Fraunhofer IMS

FRAUNHOFER-INSTITUT FÜR MIKROELEKTRONISCHE SCHALTUNGEN UND SYSTEME IMS

ANNUAL REPORT 2009

ANNUAL REPORT OF THE FRAUNHOFER-INSTITUT FÜR MIKRO-ELEKTRONISCHE SCHALTUNGEN UND SYSTEME IMS DUISBURG 2009

PREFACE

In its 25th year Fraunhofer IMS gives the starting signal for the new Microsystems technology lab to enter a new technological sector. By this strategic advancement the Fraunhofer IMS aims to develop new markets in the field of medical engineering, building technology and industrial electronics. The investment project for the MST-Lab is funded by 16 million euros. The Ministry of Innovation, Science, Research and Technology NRW and the Fraunhofer-Gesellschaft respectively incur 25% of the amount with allocations of the Federation. The European Union contributes the remaining 50%. Combining the already established CMOS of Fraunhofer IMS with the new Post-Processing technology is the perfect example of a consequent synergetic technology enhancement.

The Fraunhofer IMS operating budget in 2009 amounts to 18.5 million euros. In comparison to last year the number of employees increased by 5%. Despite the globally challenging economic situation in 2009 the Fraunhofer IMS could gain a series of public projects. The public loan programs in junction with a cost-saving program enabled the Fraunhofer IMS to achieve a counterbalanced operating budget despite the increasing number of employees. The national and international markets carry on being unsettled but Fraunhofer IMS already registers increasing incoming orders in the first months of 2010.

Project Highlights 2009

Within the BMBF-Verbund project “FIRKAM”, Fraunhofer IMS provided a cost-effective IR-imager with a VGA-resolution for a wavelength range of 8µm to 14 µm. Fraunhofer IMS realized the first micro bolometer with a pixel pitch of 25 µm.

The 2009 started Euregio project “UniHealth” should give hope to allergy sufferers. The aim of developing an easily operated and cost-effective sensorsystem is to detect and determine several allergenic substances and biomarkers.

Events 2009

In 2009 the TriDiCam GmbH, as a spin-off of Fraunhofer IMS, was awarded the business start-up prize of the "Business Promotion Agency". The developed 3D-CMOS image sensor (time of flight process) makes it possible to capture the environment tridimensionally under different ambient conditions and to analyze it in real-time.

In the first year after the opening of inHaus2 in November 2008 the business unit "Hotel" of the Fraunhofer inHaus innovation center completed a new application laboratory. The FlexLab offers the possibility to develop and test new room concepts, which are oriented on the increasing demand of a flexible use of buildings or rather hotel rooms. On the occasion of the reopening of the redesigned application laboratory "inHaus1" in May 2009 the business unit "Smart Living" presented its work by a special inHaus forum with the title "Innovative housing – Modernization with added value". The Fraunhofer-Truck complemented the forum. The exhibits shown in the impressive double-decker truck presented vividly scientific research results of the areas of health, safety, communication, mobility, energy and environment. With the help of concrete applications the visitors were able to have a realistic experience of the future.

The department "Intelligent Room – and Building Systems" has been expanded by the group "Energy Efficiency Solutions". Energy efficiency means that a designated utility can be reached by a low energy input. The objective of the newly formed group "EES" is to expose the energy consumption and to reduce the energy demand of residential and functional buildings using the conception and development of energy efficiency system solutions.

At CeBIT 2009 the exhibit "inBath – an assistive bath environment" has been well received by fair visitors. The attractive mirror is the center of the exhibit and provides reminder for the daily personal hygiene for elderly or disabled persons. During its AIM spring forum in March 2009 the "Association for Automatic Identification and Mobility"(AIM) held a meeting themed "Future Logistics and Facility Management"at Fruanhofer IMS.

On September 3rd scientists, logisticians, horticulturists and agriculturists met at Fraunhofer IMS in the innovation forum RFID Agrobusiness to exchange information about wireless technologies and their value for agricultural matters.

In the course of a colloquium on September 18th Professor Dr. Bedrich Hosticka was bid farewell on his well-earned retirement. The focus of Professor Dr. Hostickas' work during his time at Fraunhofer IMS was on CMOS image sensors where he achieved outstanding success. At this point, I would like to thank Professor Dr. Hosticka once more for his merits for the institute. As head of department "Signal processing and system design" he strongly influenced the R&D work.

In 2009 we started marketing and sales activities in Austria. The Fraunhofer IMS will increasingly operate in the major foreign market of the Fraunhofer Gesellschaft.

Particularly I would like to thank our highly motivated employees who contributed to these remarkable results in 2009 by their dedicated work and their outstanding know-how. They have helped to lay the foundations for future success in a time of rapidly changing markets. I am sure that together we are able to cope successfully with the challenges of 2010.

Anton Grabmaier

CONTENTS

III CMOS Circuits

IV Wireless Chips and Systems

V Systems and Applications

CONTENTS

PROFILE

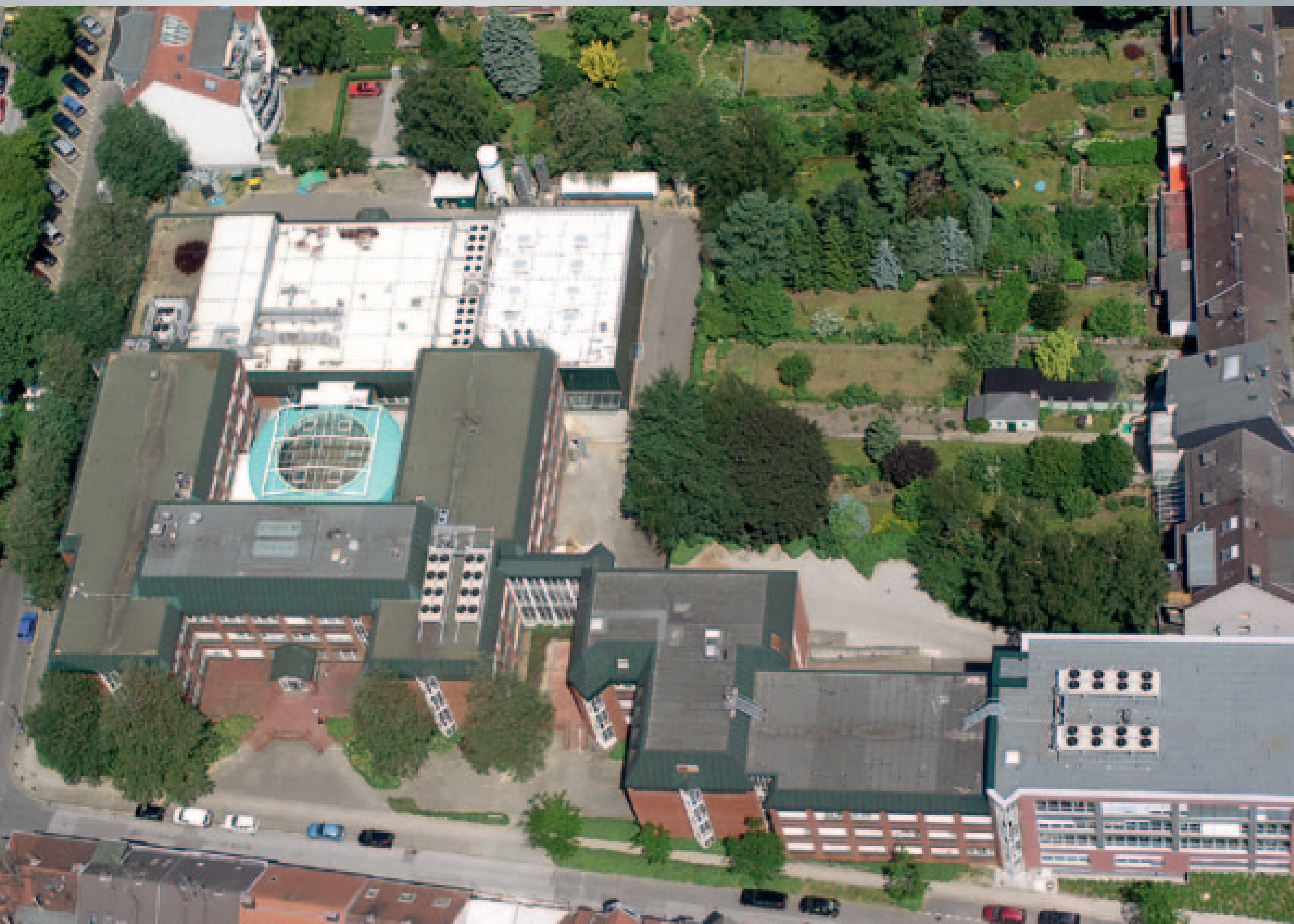

FRAUNHOFER IMS IN DUISBURG

The Fraunhofer Institute for Microelectronic Circuits and Systems (IMS) was established in Duisburg in 1984. The Fraunhofer IMS is, through continued growth and innovative research and development, one of the leading institutes in Germany for applied research and development in micro-electronics and CMOS-technology.

Fraunhofer IMS	
Employees	260
Budget	18,5 Mio. Euro
Industrial Projects	50 % of Budget
Public Projects	25 % of Budget
Fraunhofer Projects	25 % of Budget

Infrastructure

Fraunhofer IMS offers a wide range of services and production of in silicon based devices and systems.

The fabrication takes place in class ten cleanrooms, wafer-testing rooms and an assembly-line with together more than 2500 square meters.

Fraunhofer IMS CMOS Wafer Fab	
Wafer size	200 mm (8 inches, 0.35 µm)
Cleanroom area	1300 square meters
Cleanroom class	10
Employees	app. 120 in 3 shifts 7 days a week
Capacity	> 70.000 wafer/year

IMS Production and Development

Fraunhofer IMS develops, produces and assembles smart sensors, integrated circuits and discrete elements (ICs and ASICs). It also offers the fabrication of devices on a professionally managed CMOS production line in small to medium quantities.

The Fraunhofer Institute of Microelectronic Circuits and Systems (IMS)

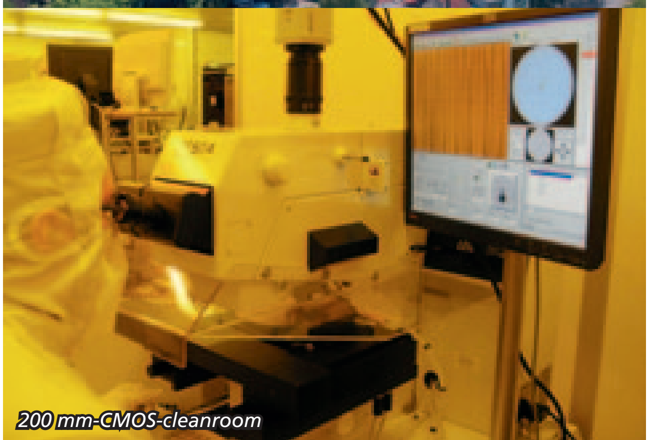

200 mm-CMOS-cleanroom

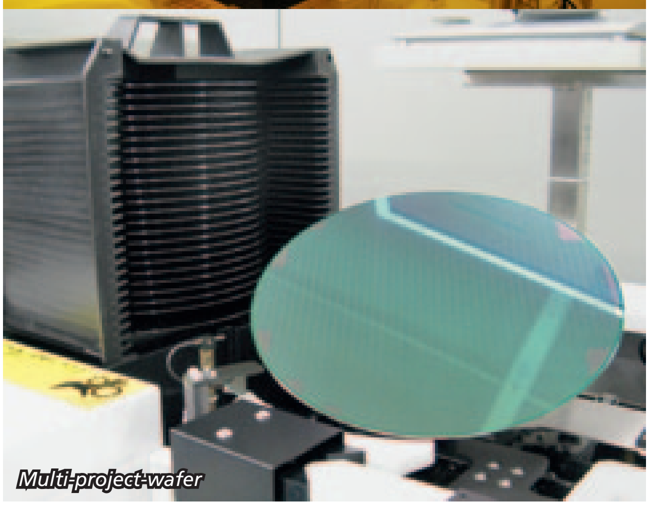

Multi-project-wafer

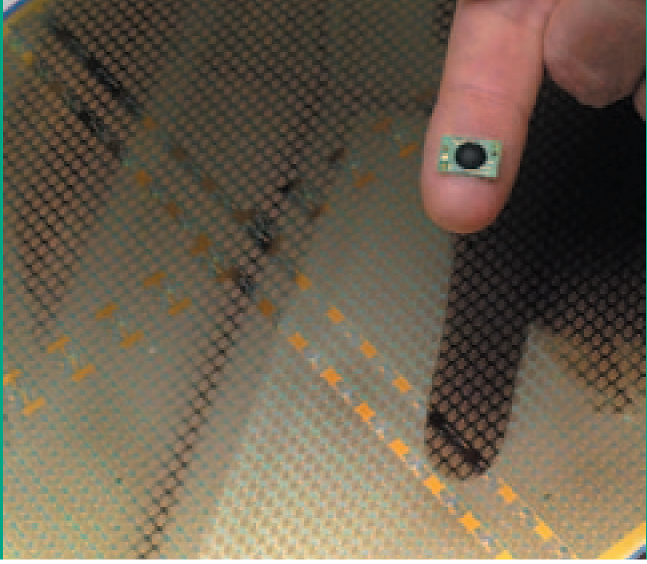

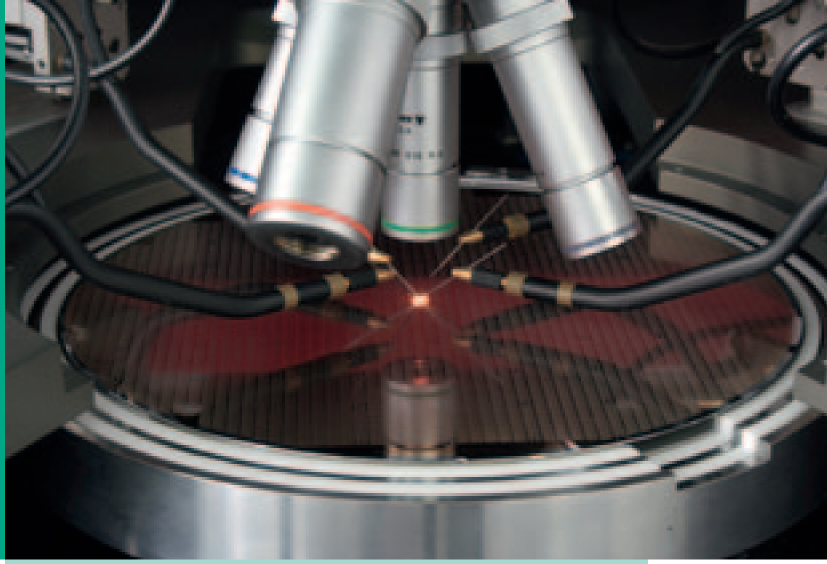

In the new microsystems technology lab (MST-Lab) we integrate different micro- and nanofunctions directly on top of the signal processing CMOS circuits. This procedure is called post-processing. (600 square meters)

The ICs are assembled in the cleanroom (400 square meters) of Fraunhofer IMS assembly facility. This facility supports the production of ICs in ceramic packages or as COB (Chip on board, COB). COB assembly is available from small quantities to several million units per year.

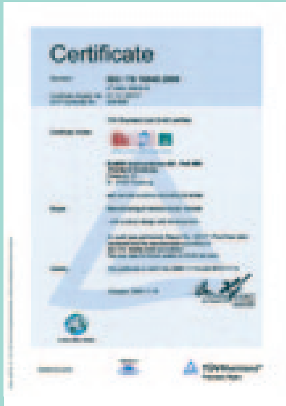

Supply and Service

The Fraunhofer IMS offers R&D services tailored to our customer needs, providing efficient solutions ranging from the initial studies to the series products.

Cooperation possibilities:

- Studies and feasibility studies
- Consulting and concept development
- Demonstrator and prototype development
- Chip production (ASIC Production)
- Development of soft- and hardware

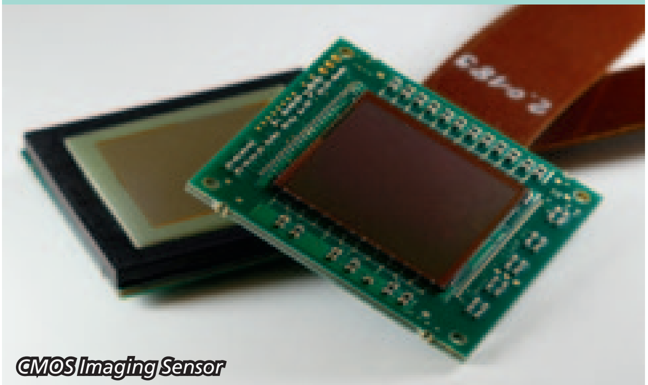

CMOS Imaging Sensor

From idea to production

RFID System

FRAUNHOFER IMS BUSINESS FIELDS AND CORE COMPETENCIES

RESEARCH AND DEVELOPMENT AT THE FRAUNHOFER INSTITUTE FOR MICROELECTRONIC CIRCUITS AND SYSTEMS

The Fraunhofer IMS conducts research and development in many different application areas including

- Automotive
- Medical
- Consumer
- Smart Buildings
- Communication
- Aero Space
- Logistics
- Industrial Automation
- Semiconductor Industry

These applications are served by our business fields:

- CMOS process
- ASIC design und development
- Sensors
  - Pressure Sensors
  - Image Sensors
  - Infrared Sensors
  - Bio Sensors
- Embedded systems hardware and software
- Wireless systems, ICs and transponders
- Smart Buildings

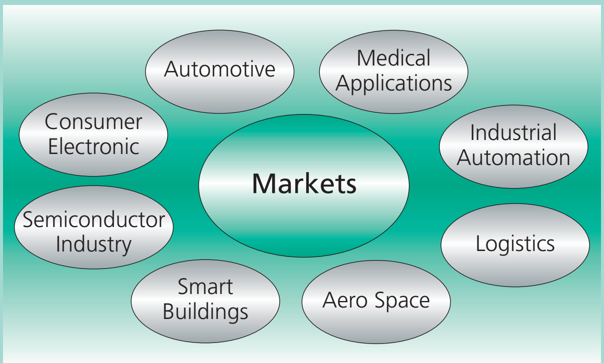

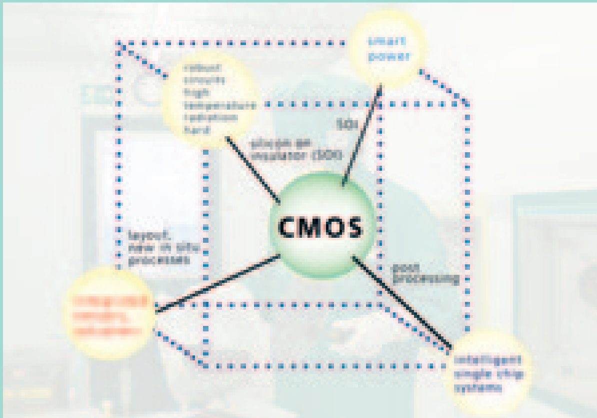

1. CMOS Process and Assembly

Based on standard CMOS process technology, IMS develops customer-specific processes and special options for standard processes (e.g. capacitors, polysilicon and thin-film resistors, high voltage transistors, EEPROM, OTP and several types of sensors).

Pressure-Sensor-Process

With a clear view on the needs of a rapidly growing sensor market, IMS leveraged its long experience in research and development of CMOS-compatible integrated sensors to establish micro-mechanical pressure sensors as one of its product lines.

At the heart of this product line is a pressure sensor that is integrated into standard CMOS technology. This micro-mechanical pressure sensor was designed for a large range of pressures, and can be monolithically integrated with many electronic devices, e.g. MOSFETs, capacitors, resistors or EEPROMs. The layout of the pressure sensor determines its pressure range, as the membrane's stiffness is directly related to its diameter.

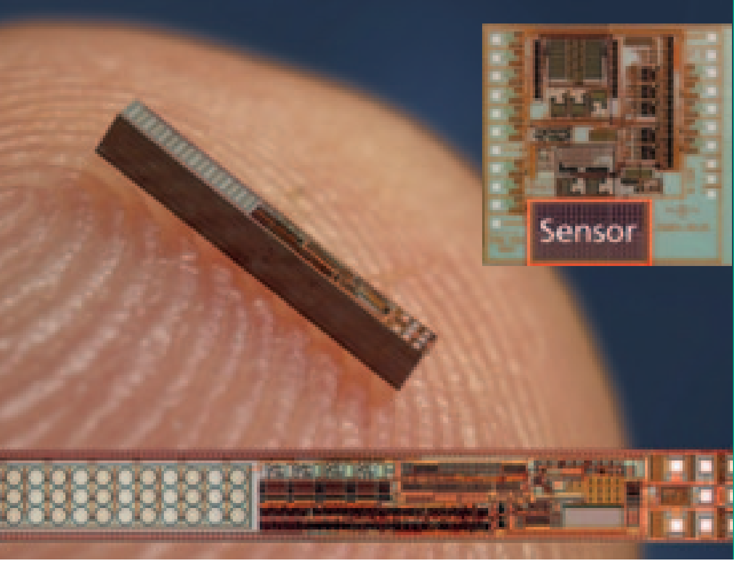

High Temperature SOI Process

The high temperature SOI CMOS process uses SOI substrates for the production of ASICs that operate at temperatures of up to 250° C.

Only fully CMOS compatible process steps are used to manufacture not only standard CMOS circuit elements, including EEPROM, but also silicon based sensors, actuators and power devices.

Power Devices

In close cooperation with industrial partners, Fraunhofer IMS provides a 600V-CMOS-process for half- and full bridge driver chips for IGBTs. Also a novel discrete power MOS transistor process based on trench technology has been developed at IMS. It features an ultra low on-resistance so that transistors with less than 1 mOhm on-resistance can be realized on a small die, while keeping the number of process steps low. Such low loss switches are used in power supply, automotive and other low voltage applications.

CMOS Fabrication

Fraunhofer IMS provides numerous semiconductor production services in its 200 mm CMOS production line. The professionally managed class 10 clean room has more than 1300 m^2 floor space. The 24 hour, 7 days a week operation ensures the uniform quality of our products.

The Fraunhofer IMS production line especially caters to the production of smaller and medium quantities of ASICs. The production line operates under an ISO 9001:2000 and TS 16949 certified quality management system, assuring stability and reliability of products and production. Timely, reliable and customer-oriented production is our and our customers key to success.

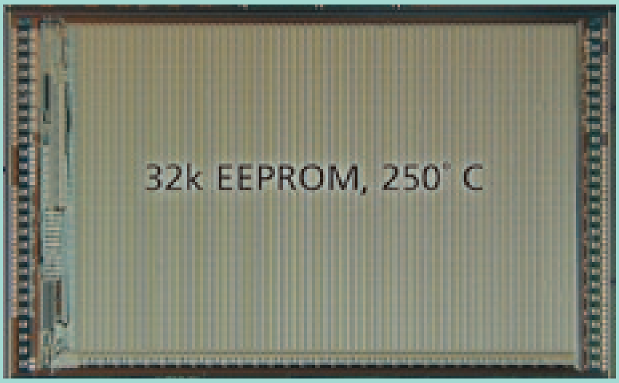

RESEARCH AND DEVELOPMENT AT THE FRAUNHOFER INSTITUTE FOR MICRO-ELECTRONIC CIRCUITS AND SYSTEMS

2. Sensors

Pressure Sensors

The basic element of our pressure sensors is a surface micromechanical sensor that is fabricated using standard CMOS processing equipment. These sensors can be realized for a wide range of pressures, sharing a single chip with all electronic devices available in a CMOS process, e.g. MOSFETs, capacitors or EEPROMs. The sensors can be configured as absolute with capacitive readout. The necessary signal conversion, linearization and amplification circuits are realized on the same chip, effectively eliminating interference on sensor wiring that is a major issue for discrete solutions. We have already created a variety of innovative products using this monolithic integration of sensors and signal processing functions like programmable amplifiers, sensor linearization, temperature compensation or wireless interfaces.

The layout of the sensor element determines its pressure range, which may be situated between 0.5 to 250 bar, as the sensor diameter controls the stiffness of the membrane: Smaller and stiffer membranes shift the pressure range to higher pressures. Thus the sensors are suitable for the measurement of pressures ranging from blood, air, and tire pressure all the way to hydraulic oil pressure. The small size of the sensor and its associated electronics enables innovative medical applications for the in vivo measurement of the pressures of blood, brain, eye or other body fluids.

CMOS Image Sensors

Fraunhofer IMS image sensors are based on CMOS technology, which enables the monolithic integration of sensor and circuit elements on a single chip. This integration is used e.g. to control the sensitivity of each individual pixel to avoid blooming. Fraunhofer IMS has developed a dedicated 0,35 µm Opto CMOS process.

A wide range of CMOS image sensors has been developed for our customers and in research projects. The realized sensors include high dynamic range sensors, high speed sensors – which deliver 1000 high quality images per second – and high-resolution sensors with “region of interest” function for faster readout of subsections of the pixel array. The CMOS image sensors suppress smearing and blooming effects and always deliver sharp images. Electronic high-speed shutters enable the realization of 3D imagers base on laser pulsed based time-of-flight measurement.

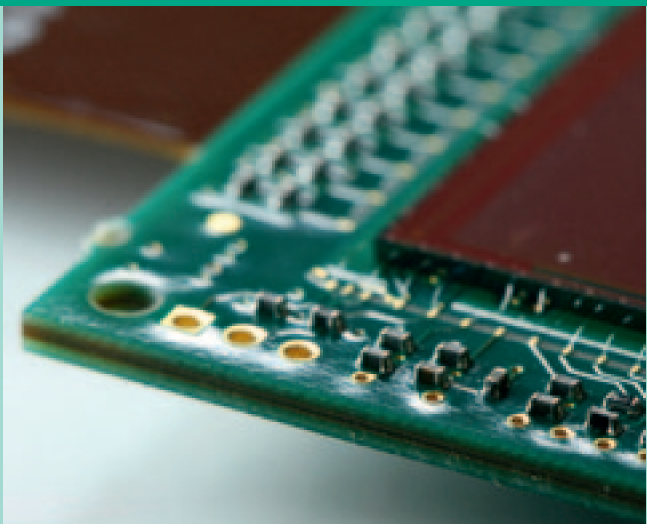

CMOS Image Sensor

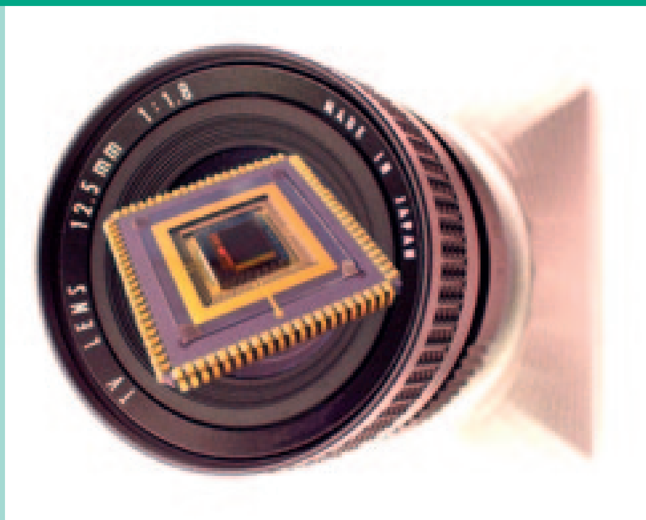

CMOS Camera

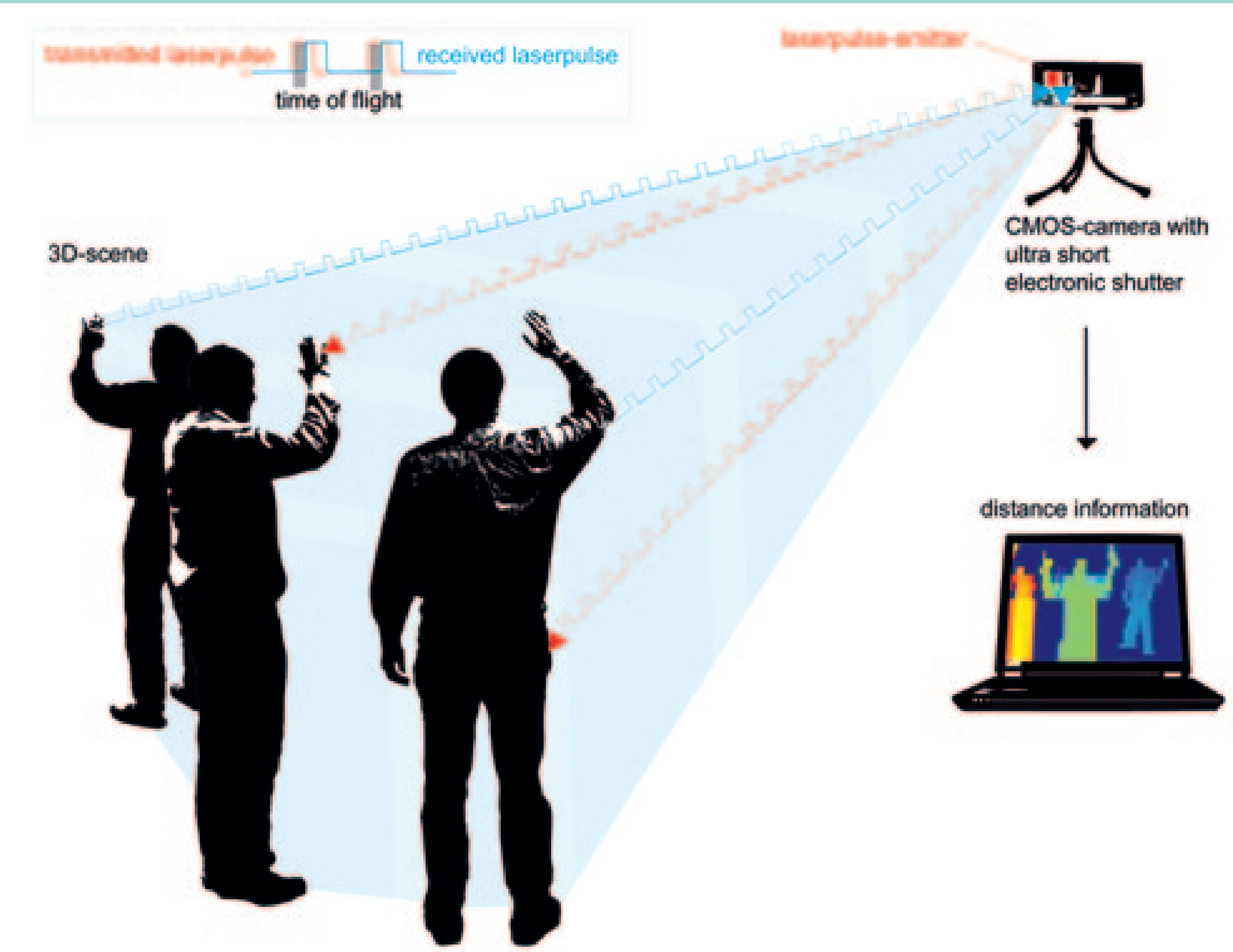

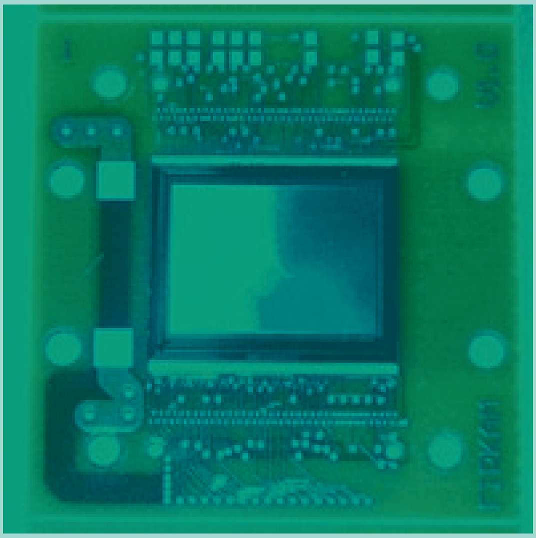

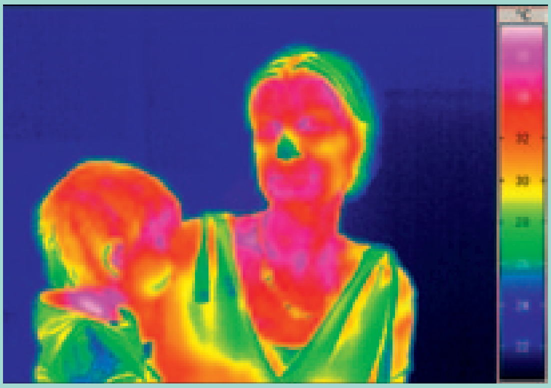

Infrared Sensor

The demand for uncooled infrared focal plane arrays (IRFPA) for imaging applications is constantly increasing. Examples for the application of IRFPAs are thermography, pedestrian detection for automotive, firefighting and infrared spectroscopy.

IRFPAs consist of an array of microbolometers located on top of a CMOS substrate which comprehends the readout circuit. Typcal array sizes are for lowcost applications 160 x 120 or 320 x 240 pixels. State-of-the-art IRPGAs achieve VGA-resolution with 640 x 480 pixels.

The microbolometer is a special infrared sensor. The IR-sensitive sensorelement based on the principle for a microbolometer is fabricated by post-processing on CMOS wafers. The microbolometer converts the infrared radiation into heart energy and this induces a temperature rise resulting in a change of the electrical resistance. Typical microbolometers have pixel pitch values of 35 µm or 25 µm.

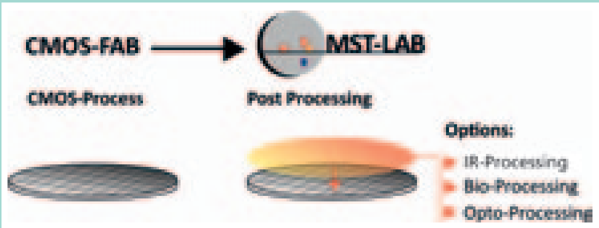

Biosensors

Biosensors for point-of-care and home diagnostics are increasingly asked for. Therefore Fraunhofer IMS advances in the development of a new generation of biosensors. These special sensors are developed in the Microsystems Technology Lab where standard CMOS circuits are prepared for or – in future – combined with bioactive layers. Typically, additional metals or oxides are added, as well as special surface treatment and activation or the dispension of anchor chemistry for later analyte receptor immobilization. This new technology is called post-processing and it enables the production of different sensors for different applications by joining biosensitive layers with CMOS electronic readout circuitry. This "Bio to CMOS" processing leads to Biohybrid Systems.

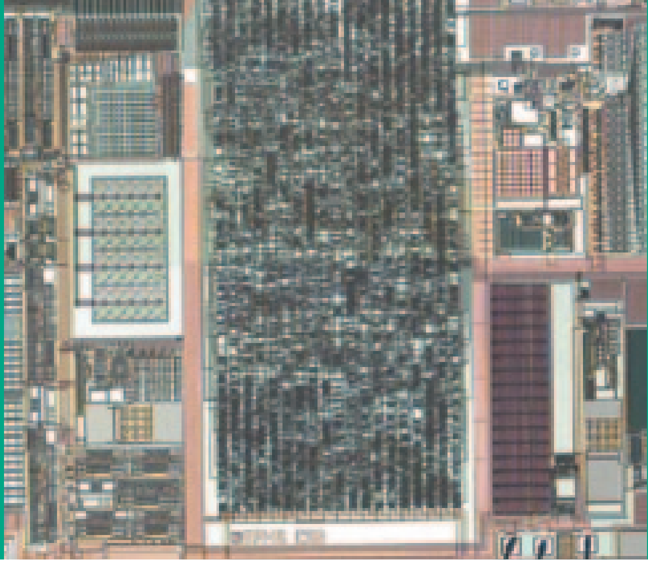

3. ASIC Design

The development of analog, digital and mixed analog-digital integrated systems is a core competence of Fraunhofer IMS. Application specific integrated circuits (ASICs) enable our customers to provide cheaper and more powerful products. We offer the full spectrum from custom to IP-based ASIC solutions.
Full-custom ASICs are designed from scratch to accommodate the specific requirements of the customer, providing a highly optimized product. The IP-based ASIC is based on proven generic components, with lower design time and cost. Using a mix and match approach both design styles can be combined to leverage the benefits of both.

The close co-operation with our in house CMOS production line provides a seamless and efficient path from concept to series production. Our long experience in the development of integrated circuits, starting from concept through design, layout, and fabrication to testing ensures a short development time and a minimized design risk.

Our fields of design expertise are:
- Embedded microcontroller
- High-temperature ASICs
- Smart power integration
- Non-volatile memories
- Mixed-signal design
- Sensor transponder

Beside standard ASIC solutions for all kinds of applications, ASICs with sensors and sensor signal processing integrated on a single chip have been realized.

These ASICs often combine our core competences in ASIC design,
- System-on-Chip (SoC) solutions,
- Mixed-signal signal processing and
- Integration of RF building blocks for wireless energy and data transfer.

Our customers benefit from our research in these areas, which provides viable solutions for their applications – applications that demand miniaturization, energy-efficiency, cost-optimization and reliability.

4. Wireless Systems and Transponders

A core-competence of Fraunhofer IMS is the development and realization of wireless systems. Research and development focuses, among other things, on wireless sensor networks. These networks comprise autonomous sensor modules that are distributed over a large area or volume, and measure physical, chemical and other quantities. The measured values are transferred to a central agency, making use of intermediate nodes for data transfer, or they can be used by similarly distributed actor modules for decision-making and control processes. Development in this field includes new methods for communication (e.g. protocol stacks, localization) and the realization of cost-efficient, miniaturized components. The realization of new products in an efficient and timely manner is facilitated by the use of modular hardware and software components that allow a quick adaptation to application requirements.

High-frequency measurement chamber at Fraunhofer IMS

The advantages of wireless sensor networks were successfully demonstrated in some projects.

Important applications of **wireless sensor networks** are in the field of:
- Industrial automation, e.g. logistics and inventory control.
- Agriculture e.g. monitoring of air and soil parameters.
- Facility management, e.g. remote monitoring of buildings and infrastructure elements.

Our customers face a number of challenges that are adressed by our R&D activities. One set these activities addresses tools for network development, deployment and maintenance. Others address the field of energy harvesting, the ability to extract module power from the environment and obviating the need for batteries or power cables.

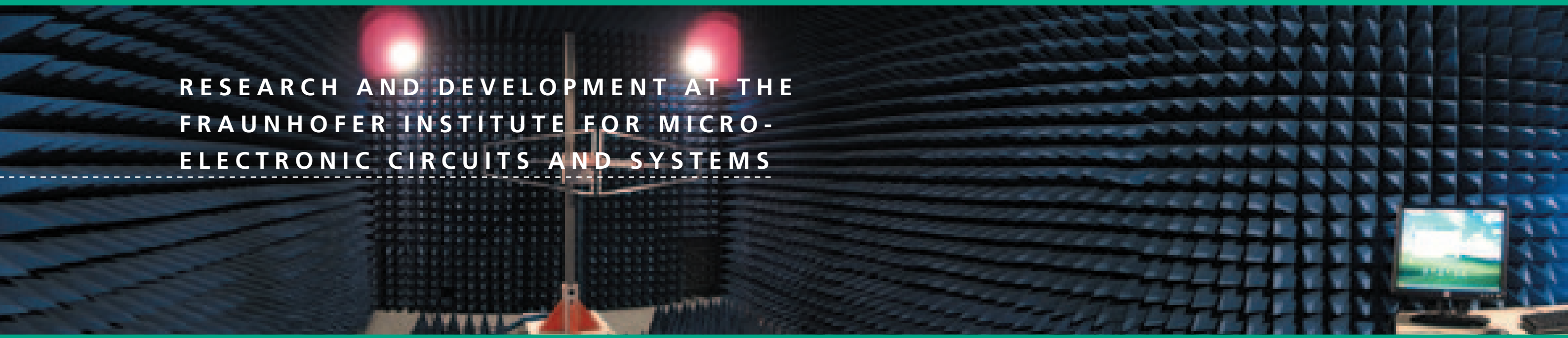

RESEARCH AND DEVELOPMENT AT THE FRAUNHOFER INSTITUTE FOR MICRO-ELECTRONIC CIRCUITS AND SYSTEMS

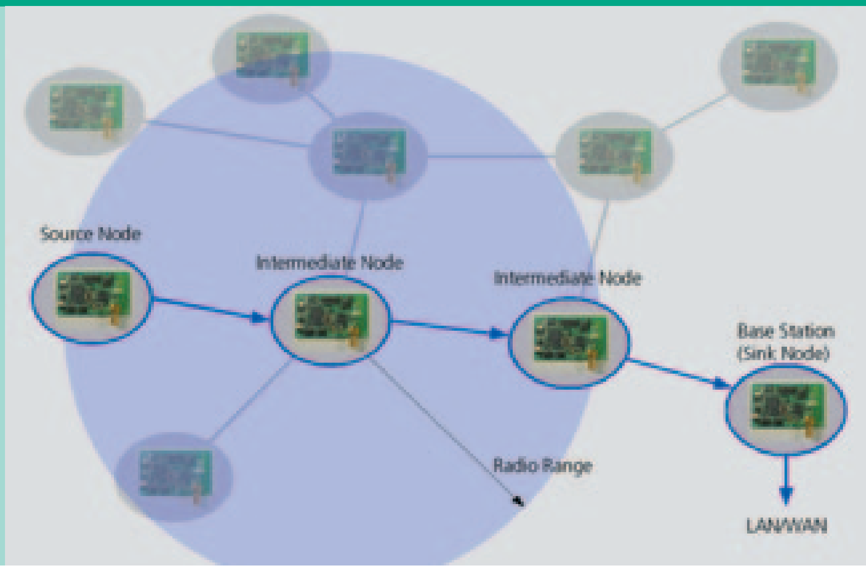

The **transponder systems** unit at the Fraunhofer IMS offers system solutions for the integration of novel portable or stationary transponder read-write devices and base stations into smart network-systems.
It also provides base stations for transponder ASICs with integrated micro sensors developed at Fraunhofer IMS, thus offering complete system solutions.
These transponder systems are used in smart buildings and vehicles, industrial automation, medical devices and logistics.

Sensor-Transponder System for Medical Applications

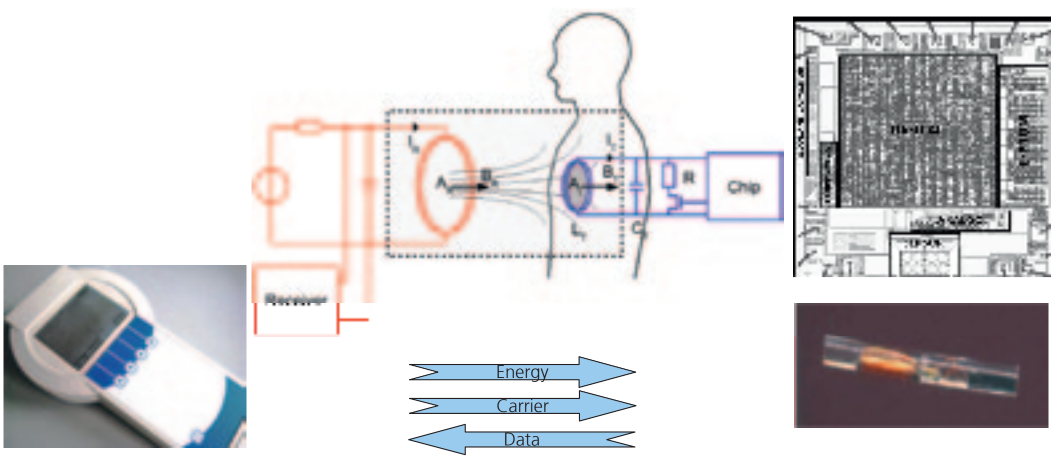

5. Smart Room & Building-Solutions

At the **Fraunhofer-inHaus-Center,** Europe's leading innovation center for smart homes and buildings, IMS cooperates with six Fraunhofer-Institutes and nearly 100 industrial partners to develop, test and demonstrate innovative solutions of all kinds for different application fields in smart buildings. In detail IMS offers research, development and complete systems-solutions to component and systems manufacturers, builders and operators of homes and commercial buildings for new and added value functions on the basis of electronics and software.

At the **inHaus1-Facility (Smart Home-Lab)** new domotic techniques to control lighting, doors and windows as well as heating and ventilation for energy efficiency in homes are developed and tested. One focus lies on solutions for smart metering for more transparency in energy consumption. In the SmartHome-Segment we have also a lot of experience in the field of user interface solutions for easyer control of technical equipment in homes. User acceptance tests in the smart home lab garantee the new industrial products to have a better success chance on the market.

At the **inHaus2-Facility (Smart Building-Lab)** new technical solutions for commercial properties are being developed, e.g. for new benefits in facility management and building operation, in the operation process of nursery homes, hotels and offices.

One main IMS focus lies on the development of new concepts and electronic systems that provide unobtrusive assistance for elderly and handicapped people in order to maintain a self-determined life at nursery homes with commercial operation and to optimize the care service process. We concentrate especially on solutions like microelectronic sensor networks in rooms with software interpretation of data to get benefits like automatic detection of problems or emergency cases (ambient assisted living AAL).

Another main field of R&D in all inHaus-application segments is energy efficiency, like in the smart home field. In cooperation with component and systems manufacturers and also energy providers next-generation-metering and building automation technologies for energy efficiency are developed, tested and demonstrated.

The inHaus Center offers R&D and complete systems-solutions to builders, modernizers or operators of homes and commercial buildings, to implement complete electronic and ITC systems for new and added value functions. This includes the following aspects:

- Safety and security
- Multimedia
- Support for the elderly
- Energy saving
- Light management

DEVELOPMENT OF THE IMS

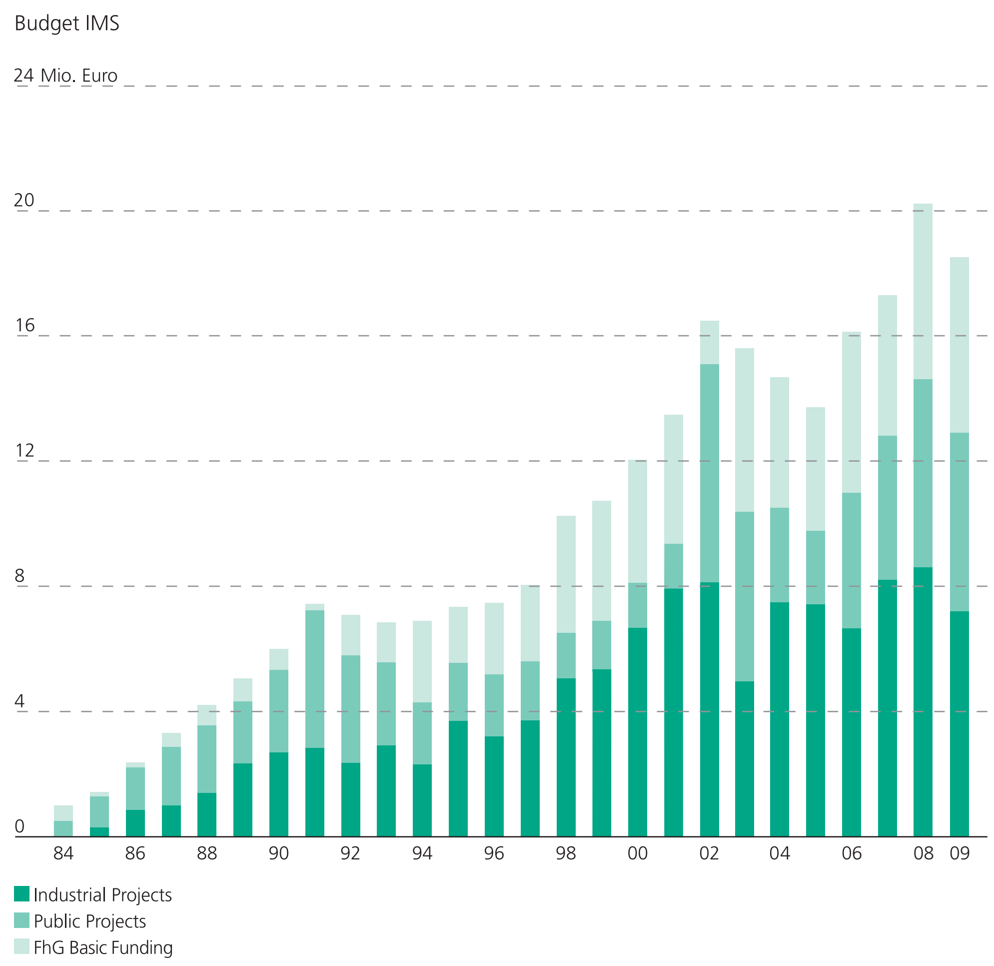
Budget IMS
24 Mio. Euro
20
16
12
8
4
0
84
86
88
90
92
94
96
98
00
02
04
06
08
09
Industrial Projects
Public Projects
FhG Basic Funding

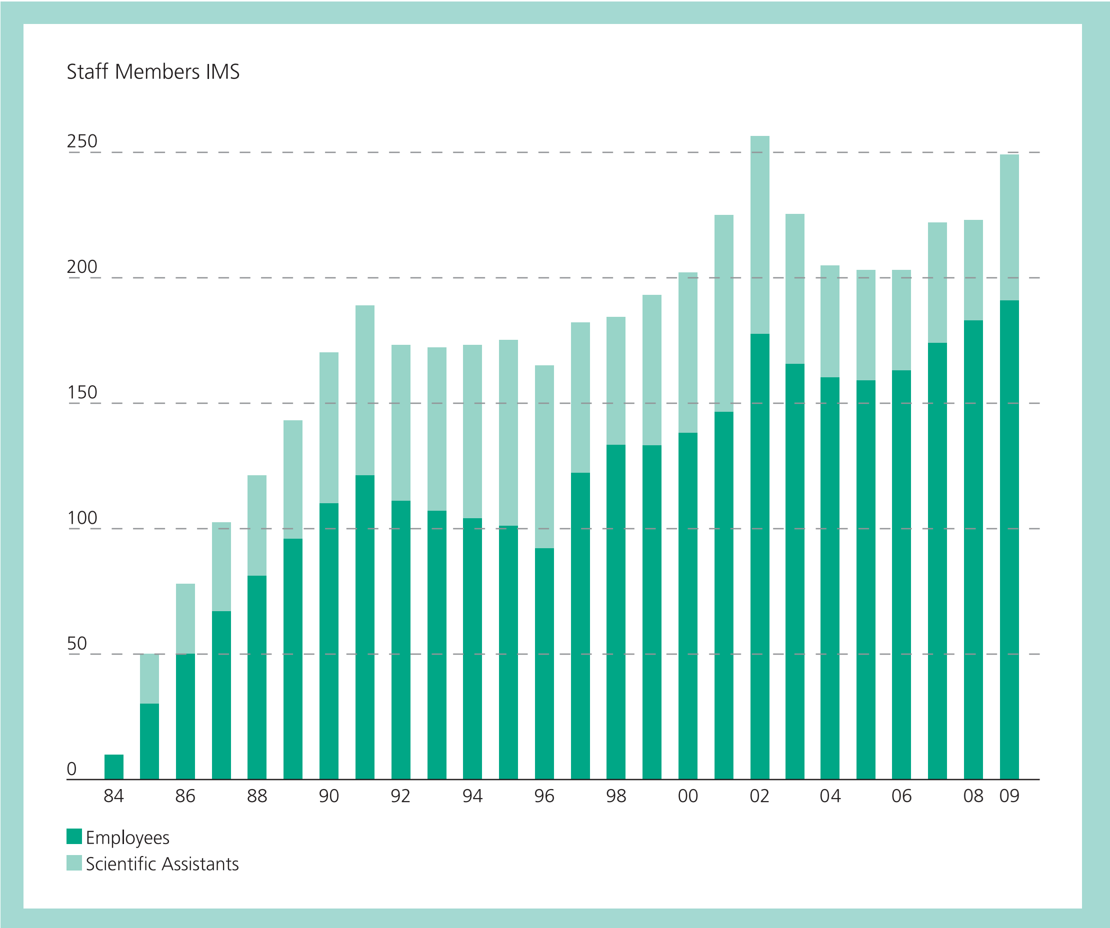

Staff Members IMS
250
200
150
100
50
0
84
86
88
90
92
94
96
98
00
02
04
06
08
09
Employees
Scientific Assistants

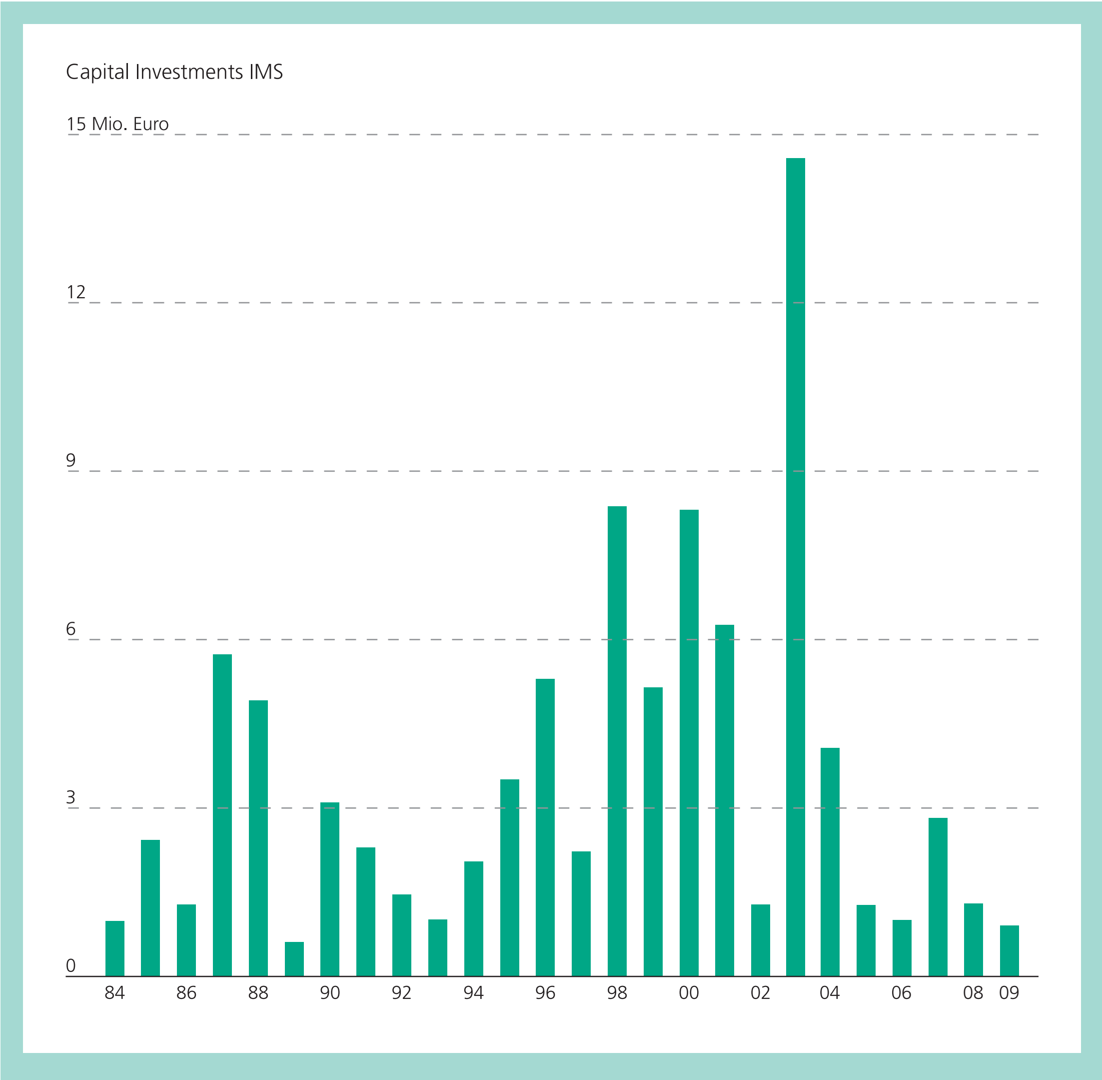
Capital Investments IMS
15 Mio. Euro
12
9
6
3
0
84
86
88
90
92
94
96
98
00
02
04
06
08
09

SELECTED PROJECTS OF THE YEAR 2009

Selected Projects of the Year 2009

CMOS PROCESSES FOR OPTICAL APPLICATIONS

F. Hochschulz, M. Jung, S. Weyers

A wide range of CMOS chips for optical applications like high speed or high dynamic range cameras have been developed and produced by the Fraunhofer IMS. Therefore, special optical CMOS devices have been developed and incorporated into standard CMOS processes down to a structure size of 0.35 µm.
In order to optimize the performance of these chips and to access new application fields new options were developed to complement the existing processes.
These new options range from optimization of the material stack in the light path of the chip over color filters to micro lenses on top of the chip.

UV-transparent Passivation

In order to prevent CMOS circuits from mechanical damage the chips are covered with a SiN passivation layer. In addition to the mechanical protection it also serves as a diffusion barrier for humidity and ions. Since this layer was initially optimized for the above mentioned protection its optical properties were no concern at the time of its development.

For optical applications a drawback of this layer is its increasing light absorption for wavelengths below 500 nm with a nearly complete absorption for wavelengths below 400 nm [Figure 1 (top)].

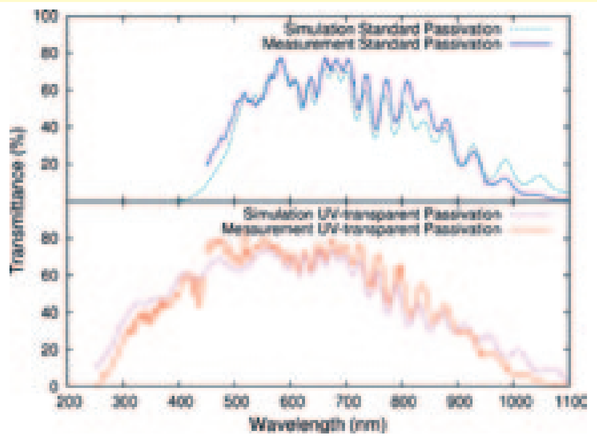

Figure 1: Comparison of wavelength dependent transmittance of light for the standard SiN passivation (top) and the optimized UV-transparent SiN passivation (bottom)

Therefore, the sensitivity of an optical sensor for blue light (400 – 500 nm) is much lower compared to other colors of the visible spectrum. Furthermore the use for spectroscopic applications that require the detection of ultraviolet light is not possible at all.

Since the optical properties of a SiN layer depend on its stoichiometric composition a protective SiN layer was developed by adjusting the deposition conditions to achieve optimized optical properties.

The improvement for wavelength below 500 nm is clearly visible in Figure 1 (bottom). Even at 300 nm 20 % of the light is transmitted through the layer while no performance loss occurs for larger wavelengths.

Optical Stack Optimization

On its way from the top surface of a CMOS chip to the detecting optical device the light has to travel through a stack of several different layers. At each interface reflection takes place which results in interferences. Therefore, the material stack on top of the photo diode acts as a spectrometer with an oscillating wavelength dependency of the transmittance of light [Figure 3 (top)].

Simulations of the stack that is used for our CMOS processes show periods for the oscillations in the range of 5 to 20 nm. For applications with a bandwidth of the incoming light much wider than these periods the detected intensity will depend

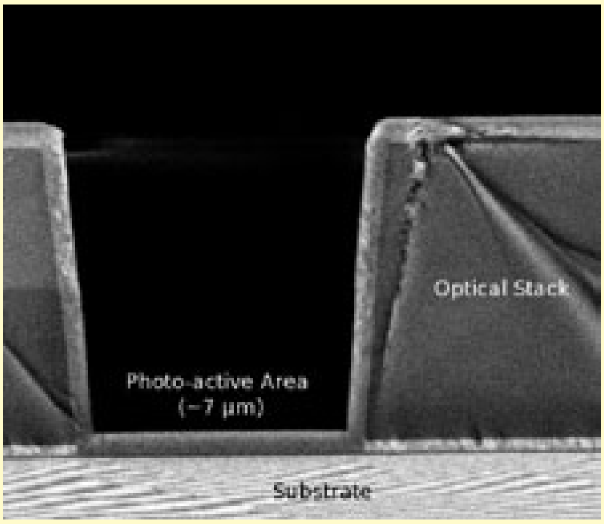

Figure 2: SEM-cross section of the optimized stack

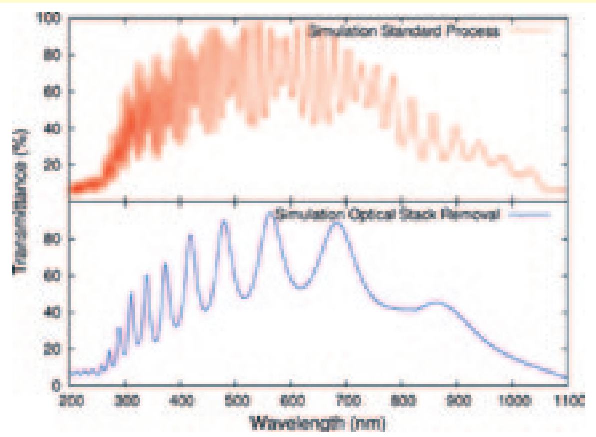

Figure 3: Simulation results for the wavelength dependent transmittance of the material stack on top of a photodiode for the standard CMOS stack (top) and the optimized stack shown in Figure 2 (bottom)

on the average transmittance of the material stack and the oscillation can therefore be neglected.

For nearly monochromatic light likely to be found in spectroscopic applications the transmittance of the optical stack will directly influence the detected intensity. For example in the structure simulated in Figure 3 (top) the transmittance for 530 nm is 97 % while for 538 nm it is decreased to 41 %. The actual oscillations are highly sensitive to the thickness of the involved layers and therefore sensitive to process variations during the manufacturing of the chip. Thus for larger chips the behavior might even change significantly for different positions on the same chip and the intensity detection of light with a small bandwidth can result in a large unpredictable error.

In order to reduce the influence of the material stack the stack itself was removed as far as possible from top of the photo diodes while keeping it for the remaining chip area. For protection purposes the top passivation layer of SiN was left on top of the photo diode [Figure 2].

By doing so the period of the oscillation can be increased significantly [Figure 3 (bottom)]. Due to the fact that only one remaining layer and its process variations are involved, the behavior of the photo diode is more stable and can be compensated numerically. This allows for the use for spectroscopic applications that require a high wavelength resolution.

CMOS PROCESS FOR OPTICAL APPLICATIONS

Color Filters

While for spectroscopic application the afore mentioned improvements are crucial, for imager applications additional qualities like color separation and sensitivity are important. Therefore, we have integrated a color filter system in our CMOS process, so the sensors are not longer color blind. To realize this, each pixel receives a color filter by coating a layer of polymer dyed in red, green or blue. The transmittance curves of these color filters are measured and are shown in Figure 4. Even after temperature cycling the transmittance characteristic does not change, confirming that the color filter system is very stable over time.
As an example a color sensor fabricated at the Fraunhofer IMS is shown in Figure 5. It is realized with alternating single-color RGB stripes (see Figure 5). A cross section of the pixel matrix can be observed in Figure 6.
We also offer a blue cover over the chip around the matrix serving as a light shield to protect the matrix from scattered light entering the chip from the side.
The implementation of color filters allows using these sensors for a wide field of applications, for example driver assistance systems or for print inspection.

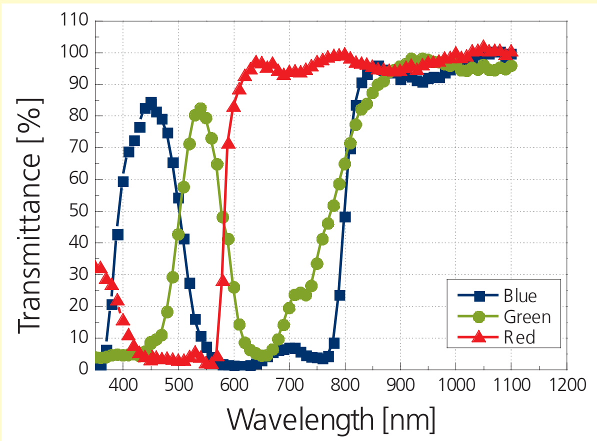

Figure 4: Transmittance curves measured at the Fraunhofer IMS

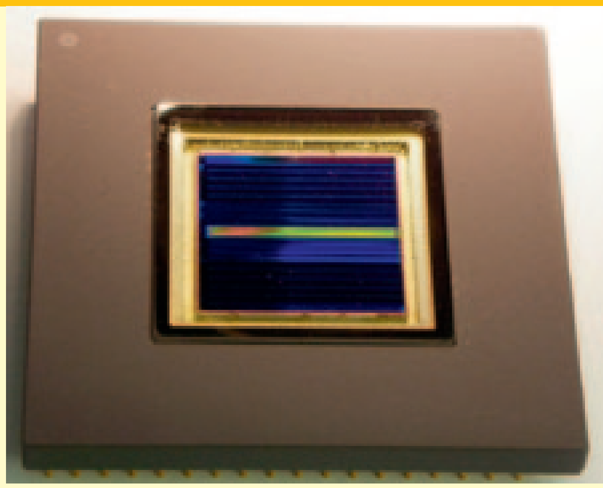

Figure 5: Color sensor chip (top) and detail of the color filter lines (bottom)

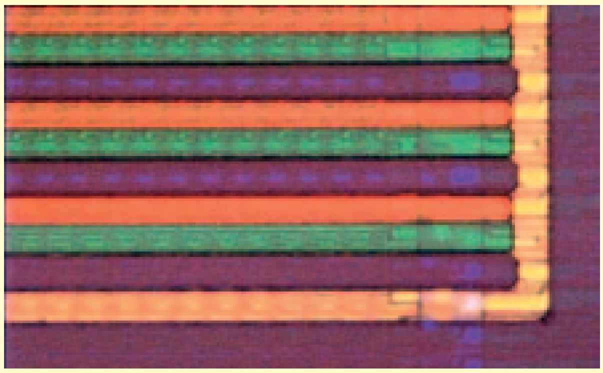

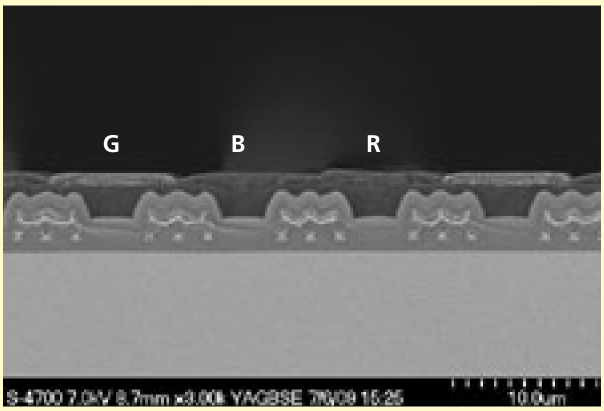

Figure 6: SEM cross section of a pixel matrix covered by color filter (R: Red, G: Green, and B: Blue)

Micro Lenses

For imager applications part of the readout circuit for the photo diodes have to be placed directly next to the photo diode itself. Therefore, a pixel consists of a photo active area and a non active area. Light that enters the non active area will not be detected and decreases the sensitivity of the pixel. In order to increase the sensitivity of the imager micro lenses can be used to focus the incoming light onto the photo active area.

These lenses are fabricated in a CMOS compatible process on top of the CMOS imager. The size and the shape of the micro lenses are individually adjusted for any imager layout to give the best performance for a chosen application [Figure 7]. The micro lenses process is also compatible with color filters. Combining these two options allows accessing a much wider field of application than before.

In addition to the improvement of an imager performance our ability to individually adjust the micro lens design enables their use for more advanced application like stereoscopic imaging. In this case the micro lenses are shaped cylindrically [Figure 8] and used to focus the light from the two objective lenses representing the right and the left optical channel onto two adjacent pixels. For this kind of application the separation of the two optical channels is very important resulting in much tighter requirement for the optical properties of the micro lenses.

Therefore, the whole system consisting of the chip and the micro lenses is simulated using optical as well as electrical simulations. The results are used to optimize both the micro lens design as well as the chip layout.

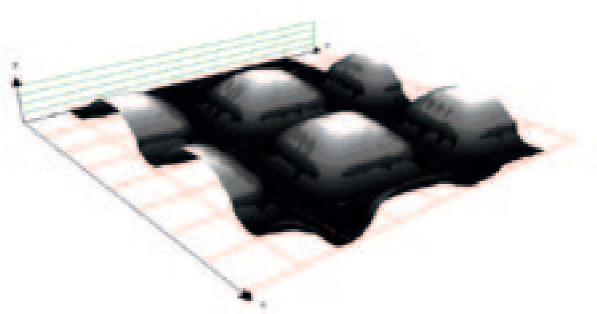

Figure 7: Shape of square micro lenses (20 µm × 20 µm) measured using a phase shift microscope

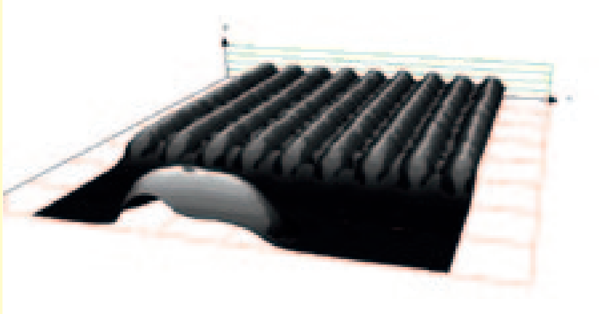

Figure 8: Shape of cylindrical micro lenses (pitch = 6 µm) measured using a phase shift microscope

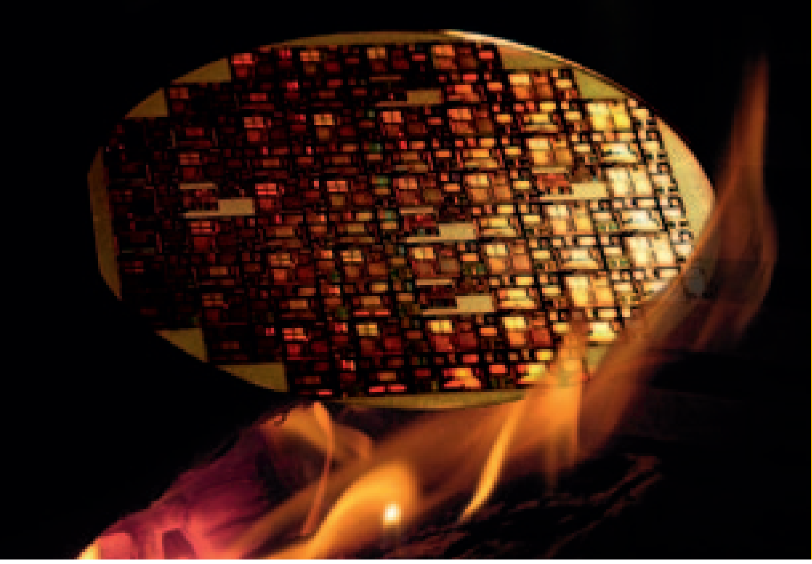

HIGH TEMPERATURE ELECTRONICS

H. Kappert, R. Lerch

Today numerous industrial applications have a demand for high temperature electronics which is already used in the fields of oil or gas exploration as well as geothermal development.
In these fields the circuits used to control and monitor the deep hole drilling process call for solutions withstanding the harsh environment. Additional applications are in the field of measurement instrumentation especially for industrial processes. While factors like shock or vibration can be taken into account with special assembly or housing techniques, the high temperature environment is often dealt with extensive cooling measures to assure the operation of the electronics in the specified industrial temperature range.
Fraunhofer IMS has investigated for more than fifteen years the use of Silicon on Insulator CMOS technology for the realization of high temperature integrated circuits. With this technology integrated circuits can be expressly designed for operating temperatures of up to 250°C, eliminating the customary screening process for pre-selection of standard components.
Due to the increasing demand for highly integrated high temperature electronics and the need for co-design with external customers, Fraunhofer has started some challenging activities in an internal project.

Technology
Based on an industrial proven 1.0 µm thin-film SOI CMOS process used for high voltage devices like an “Integrated 3 Phase Gate Driver” Fraunhofer IMS has developed a process option for high temperature applications. This option includes HT-EEPROM, additional devices as well as a high temperature metallization based on tungsten. In the course of this project Fraunhofer IMS has revised the metallization process to adapt it to new technology constraints of the 8 inch fabrication line. Furthermore the metallization process supports 3 layers of metal now, which increases the gate density for digital circuitry by approximately 40 % allowing more complex digital designs.

Process Design Kit
Up to now, the simulation environment was based on a Fraunhofer IMS proprietary SOI model. In the course of the project the SOI transistor devices have been recharacterized and fitted to an industrial standard BSIM SOI model. Additionally Fraunhofer IMS has revised the whole Process Design Kit (PDK), which is ready to use for external customers now.

Technology Preview
Addressing the demand for higher complexity of digital circuits also in the field of high temperature electronics, Fraunhofer IMS has kicked-off the development of a next generation SOI CMOS process. The new process aims for a structure size of 0.35 µm. It features two gateoxides to support the original 1.0 µm devices for analog and high voltage operation as well as area-optimized 0.35 µm devices for digital circuits. The new process includes a high voltage option for devices up to 600 V as well as the high temperature option with EEPROM, additional analog devices and a high temperature metallization.

Conclusion
High Temperature Electronics gives the opportunity to realize complex integrated systems for harsh environments without the need for extensive cooling measures and opens a broad range of new applications. Fraunhofer IMS provides powerful solutions based on the in-house SOI CMOS process. The actual technology and PDK developments augment the existing platform to support more complex designs and opens new business models with our customers. Finally the technology shrink to 0.35 µm will open up new possibilities for the realization of more complex and capable high temperature integrated circuits.

DIGITAL VGA-IRFPA FOR THERMAL IMAGING APPLICATIONS

D. Weiler

Fraunhofer IMS has fabricated in 2009 the first uncooled infrared focal plane array (IRFPA) throughout Germany. IRFPAs measure the emitted radiation of warm bodies in the long-wave infrared band (8 µm … 14 µm) and provide the IR-image in an IR-camera system. Examples for applications of IRFPAs are thermography, pedestrian detection for automotive, firefighting, and infrared spectroscopy.
IRFPAs consist of an array of microbolometers located on top of a CMOS substrate which comprehends the readout circuit. The microbolomters are located in a vacuum package to achieve a higher sensitivity due to thermal isolation.

IRFPA

The IRFPA based on uncooled microbolometer with a pixel pitch of 25 µm and is realized with a VGA resolution of 640 x 480 pixel. The IRFGA is designed for a high sensitivity (noise equivalent temperature difference NETD) of NETD < 100 mK at a frame frequency of 30 Hz. A novel readout architecture which utilizes massively parallel on-chip Sigma-Delta-ADCs located under the microbolometer array results in a high performance digital readout. Sigma-Delta-ADCs are inherently linear and a high resolution of 16 bit for a second-order Sigma-Delta-modulator followed by a third-order digital sinc-filter can be obtained. In addition to several thousand Sigma-Delta-ADCs the readout circuit consists of a configurable sequencer for controlling the readout clocking signals and a temperature sensor for measuring the temperature of the IRFPA. Since packaging is a significant part of IRFPA's price Fraunhofer-IMS uses a chip-scaled package consisting of an IR-transparent window with double-sided antireflection coating and a soldering frame for maintaining the vacuum resulting in reduced production costs. The IRFPAs are completely fabricated at Fraunhofer-IMS on 8" CMOS wafers with an additional surface micromachining process.

Microbolometer

The IR-sensitive sensorelement is a microbolometer and it is fabricated by post-processing on CMOS wafers in the IMS Microsystem Lab. The microbolometer converts the infrared radiation absorbed by a membrane into heat energy and this induces a temperature rise resulting in a change of the electrical resistance. The top view of a microbolometer is shown in Fig. 1. A micromachined membrane consisting of amorphous silicon as a sensing layer absorbs the IR-radiation. To increase the thermal resistance and therefore the temperature raise due to IR-absorption the membrane is fixed by two long legs with a small width. The legs are suspended by two via stacks of metal from the CMOS substrate [1]. Fig. 2 depicts the cross section of a microbolometer. The membrane is deposit using a sacrificial layer at a distance of approx. 2 µm over a reflection metal on top of the CMOS substrate. After the release process the membrane forms with the reflection metal a interferometric structure [2]. The bolometer are realized with a pixel pitch of 25 µm. The amorphous silicon as the sensing layer is optimized to achieve a high temperature coefficient TCR with low-noise.

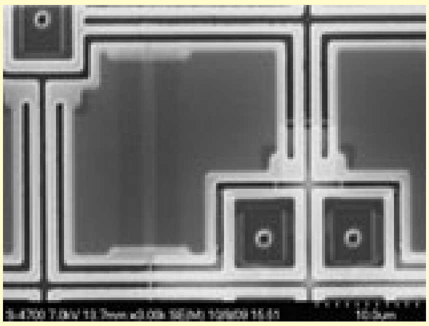

Figure 1: SEM micrograph of a bolometer (top view)

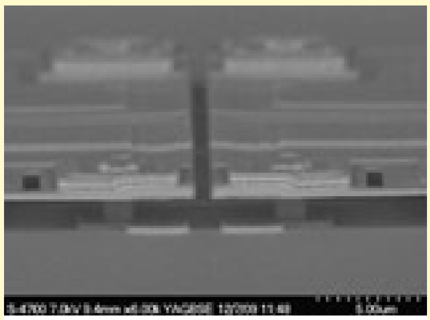

Figure 2: SEM micrograph of a bolometer (cross section)

DIGITAL VGA-IRFPA FOR THERMAL IMAGING APPLICATIONS

Package

To reduce thermal losses by gas conduction a vacuum package with an infrared window is required. The principle of a chip-scale package is shown in Fig. 3. A IR-transparent shell consists of silicon with a doubled-sided antireflection coating is placed using a solder frame on top of the substrate which includes the readout electronic and the bolometer. By using a flip-chip technique the shells are placed only on top of "good-tested" chips. Fig. 4 illustrates a wafer with partly assembled chip-scale packages. A chip-on-board package (Fig. 5) is used as a detector-board in a IR-camera system.

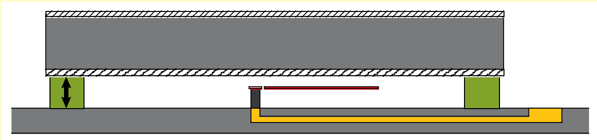

Figure 3: Chip scale package

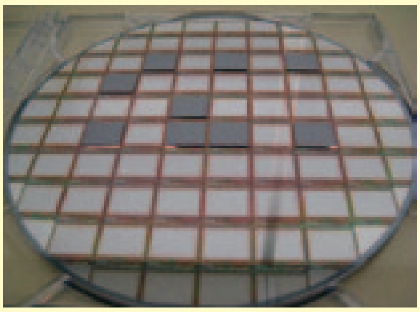

Figure 4: Wafer with chip scale packages

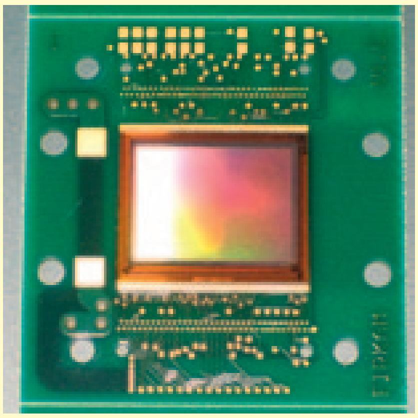

Figure 5: PCB with VGA-IRFPA

Digital readout

The electrical signal of a microbolometer is a radiation dependent change of the electrical resistor [3]. A sophisticated readout of a bolometer array is to integrate the readout principle directly into an ADC. This can be done by using the principle of a sigma-delta (ΣΔ) modulator. A ΣΔ modulator achieves a high signal to noise ratio (SNR) by combining over-sampling, interpolation, and noise shaping while dispensing with the need of high precision analog components. It relies on the noise spectrum of coarsely quantized input signal being shaped and shifted out of the signal band to higher frequencies to achieve fine quantization. The IMS developed a highly innovative IRFPA using the ΣΔ principle in a public funded project called FIRKAM.
The readout of the microbolometers based on the use of a 2^{nd} order ΣΔ modulator followed by a 3^{rd} order sinc-filter with a resolution of 16 bit. The 2^{nd} order sigma-delta modulator is realized using single-ended switched capacitor (SC)-technique (Fig. 6). For noise requirements the 1^{st} integrator is realized as a time-continuous type with two SC current sources. The current throw the resistor of the microbolometer is integrated using the feedback capacitor C_{int1} of the left OTA. The first current source subtracts the radiation independent part of the resistor current. This current source is realized by a switching network and the capacitor C_{offset}. The ΣΔ principle requires a feedback loop with the output signal with is realized by the 2^{nd} SC current source.

The 2^{nd} integrator is realized as a time-discrete type with a non-overlapping two phase clock. The output voltage of the 2^{nd} integrator is valid at the end of phase Phi1 and fed into a comparator. The output of the ΣΔM is digitally filtered using a 3^{rd} order sinc-filter. The output of the sinc-filter is a 16 bit digital value.

Over 10000 ΣΔ modulators and sinc-filters are integrated for a parallel readout of the microbolometers. A sequencer controls the readout circuits and multiplexes the digital output data. The state machine is programmable using an I²C bus. A build-in selftest supports the wafer test und reduces test time. The IRFPA is completed by a temperature sensor for calibration issues. The IRFPA is fabricated in a 0.35 µm CMOS technology with micromachining extension and occupies an area of approx. 326 mm² with 13.6 million transistors (Fig 7).

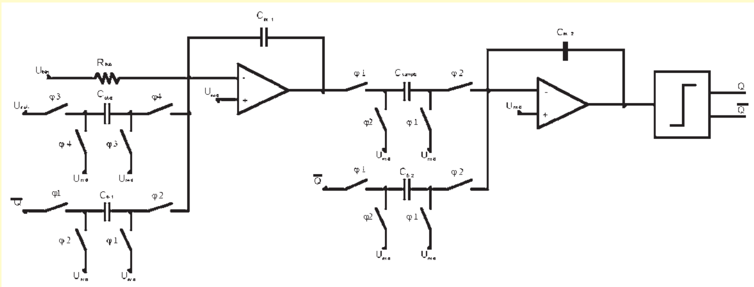

Figure 6: 2nd order ΣΔ-modulator

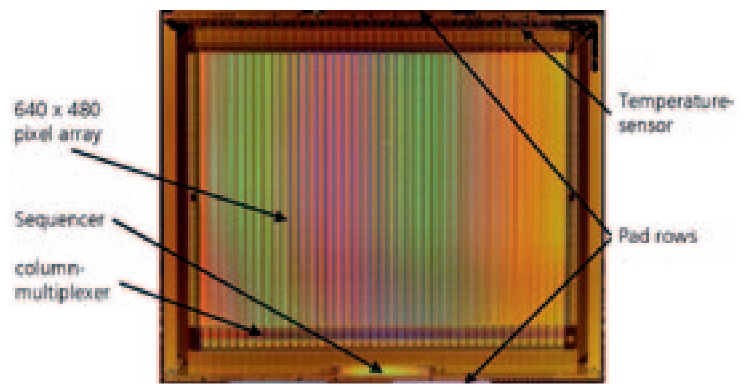

Figure 7: Chip photo VGA-IRFPA

Electro-optical results

The IRFPAs are electro-optical characterized using a black body radiation source. The local distribution of the responsivity shows Fig. 8. The responsivity is measured at an IRFPA temperature of T = 300 K is defined as the change of the digital values as the temperature of the black body is changed from 25 °C to 35 °C. The local distribution shows a homogeneous image. Fig. 9 depicts the histogram of the responsivity which shows a Gaussian distribution with a mean values of R_{mean} = 238 LSB/K and a standard deviation of R_{std} = 13 LSB/K. An IR image of a human hand illustrates Fig. 10 using a f/1.2 lens. Apart from a simple offset correction the shown image is uncompensated, i.e. no gain, defect pixel, or noise correction has been done. Further electro-optical characterizations are ongoing.

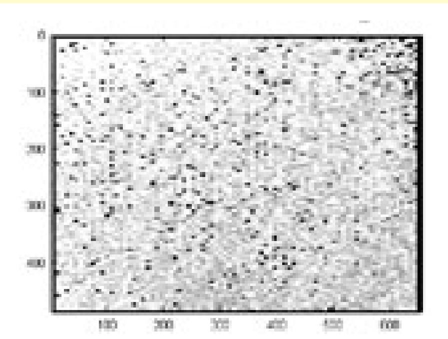

Figure 8: Responsivity (local distribution)

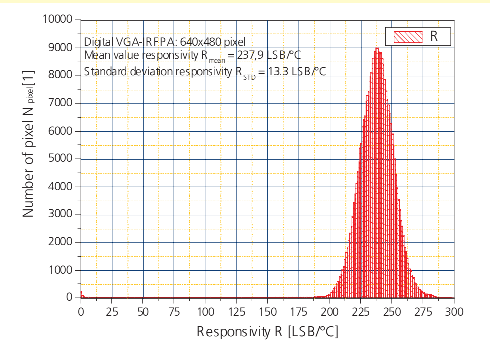

Figure 9: Responsivity (histogram)

Figure 10: Uncompensated IR image with f/1.2 optics

DIGITAL VGA-IRFPA FOR THERMAL IMAGING APPLICATIONS

Conclusion

A digital IRFPA with 640 x 480 pixel and a 16 bit output signal has been designed, fabricated and electro-optical tested. The microbolometers feature a pixel pitch of 25 µm and consists of amorphous silicon as the sensing layer. The digital read¬out of the microbolometer based on a massive parallel use of SD modulators followed by sinc-filters. To complete an IRFPA a vacuum package is necessary which is realized as a "chip scale package".

The IRFPA consists of an array

References

[1] M. Ruß, J. Bauer, and H. Vogt, "The geometric design of microbolometer elements for uncooled focal plane arrays", Proc. SPIE Conference Infrared Technology and Applications XXXIII, Volume 6542, 2007

[2] F. Niklaus, F. Forsberg, A. Fischer, N. Roxhed, G. Stemme, "Performance model for uncooled infrared bolometer arrays and performance predictions of bolometers operating at atmospheric pressure", Infrared Physics & Technology Volume 51, Issue 3, January 2008, Pages 168-177

[3] Hwang, C.H.; Kim, C.B.; Lee, Y.S.; Lee, H.C., "Pixelwise readout circuit with current mir¬roring injection for micro¬bolometer FPAs", Electronics Letters Volume 44, Issue 12, June 5 2008 Page(s):732 – 733

FEASIBILITY STUDY OF AN INTEGRATED PRESSURE SENSOR TRANSPONDER FOR TRIGGERING OF A PACEMAKER IN THE TREATMENT OF DYSPHAGIA

W. Betz, M. Görtz*, H. Feussner**, A. Schneider**, H. K. Trieu**

** Fraunhofer IMS, Duisburg, Germany; ** Research group MITI, Klinikum rechts der Isar der TUM, Munich, Germany*

Dysphagia is the difficulty in swallowing, often combined with pain. In a more serious form of dysphagia, people may be completely unable to swallow. Dysphagia has many reasons and could be caused by diseases of the nervous system, like cerebral palsy or Parkinson's disease. Additionally, stroke or head injuries may affect the coordination of the swallowing muscles or limit sensation in the mouth and throat. In Germany, several 10,000 people are suffering from dysphagia every year. Dysphagia is often related to other diseases and accelerates their progress as it precludes the patients from eating. Therefore many of them require artificial feeding.

One of the main problems of dysphagia is the initiation of the swallowing act, which is caused by weak throat muscles. Therefore we focused our research, in cooperation with the Research group MITI at the Klinikum r.d. Isar der TUM on this indication. The goal was to develop an implantable device to stimulate these muscles after a trigger signal by the specific tongue movement towards the hard palate, which is the start of the pharyngeal transport phase.

Figure 1: In silicone encapsulated telemetric pressure sensor fixed to an imprint of the hard palate that is placed on a model of the upper jaw.

During swallowing, each time one intents to swallow the tongue is moved against the hard palate to force the food towards the pharynx. Consequently, if it would be possible to derive advantage from the tongue's characteristic movement by detecting the contact of the tongue with the hard palate, one could trigger the muscles in the throat. This approach was investigated in the feasibility study shown here.

The sensor that was used to detect the contact of the tongue with the hard palate consists of a capacitive pressure sensor that was produced in our CMOS line, a coil with ferrite core, some discrete electronic components for signal transformation, a circuit board and a silicone encapsulation. The size of the senor is about 18 mm in diameter and 5 mm in height. The sensor's data and energy transfer is wireless and is effected by a magnetic field at a frequency of 133 kHz. The magnetic field is generated by a coil that is connected to a handheld reader that records the sensor's pressure values at a rate of 50 Hz. For experiments the sensor is fixed to an imprint of the proband's hard palate and the coil of the reader is held next to his cheek. Exemplary an imprint with pressure sensor placed on a model of the upper jaw is shown in Figure 1.

First measurements showed that the event of the tongue's pushing against the sensor in the imprint gives a strong, characteristic raise in pressure of about 400 mbar. This signal is clearly distinguishable from changes in pressure caused by speech or food during chewing.

To show the chronological dependence between swallowing and the sensor signal, high speed fluoroscopy was performed. The proband takes a mouthful of contrast agent, which makes his oral cavity appear very bright on the angiograph shown in Figure 2. Because of the load of the contrast agent and the position of the tongue the sensor's pressure reading is 219 mbar. Now the proband intends to swallow and presses

FEASIBILITY STUDY OF AN INTEGRATED PRESSURE SENSOR TRANSPONDER FOR TRIGGERING OF A PACEMAKER IN THE TREATMENT OF DYSPHAGIA

Figure 2: Angiograph of the proband's oral cavity and throat. The oral cavity is filled with contrast agent. This causes a pressure of 219 mbar to the sensor.

Figure 3: Angiograph of the proband's oral cavity and throat. The proband intends to swallow and the natural movement of the tongue towards the hard palate causes a high pressure of 545 mbar to the sensor.

Figure 4: Angiograph of the proband's oral cavity and throat. The proband is swallowing and the contrast agent enters the esophagus. The pressure decreases to 92 mbar while the oral cavity is emptied.

his tongue automatically against his hard palate and thus the contrast agent towards his pharynx. This causes a strong increase of the pressure to 545 mbar indicating that swallowing starts immediately (Figure 3). Right after swallowing, the contrast agent flows down the proband's throat, the oral cavity empties and the pressure reading decreases to 92 mbar (Figure 4).

These first investigations gave very promising results and show that the approach to trigger swallowing by the signal of a pressure sensor that is caused by the natural movement of the patient's tongue is feasible. Further research will now focus on miniaturization of the sensor and its integration with electrodes for muscle stimulation. This gives future prospects to improve the treatment of dysphagia and to allow patients to continue eating in a natural way.

CMOS BASED BIOSENSOR WITH INTEGRATED BIOMEMBRANE

S. Dierk, S. Ünlübayir*, T. van den Boom*, H. K. Trieu*, I. Köper***
** Fraunhofer IMS, Duisburg, Germany; ** 2: Flinders University, Adelaide, Australia*

Point-of-Care testing (POCT) has become more and more important in clinical diagnostics. It is an alternative to diagnoses in laboratories which are often time consuming and expensive. The samples have to be taken to a laboratory, the analysis must be performed by trained personnel and in most cases sample pre-treatment is needed.
In POCT on the other hand small and robust devices with an easy and fast handling provide the possibility to carry out the diagnoses close to the location of the patient, which is less costly and time-saving. Therapy can start immediately.
BioPROM is a biosensor being developed for POCT. As a CMOS-based sensor, it can be integrated into established silicon electronic devices and as no sample preparation is needed, handling will be very easy.

Biological recognition
For detection of analyte molecules, there is an electrode on the chip, which is covered by a tethered bilayer lipid membrane (tBLM). Bilayer lipid membranes (BLMs) consist of two layers of lipid molecules. They form a barrier for ions, proteins and other molecules.

For BioPROM the BLM is tethered via an anchor lipid (spacer) to the electrode of the microchip. It insulates the electrode from the surrounding analyte solution. The tethering improves the stability and the life-time of the BLM [2]. Additionally the fluidity of the membrane is kept; hence it is possible to incorporate proteins, e.g. ion channels. Therefore tBLMs are very interesting for biosensor use. Ion channels enable the transport of ions through BLMs. When an ion channel is ligand gated, ions can only pass, when the ion channel is activated by a specific analyte. Once an analyte molecule binds to a receptor of the ion channel, the channel is opened; ions reach the electrode and generate an electrical signal, which can be read out by the microchip. There is a great variety of application areas. One is the pharmaceutical industry. The influence of medicaments on ion channels can be observed directly. Another application is the detection of glutamate in food for people with glutamate allergy.

Simulation
To get an impression of the sensitivity and the ability of the sensor, a simulation of the readout circuit has been carried out with the simulation program Spectre. In order to simulate the output signal of the sensor, an equivalent circuit of the membrane and the sensor surface has to be considered. The simplest model for a tBLM on a gold surface consists of a resistor for the electrolyte R_E, an RC-element R_M C_M in series and a capacitor C_D for the electrical double layer of the substrate and the spacer-region (Fig 1).

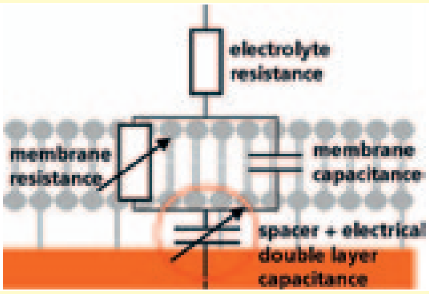

Figure 1: Equivalent circuit of the membrane and the sensor surface.

In case of ion channel opening R_M decreases and C_D increases. So there are two elements that can be used as read-out signals for the sensor. As R_M is in the giga-ohm-range, it is not suitable for CMOS technology. Noise would be too high. Instead the change of C_D is chosen as read-out-signal. Reference [2] reports changes from 3.5 μFcm^{-2} to 7.1 μFcm^{-2} for C_D for the pore forming segment of AChR M2[1]. This means 350pF to 710pF for a 0.01 mm^2 electrode.

[1] *M2 is the pore forming segment of the nicotinic acetylcholine receptor*

CMOS BASED BIOSENSOR WITH INTEGRATED BIOMEMBRANE

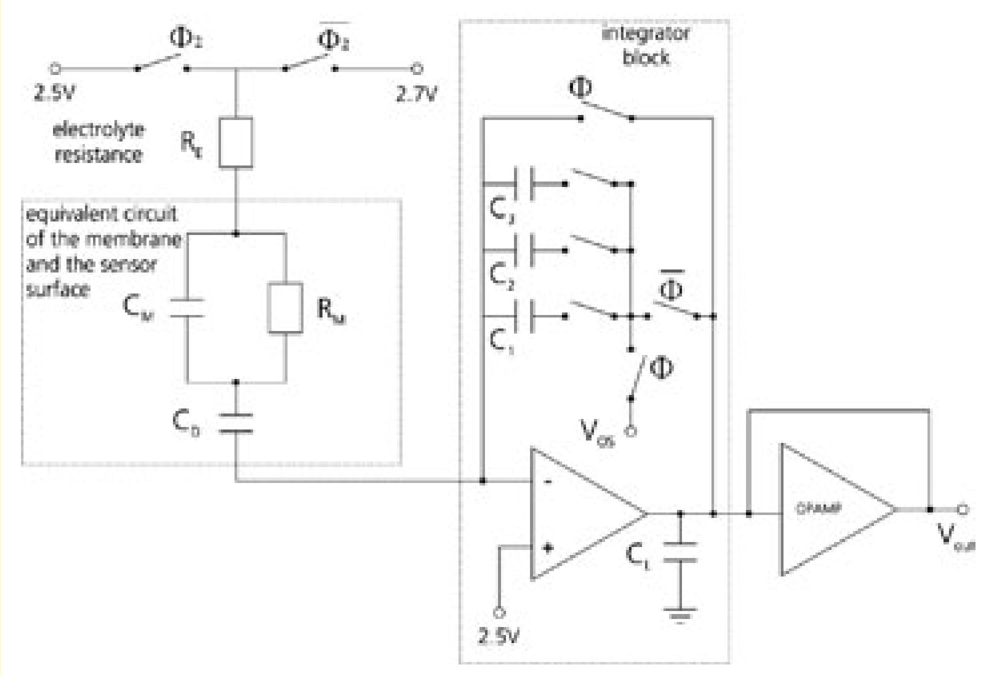

Figure 2: Schematic of the readout circuit: A programmable capacitor array assures an adjustment to the range of the spacer/electrical double layer capacitance C_D.

The readout circuit consists of an integrator (Fig. 2). A programmable capacitor array with three capacitors in the feedback loop assures an adjustment to the range of the spacer/electrical double layer capacitance C_D (Figure 2). The circuit also provides the possibility to apply an additional bias voltage to the capacitors in the feedback loop during the reset-phase Φ to shift the output voltage.
The output voltage can be calculated by

$$V_{out} = V_{OS} - \frac{C_S}{C_i} \cdot 0.2V, \ (1)$$

where $C_S = \dfrac{C_D \cdot C_M}{C_D + C_M}$,

and V_{OS} is the bias voltage of the capacitances C_i in the feedback loop.

In order to determine the parameters R_E, R_M, C_M and C_D, impedance spectra from a tBLM on a gold surface were taken in dependency of the concentration of an ion channel species (Fig. 2). From the fitted curves R_E, R_M, C_M and C_D were determined. To simplify the system α-hemolysin was used as ion channel instead of a ligand gated ion channel. α-hemolysin is permanent open. Therefore the existence of α-hemolysin in the membrane is equivalent to the open state of a ligand gated ion channel.

Figure 3 shows the resulting output voltage in dependency of the α-hemolysin concentration. The simulation confirms that the readout circuit is well suited to measure the sensor signals which are expected during a measurement.

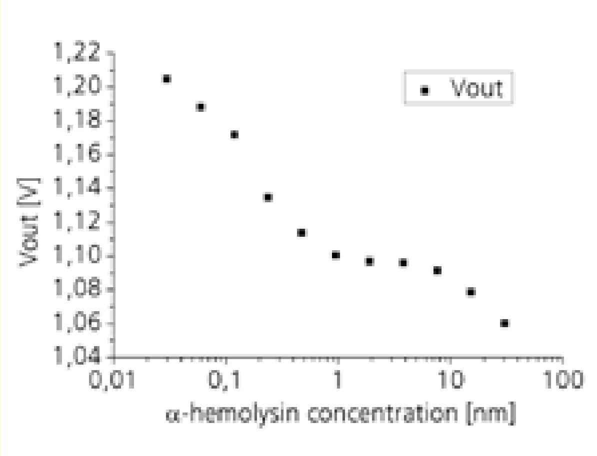

Figure 3: Simulated output voltage V_{out} in dependency of the α-hemolysin concentration.

evaporation. Then it is glued with a conductive silver Epoxy (EPO-TEK® H20E) to the electrode on the chip. Afterwards the silicon wafer can easily be removed, because of the low adhesion of the gold on the silicon wafer.

Small electrodes are preferable because the membrane resistance increases with decreasing electrode size.
They can be accomplished by structuring the surface with a gold electrode surrounded by SiO_2. Structuring of the gold electrode can be accomplished with lithography procedures or a shadow mask e.g. Then a polymer with silane end groups covalently bonds to the SiO_2 and insulates the membrane boundaries. Gold electrodes with a diameter of 0.1 mm are planed.

Fabrication of the sensor surface

For tBLMs a very flat surface is essential, as the tBLM forms a very thin film of only about 6 nm. The effect of a rough surface on a tBLM is illustrated in Figure 4. [3] Low roughness (0.5 nm) cannot be reached with techniques used in the production process of the microchip. To overcome this problem so called template stripped gold method is used [4] (Fig. 5).
A 70 nm gold film is deposited on a silicon wafer by thermal

Membrane assembly

Membrane assembly consists of two parts:
At first a lipid monolayer with anchor lipids is covalently bonded to the gold sensor surface by self-assembling (SAM)[2]. Then the outer leaflet is deposited by vesicle fusion to complete the bilayer. [5] Vesicles are small bubbles of liquid surrounded by a lipid membrane. Once a vesicle contacts the SAM it adsorbs, bursts and then spread all over the monolayer (Fig. 6). The bilayer formation can be monitored by electrochemical impedance spectroscopy (EIS).

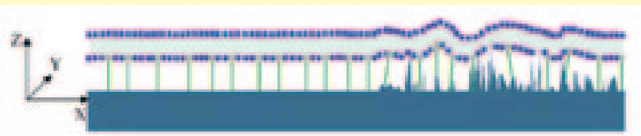

Figure 4: Schematic representation of the effect of surface roughness on tBLMs. [3]

Figure 5: Fabrication process for template stripped gold.

2 *In case of a gold surface thiol end groups are used as anchor molecules.*

CMOS BASED BIOSENSOR WITH INTEGRATED BIOMEMBRANE

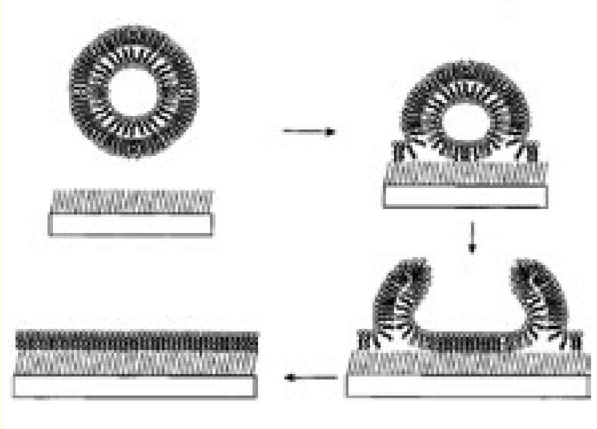

Figure 6: Vesicle fusion [5]

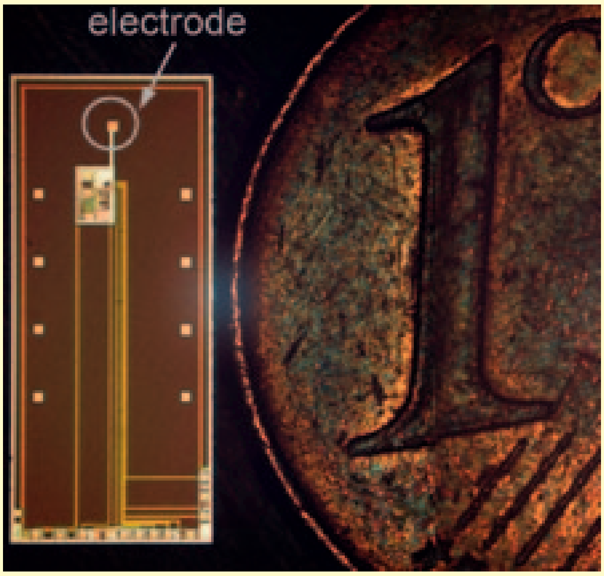

Figure 7: BioPROM- microchip with readout circuit and sensor electrode.

Sensor chip test

To test the sensor chip (Fig. 7), the equivalent circuit of the membrane and the sensor surface has been assembled with concrete devices. To simplify the measurement the electrolyte resistance was neglected just as the membrane resistance. The capacitances C_D and C_M were united to one capacitance. This capacitance was imitated by a trimmer capacitor. The control signals were produced by a pattern generator. The output signal was observed on an oscilloscope. Figure 8 shows the output voltage in dependency of the capacitance. The measured signal is compared with the calculated simulated output voltage Vout.

Results

Electrochemical impedance spectroscopy was performed to determine the change of the capacitance of the electrical double layer and the spacer-region C_D of a tBLM. The parameters were extracted by fitting the curves and used to simulate the behaviour of the readout circuit. The Simulation confirms that the sensor is well suited to measure the expected changes in the signal. The microchip was tested with a trimmer capacitor to imitate C_D. As the simulated and the measured output voltages fit well, the functionality of the microchip has been successfully verified. Thus the chip is very promising to measure the change in ion channel concentrations.

Next step will be to measure the influence of the change in the electrical double layer of the substrate and the spacer-region of a tBLM on the output voltage and the change due to ion channel incorporation.

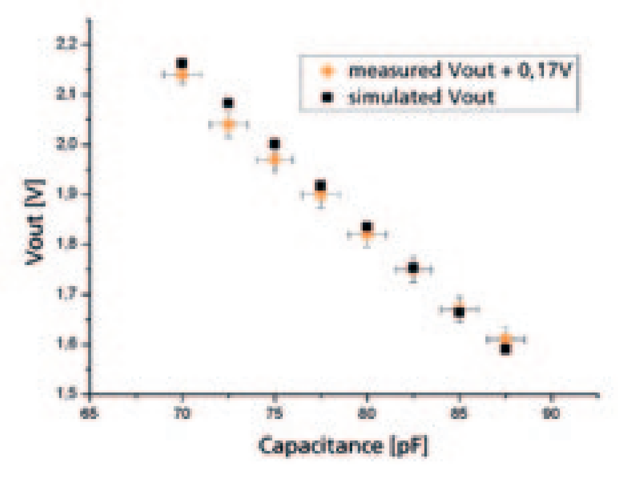

Figure 8: : Sensor chip test: Apart from an offset of 0,17V the measured and simulated sensor signals fit well.

References

[1] Ingo Köper, “Insulating tethered bilayer lipid membranes to study membrane proteins”, Mol. BioSyst., 3, 651–657, 2007.

[2] Inga K. Vockenroth et al., “Functional incorporation of the pore forming segment of AChR M2 into tethered bilayer lipid membranes”, Biochimica et Biophysica Acta, 1768, 1114–1120, 2007.

[3] Mathieu Jung, „Patterning of tethered Bilayer lipid membranes”, Dissertation MIPI Mainz, 2008.

[4] R. Naumann et al., “Tethered Lipid Bilayers on Ultraflat Gold Surfaces”, Langmuir, 19, 5435, 2003.

[5] Steffen Lingler, Israel Rubinstein, Wolfgang Knoll and Andreas Offenhäusser, “Fusion of Small Unilamellar Lipid Vesicles to Alkanethiol and Thiolipid Self-Assembled Monolayers on Gold”, Langmuir, 13, 7085-7091, 199.

CUSTOMIZED MEMS PROCESS DEVELOPMENT: A PRESSURE SENSOR FOR HIGH TEMPERATURE AND HIGH PRESSURE APPLICATIONS

A. Goehlich, H. Vogt*, K. Debusmann*, H. K. Trieu*, J. v. Berg***

** Fraunhofer IMS, Duisburg, Germany; ** Kistler Instrumente AG, Winterthur, Switzerland*

1. Abstract

This work describes a novel technology development of a stand alone pressure sensor for an industrial customer (Kistler Instrumente AG). The sensor element is intended for the measurement of high pressures (up to 5000 bar) in a high temperature environment (up to 350° C). A deep trench technology in connection with bonded SOI (silicon on insulator) wafers is applied for the production of the sensor chips.

2. Introduction

The measurement of high pressures in high temperature environments is of importance in many industrial applications. An example of such an application in the plastic fabricating industry is the measurement of the pressure in the nozzle of a plastic injection moulding installation. Another example of an automotive application is the pressure measurement in fuel injection nozzles of diesel engines [1].

A piezoresistive sensor chip for this type of application is developed in a customized MEMS process. The sensor element is realized as a resistive Wheatstone bridge circuit made of four discrete doped silicon resistors. Due to the high temperature requirement a SOI-technology with dielectric isolation in contrast to isolation by pn-junctions has been chosen. The bulk silicon substrate itself serves as a flexible "mechanical plate", which deforms under pressure loading. The mechanical deformation (strain) in turn generates a surface near stress field, that leads to a measurable resistance change in the resistors [2]. A tungsten metalization has been applied for extended lifetime at high temperatures. A planar surface minimizes the occurrence of metallic residues after the metal etch. These residues could lead to electrical short circuits. These aforementioned requirements have to be taken into account for the development of a technology compatible to the existing 8 inch CMOS production line.

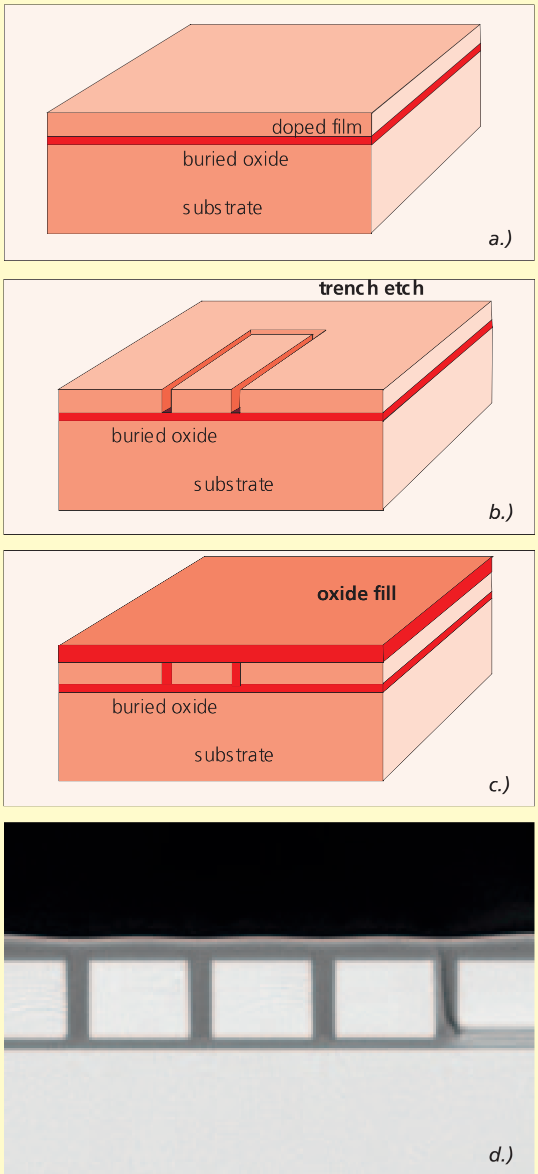

Figure 1: Realization of embedded silicon resistors:
a.) thick film SOI substrate
b.) trench etch with stop on silicon
c.) oxide filling
d.) SEM micrograph of the oxide filled trenches after the reflow process. The void free filling of the trenches is obvious

3. Technology Development

The novel pressure sensor element is based on a bonded thick film SOI substrates. The thick film SOI substrates have been generated from a standard thin film SOI-substrate by epitactical growth of a thick silicon film. The required square resistance of the resistors is adjusted by doping through an ion implantation and a diffusion step.

The doped silicon resistors are isolated from the surrounding silicon film by narrow trenches. The trenches are etched down to the buried oxide with the aid of a plasma deep trench etch process, which was adopted from existing trench etch modules. The trenches were filled with a SACVD (subatmospheric chemical vapour deposition) oxide and were subsequently smoothened with the aid of a reflow technique. The SACVD- oxide layer also serves as the interlevel dielectric. This process sequence results in a very smooth surface. In this way problems with metallic residues are avoided. The trench etch and oxide filling process is shown schematically in figures 1 a-c together with an SEM micrograph of trenches filled with this technique .

As shown in figure 1d crystalline silicon structures are generated, which are fully encapsulated in oxide. The trench filling step is followed by the patterning of the contact holes and the contact ion implantation. This implantation is activated by a rapid thermal annealing step. Subsequently the tungsten metal is deposited and patterned. The whole process sequence is completed with the deposition of the passivation layers and the opening of the bonding pads. The process flow involves 4 lithographic layers. The flow is depicted in Figure 2 in a simplified form.

Implantation and diffusion

trench patterning deep trench etch

trench filling (oxide) and smoothening by reflow

patterning an etch contact holes

contact implantation and anneal

metal deposition and metal patterning

deposition of passivation and pad opening

Figure 2: simplified process flow for the production of SOI-pressure sensor chips In the IMS 8-inch line

4. Results

A test lot was runned in order to explore the novel process set-up and in order to adjust the required resistance to the desired value. The novel process set-up worked without problems. The resistance was tuned by the variation of the implantation dose. In figure 3 the measured resistance versus dose dependence is depicted and compared to simulation results. The experimental results are – as expected – close to the simulation results for the trench etch process.

CUSTOMIZED MEMS PROCESS DEVELOPMENT: A PRESSURE SENSOR FOR HIGH TEMPERATURE AND HIGH PRESSURE APPLICATIONS

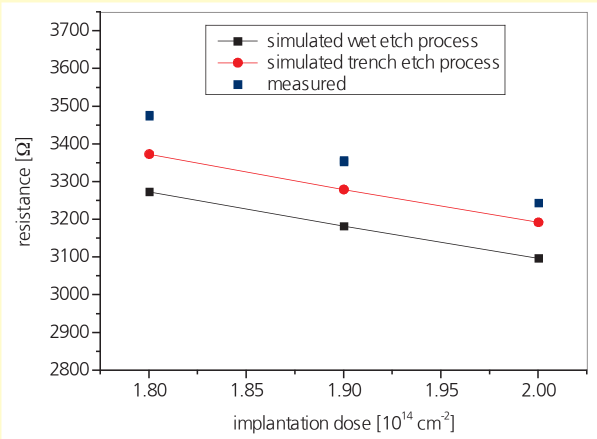

Figure 3: dose dependence of the resistance

The test lot was electrically tested on wafer level after the completion of the test run with yields exceeding 95%.
The dielectric isolation allows a voltage stress more than100 V. The thermal and mechanical behaviour of the sensor elements were characterized at the Kistler Instrumente AG. In order to perform these characterizations the wafers were gold bumped and diced. Subsequently the chips were assembled in a high pressure sensor housing equipped with a rugged steel diaphragm. The whole pressure sensor assembly is shown figure 4.

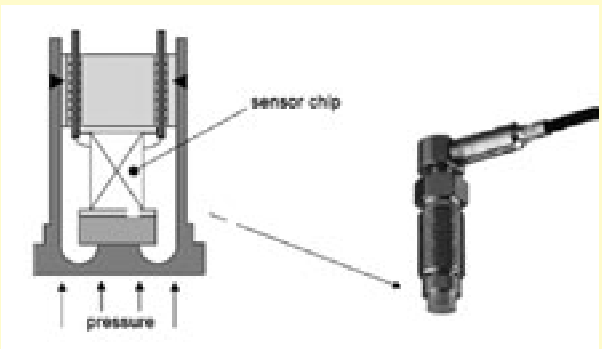

Figure 4: pressure sensor assembly (from reference [1])

The mechanical and thermal results of the novel sensor were found to be very close to the performance as expected for this design. The typical dependence of the bridge resistance and the sensitivity on temperature is depicted in figure 5.

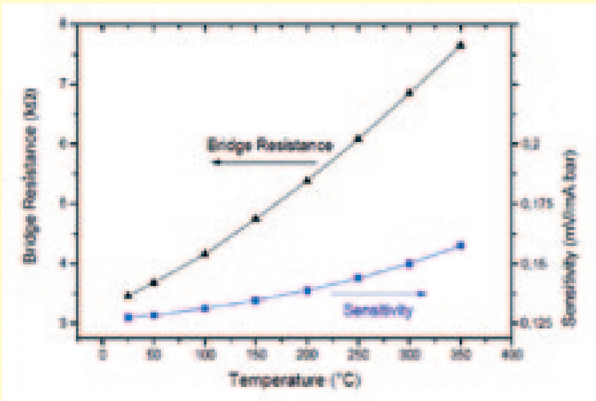

Figure 5: typical temperature behaviour of the bridge resistance and of the sensitivity (taken from reference [1]).

5. Conclusions

A novel process set-up for the production of a piezoresistive high temperature pressure sensor chip has been developed and successfully tested. A high degree of process simplification has been achieved. The realized sensing elements exhibits mechanical and thermal parameters as expected for the design.

References:

[1] J. von Berg, C. Sonderegger, S.Bollhalder and C.Cavalloni, "Piezoresistive SOI-Pressure Sensor for High Pressure and high Temperature Applications", Sensor 2005, Vol. 1, pp.33-38 .

[2] A.A. Barlian et al., "Review Semiconductor Piezoresistance for Microsystems",
Proceedings of the IEEE, Vol. 97, No.3 (2009)

HIGH TEMPERATURE IMAGE SENSOR

C. Nitta

The following sections describe a CMOS image sensor, which was developed at the IMS Duisburg in the course of a research and development project. It is fabricated at the institute's own 0.5 µm CMOS technology line for the exclusive use by an industrial partner. The main feature of this device is that it can be operated at temperatures ranging from -40°C up to +115°C all in compliance with the specified electro optical requirements. A further noteworthy aspect of the device is the large physical dimension of the active pixel matrix of 2.5 cm x 2.5 cm. This size prevents the use of conventional exposure techniques during fabrication. Hence, only a subdivision of the whole chip into individual tiles and a stepwise exposure of these chip sections allows a mapping of the device on the silicon wafers.
Concerning its readout modalities, the imager can be operated with a synchronous and an asynchronous shutter. It furthermore features an on-chip binning mode, which combines four neighbouring pixel into a single one.

Sensor principle
Figure 1 shows a schematic diagram of the pixel cell. As illustrated, the general design of the pixel cell is based on a four-transistor circuit with an internal storage element. This core setup was extended by an antiblooming and a binning transistor and therefore it can be used in a *rolling frame shutter mode* as well as a *synchronous frame shutter mode,* both with and without pixel binning. When operating in the binning mode, every two neighbouring photo diodes of each column are connected. Like this the full field of view is retained even though the total number of read out picture elements is halved. In applications, which rely on image processing but which can also tolerate lower image resolutions, this method can be advantageous as the hardware requirements for the image processing unit can be relaxed.

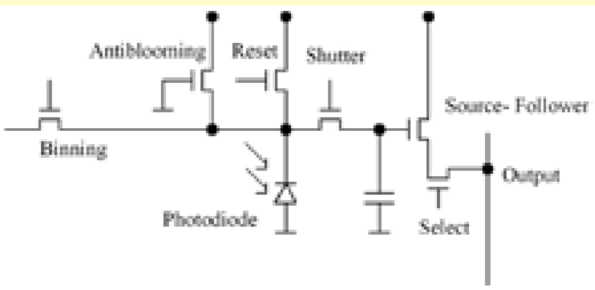

Figure 1: Schematic drawing of the pixel cell

The photo diodes used in the device are optimized buried photo diodes, which feature a very low dark current. With this optimization the imager is able to achieve operating temperatures significantly above 85°C.

The pixel operation is handled in the following way: initially the parasitic capacitance of the photo diode and the storage capacitor are charged via the reset transistor during a reset phase. After this reset phase the charge on the storage capacitor is decreased by means of the illumination-dependent photo current of the photo diode. This in turn generates a voltage drop across the storage capacitor, which is proportional to the illumination and to the duration of the discharge, i.e. the integration time. This integration interval is set by the shutter transistor. Finally, the voltage at the storage capacitor is read out through the pixel source follower and the select transistor, which serves to select an individual pixel address.

Sensor Layout
The sensor layout is determined by the sizes of the photo diode and the storage capacitor. In order to guarantee a direction-independent spatial sampling of the imaged scene, the pixels feature a quadratic photosensitive area (see Figure 2). In the design phase, the dimension of the storage capacitor was chosen such that it takes into account the device's wide temperature range, which is in-turn reflected in the elevated requirements concerning the electro optical

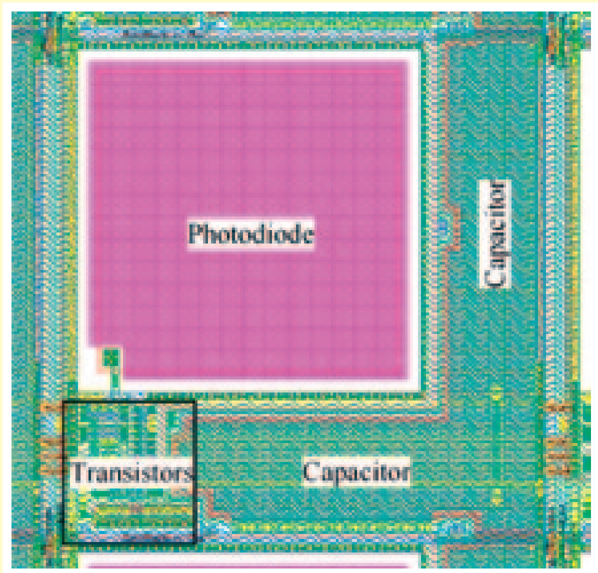

Figure 2: Layout of the pixel cell

properties of the pixels. Considering the routing of the control and supply lines, a number of optimization rules have been applied. For instance, all control lines of the pixel matrix are routed horizontally placing the control blocks to the side of the matrix. In order to guarantee an optimal voltage supply configuration all supply lines run vertically. Thereby during readout the supply of each pixel of a selected row is decoupled from its neighbors. In addition, the output lines are also running vertically in order to decouple the readout signals from the control lines. Finally, the storage capacitor and the pixel electronics are all covered by metal layers such that these parts of the pixel cell are rendered light-insensitive. If this were not the case, these elements could introduce additional illumination-dependent noise contributions. Apart from the regular, i.e. light sensitive, pixels the imager contains reference pixels, which are fully covered by a metal layer and are thus insensitive to illumination. These pixels can be used to run correction algorithms on the pixel matrix.

Readout circuit

The pixel matrix is read out in a row-wise fashion through column parallel *double delta sampling* (DDS) circuits (see Figure 3). In this particular approach, the conventional DDS design was enhanced by an additional binning option, which allows the accumulated readout of two adjacent pixels from neighboring columns. Thus, together with the binning option implemented in each pixel cell, a combination of four neighboring pixels into one large picture element becomes possible. As has been mentioned in the introduction, this option reduces the image resolution but at the same time still guarantees a full coverage of the field of view.

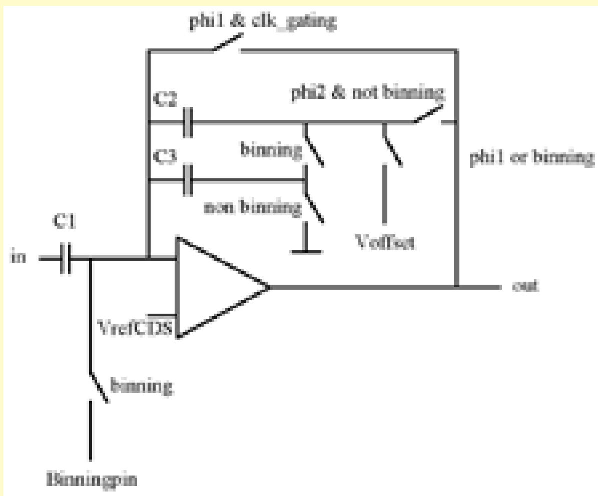

Figure 3: DDS readout circuit with binning option

Figure 4 shows a schematic view of the complete readout path. As indicated, the pixel values that are processed by the DDS circuit are subsequently sampled and stored by a *sample und hold* (S&H) element. From there the analog pixel data are transferred to off-chip circuits via a multiplexer stage and an output buffer. In terms of an increased readout speed, the imager profits from the simultaneous operation of the DDS circuit and the S&H stage. In detail this means that while one

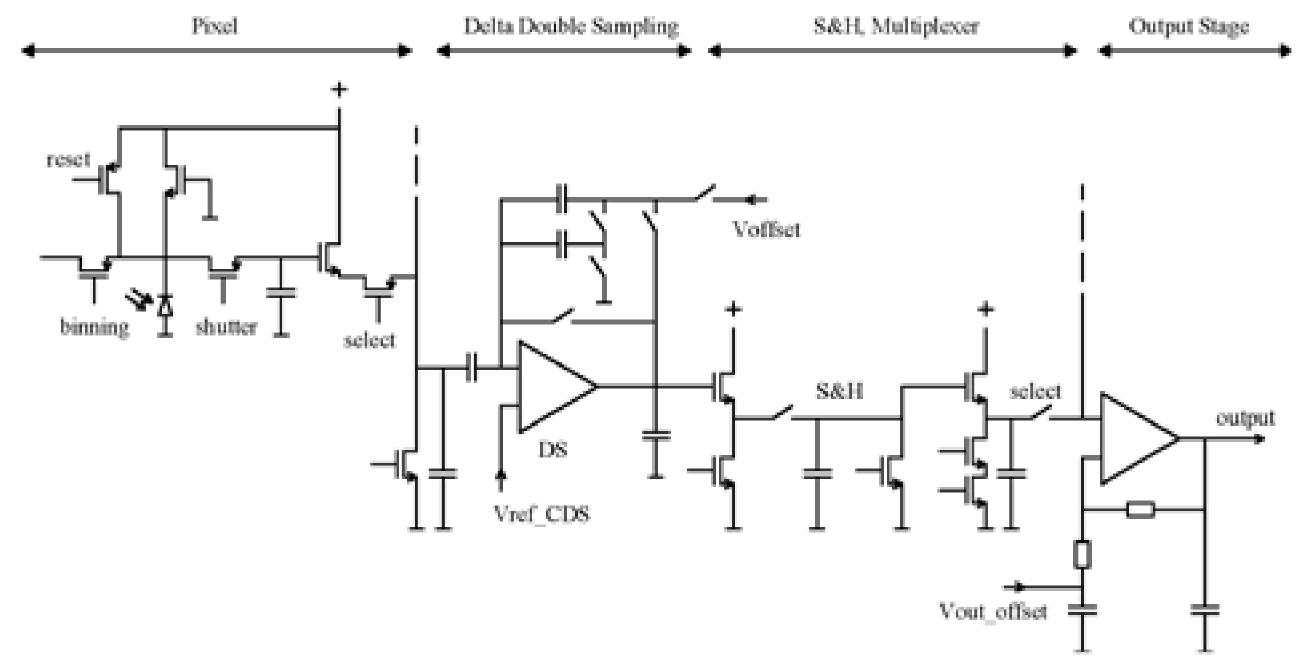

Figure 4: Readout path

row is being read out from the S&H elements, the next row is already being transferred into the DDS circuit.

Sensor architecture

The sensor consists of an active pixel matrix, which is located at the center of the device (see Figure 5). Below the matrix there are two rows of reference pixels, both fully covered with metal. The digital control of the imager can be found on the left side of the device. It consists of the control elements for the active pixels of the matrix as well as the reference cells. Also located on the left side are the control elements for the DDS stages, the S&H blocks, the multiplexer and the shift register. The aforementioned four building blocks are all situated at the bottom of the pixel matrix. All reference voltage sources and the output buffers are placed on the right side of the sensor. Furthermore, all circuits apart from the active pixel matrix were fully covered with metal so as to eliminate any unwanted light sensitivity of these elements.

The pixel area is read out from bottom left to top right. Systems with a simple objective therefore obtain the image data from top right to bottom left when viewed from the observer's perspective.

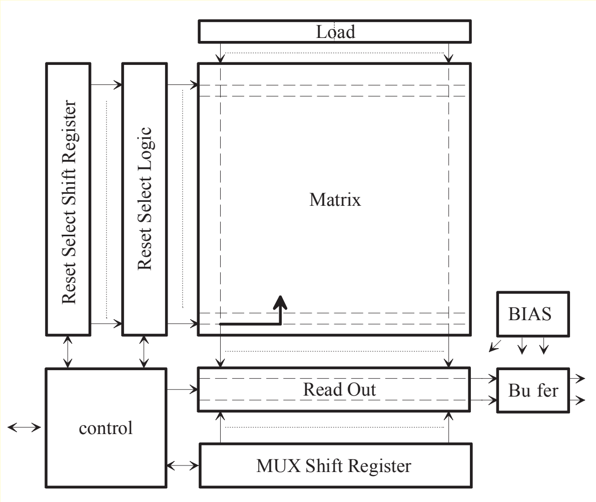

Figure 5: Sensor architecture

Stitching

Due to its large size, the image sensor can not be placed onto a single mask reticle. Hence, it is not suited for a conventional exposure of the wafer surface during fabrication. So, to produce the device with the standard equipment available in a CMOS line irrespective of the chip size, the layout was divided into 12 subsections. These sections were chosen such that some could be used repeatedly in the imager and therefore only seven different reticles had to be fabricated. Thus, by stitching the seven elements the full image sensor could be realized. The final production mask for the stitching is shown in Figure 6.

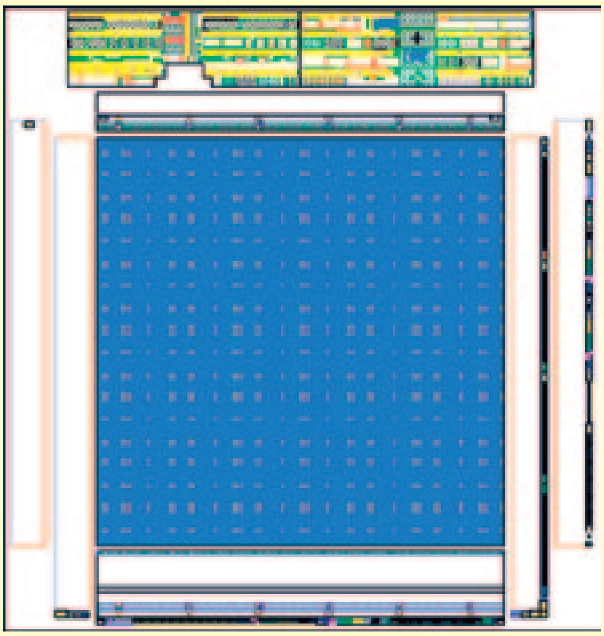

Figure 6: Production mask for stitching

Fabrication, test, assembly and shipping

The image sensor is fabricated on 8'' wafers in the IMS own 0.5 µm CMOS technology. In this technology the circuits can be operated at 3.3 V supply voltage. As the wafers are diced by the customer, the IMS performs extensive tests of the electro optical properties at wafer-level. In order to allow machine-controlled processing of the sensors, which were qualified as "good" during the wafer tests, all tested wafers are shipped with electronic wafer maps. Furthermore, the customer receives a summary of the test results for each one of the "good" imagers. Finally, each production lot also includes a *Certificate of Conformity.*

The following figure (Figure 7) shows an assembled image sensor with and without fiber glass plate.

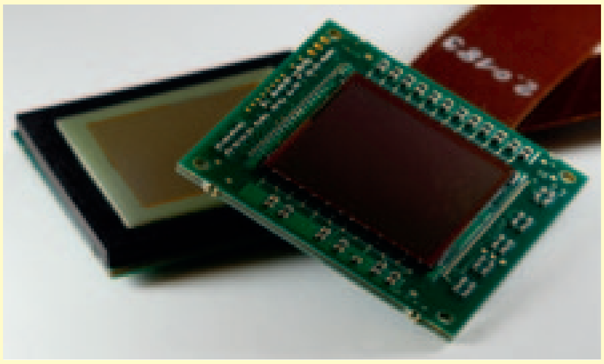

Figure 7: Assembled image sensors with and without fibre glass plate

NEW CMOS PIXEL STRUCTURES FOR TIME-OF-FLIGHT IMAGING

A. Spickermann, D. Durini

I Introduction

Nowadays, three different techniques for optical contactless distance measurements have become well established in a variety of applications: those based on interferometry, those based on optical triangulation, and finally those using the emitted beam time-of-flight (ToF) principle. Optical three-dimensional (3D) image sensors can be found in safety and security applications or the automotive industry, and have a huge potential to make it some day into video game consoles, weather forecast and research activities, or to be used in fully automated industrial processes. Low cost 3D image sensors based on standard CMOS technology could generate a huge market for these applications and many others.

The CMOS Imaging group at the Fraunhofer IMS is highly involved in the development of innovative ToF pixel structures to be fabricated, for example, in its 0.35 µm CMOS process. This work is focused on issues concerning the ToF pixel structures based on charge coupling between separated photoactive and readout node regions, e.g. the photogate (PG) active pixel, the pinned photodiode (PPD) active pixel or the novel lateral drift field photodetector (LDPD) structure, all aiming to enhance the signal-to-noise ratio (SNR) of the sensors, increase the response speed of the detector and improve its dynamic range. In order to do so, all these pixel configurations must be well designed to reach the high performance requirements of the ToF application. The complete charge transfer from the photoactive into the readout node region in a very short time, and the low-noise readout of this charge, are some of the essential challenges to be solved.

II Time-of-Flight Distance Measurements

The ToF distance measurement technique provides the possibility to measure distances between any object situated within a certain distance in a 3D scene and the sensor system developed for such a purpose. To achieve this, the sensor system emits a widened light beam with the irradiance E_{laser} in direction of the 3D scenery, and a photodetector array forming part of the same system receives the radiation ($E_{laser,r}$) reflected from all the existing objects found on its path added to the ambient light (E_{amb}) existent in the scene itself. The distance information d can be extracted from the time delay T_d elapsed between the emission of the light beam and the return of the beam reflected from any object to the photodetector after the light has travelled the distance of 2_d (see Fig. 1). The object distance to the photodetector array can be obtained as shown in (1), where c = 3 x 10^8 m/s represents the velocity of light.

$$d = \frac{c}{2} T_d \quad (1)$$

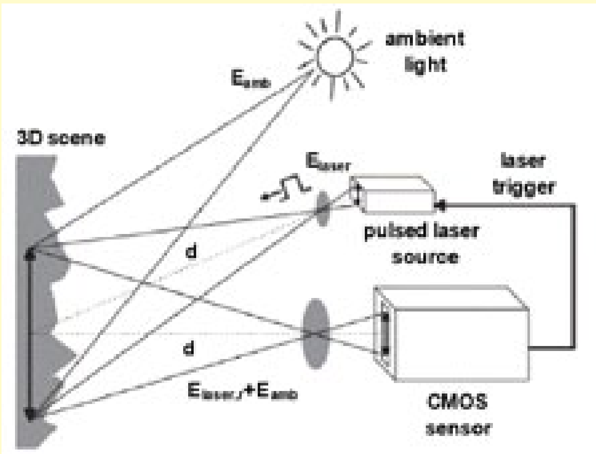

Figure 1: Principle of ToF distance measurements

Depending on the modulation of the emitted light beam, the ToF measurement systems can be divided into two basic groups: (a) those using radiation sources emitting continuous-wave beams [1], and (b) those using radiation sources emitting pulse-modulated beams [2]. In this work, a pulsed NIR (near infrared) laser diode emitting radiation with 905 nm wavelength is used with pulse widths ranging from 30 ns up to 60 ns. The maximum measureable distance d_{max} is limited by the width (T_{pulse}) of the laser pulse and can be defined as shown in (2).

$$d_{max} = \frac{c}{2} T_{pulse} \quad (2)$$

NEW CMOS PIXEL STRUCTURES FOR TIME-OF-FLIGHT IMAGING

III Photogate-based ToF Pixel structure

In the previous works published by the Fraunhofer IMS CMOS Imager group, different pixel configurations had been used together with pulse emitting radiation sources for ToF applications, mainly based on standard pn-photodiodes used as photodetectors. These approaches resulted in the need of using large pixel pitches in order to achieve high SNR. Other researchers used for ToF-sensors either hybrid CCD/CMOS technologies [1] or modified CMOS processes [3]. In contrast to this, our approach presented here uses a 0.35 µm CMOS process that requires no additional modifications and still yields very good results. Fig. 2 shows the cross sectional and top views, respectively, of the proposed ToF pixel structure.

In Fig. 2, the photoactive area (photogate, *PG)* is defined by an *n*-type MOS-capacitor *(MOS-C)* consisting of a polysilicon layer (poly 1) deposited on a thin silicon gate-oxide grown on top of a *p*-well diffused in a *p*-type epitaxial layer. For transfer of photo-generated charge carriers collected beneath the PG, a second *n*-type MOS-C, consisting of an overlapping second polysilicon layer (poly 2) deposited on top of an oxide-nitride-oxide *(ONO)* isolation stack is used. The four poly 2 MOS-C's form four transfer gates *(TX),* which overlap the four edges of the square PG and enable charge transfer between the PG and the n^+ diffusion areas (floating diffusions, *FD).* Each FD is connected to a reset transistor and an in-pixel buffer stage in source-follower *(SF)* configuration. Each of the four pixel outputs can be addressed using additional row-select transistors.

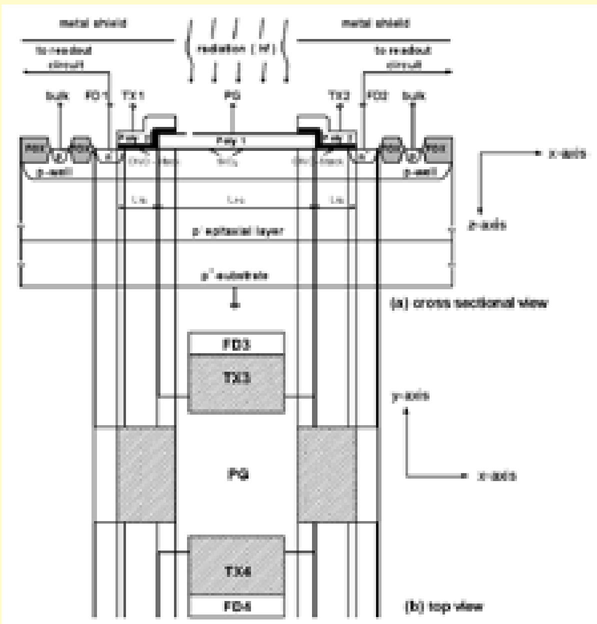

Figure 2: Cross sectional (a) and top view (b) of the proposed PG based ToF pixel structure.

Exemplarily, in Fig. 3 sketches of the PG pixel during charge collection and during charge transfer from the PG into FD1 can be observed. For the successful charge collection and transfer, the electrostatic potentials inside the silicon should obey the relation expressed by (3), namely

$$\phi^{+}_{TX} > \phi^{+}_{PG} > \phi^{-}_{PG} > \phi^{-}_{TX}\,, \quad (3)$$

where ϕ represents the electrostatic potential for each region. During charge collection, a space charge region *(SCR)* under the PG is generated by pulsing the PG to V_{PG+}, while the TX electrodes are set to a much lower potential V_{TX-} and the FD nodes are charged to V_{REF}. After charge collection is finished, the transfer of photogenerated charge starts with the setting of the TX electrode to a higher potential V_{TX+} and decreasing the PG voltage to a lower potential V_{PG-}. By this means a potential profile shown in Fig. 3 is created, and the photogenerated charge carriers are transferred to the selected FD. This causes a discharge of the FD node, the potential of which results proportional to the amount of photogenerated charge transferred into it.

To perform ToF measurements, FD1 and FD2 are used to collect the charge carriers generated by the reflected laser pulse impinging into the PG photoactive area. As it can be observed in Fig. 4, the first shutter activation *($T_{TX1} = T_{pulse}$)* begins synchronously with the emission of the laser pulse, followed by the second shutter activation *($T_{TX1} = T_{pulse}$)* starting directly at the end of the TX1 pulse. If the time delay T_D

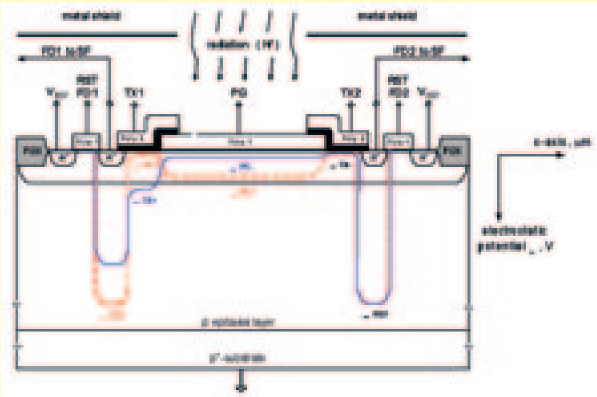

Figure 3: Schematic representation of the surface-channel photogate pixel and the electrostatic potential profile in Silicon during charge collection, and charge transfer to FD1, respectively.

between the laser emission and the impinging light of the reflected laser pulse on the photodetector is equal to zero, the whole laser pulse is included in the first shutter (TX1) window. Otherwise, the laser contribution is splitted into two parts and the amount of charge transferred to FD1 and FD2 includes the information about the time delay. After the end of the TX2 pulse, a short cycle of charge draining follows (TX4 is ON) to clear the SCR under the PG by using FD4 connected to the reset voltage (see Fig. 2). Afterwards, an additional measurement is performed using FD3 and TX3, during an integration time *($T_{TX3} = T_{pulse}$)* identical to the one used in the previous cycle, only without the reflected laser pulse radiation impinging on the photoactive area of the pixel. This additional measurement is used to determine the amount of charge generated by the ambient light alone. During all other operation times, TX4 remains ON to drain the unwanted charge carriers from the PG area.

After one laser pulse acquisition cycle, the amount of transferred charge to FD1 and to FD3 can be used to calculate the distance as shown in (4), assuming the capacitances of the readout nodes FD1 to FD3 to be equal.

$$d = \frac{c}{2} \frac{V_{FD2} - V_{FD3}}{V_{FD1} + V_{FD2} - 2V_{FD3}} T_{pulse} \quad (4)$$

The complete pixel readout circuit is also shown in Fig. 4 including the ToF pixel structure with the four FD's, the reset transistors and source followers and also the correlated double sampling *(CDS)* stage that allows the readout of the output voltages from the ToF pixel and the elimination of the low-frequency correlated noise embedded in them.

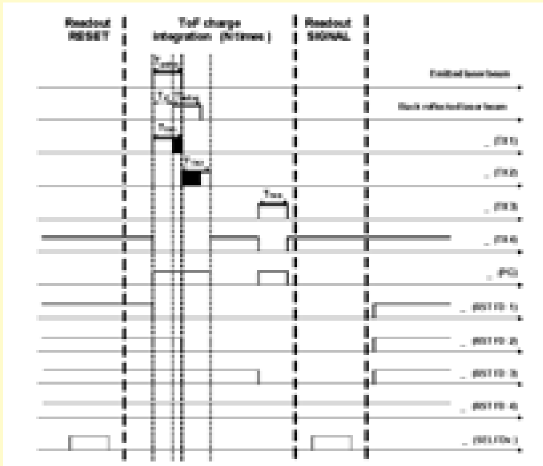

a.)

Figure 4: PG based ToF pixel timing diagram for readout (a) and dedicated circuit including a CDS-stage (b)

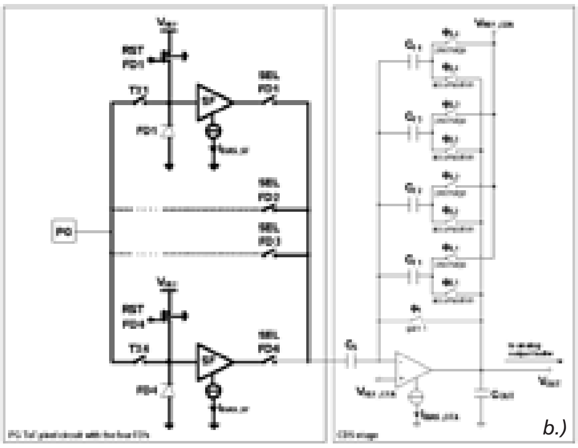

b.)

NEW CMOS PIXEL STRUCTURES FOR TIME-OF-FLIGHT IMAGING

The proposed PG-based ToF pixel structure has been realised as a 4 x 16 sensor array with several layout variations, as shown in Fig. 5.

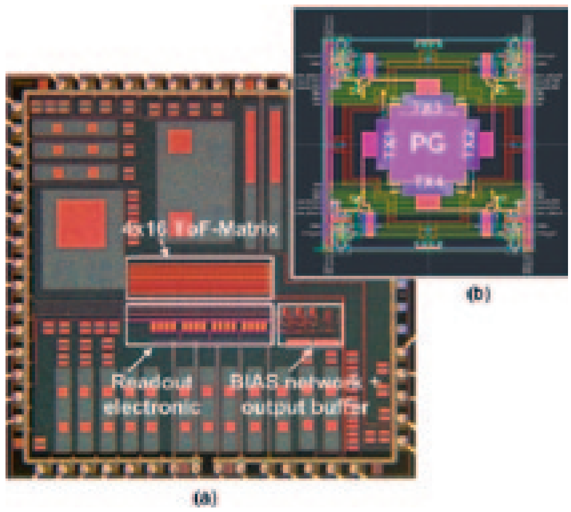

Figure 5: Chip photomicrograph of the fabricated PG-based ToF chip (a) and layout of the pixel structures (b)

For the characterisation and distance measurements, an NIR (near infrared) laser pulse source with an emitting wavelength of 905 nm and an effective laser pulse width of 60 ns has been used and acceptable distance measurements were achieved. According to these measurements, Table 1 summarizes the geometries and the measured data of our fabricated ToF image sensor.

The transfer speed and variations of the transfer time have also been investigated for several laser pulse widths *(T_{pulse})* and variations of the transfer time *(T_{TX})* applied together with the PG pixel configuration described. As expected, the transfer times of several ns are too short to transfer the complete amount of photogenerated charge carriers collected under the PG to any FD due to the absence of strong electrical drift fields in the transfer path.

Parameter	Data
Technology	0.35 µm standard CMOS process with 2 poly and 4 metal layers
Power Supply	3.3 V
Photoactive Area	30 x 30 µm²
Laser source	pulsed (T_{pulse}=30ns up to 60ns), infrared (λ = 905 nm)
Dynamic Range	56 dB (4 laser pulses)
Responsivity of one FD (@T_{pulse}=30ns, T_{TX}=60ns)	224 µV/(W/m²)
Noise Equivalent Power (@T_{pulse}=30ns, T_{TX}=60ns)	4.46 W/m²

Table 1: Sensor Data of the PG-based ToF chip [4]

A special type of "buried" photodetectors is used in the well-known *pinned* photodiode (PPD) [5] active pixel configuration. It solves the problem of the fast surface states present in surface channel PG pixels, as it uses a "shallow" *n*-well fabricated on the *p*-type epitaxial layer as a *p-n* junction based photodetector, sandwiched between the epitaxial substrate and an additional grounded p^+ implantation on its surface. The p^+ layer "pushes" the electrostatic potential maximum away from the silicon surface (voltage pinning), thus avoiding all the already discussed effects of the surface fast states. It also reduces the recombination rate of the minority carriers at the surface, as they are almost immediately drifted into the electrostatic potential maximum generated below, which boosts the optical sensitivity in the soft UV and blue parts of the spectra. The rest of the pixel configuration is identical to the one described for the PG pixel, as far as the TX, the FD, the SF buffer stage, and the CDS readout are concerned.

Both configurations exhibit image-lag [6] and charge transfer speed problems. On the one side, this is due to the lateral flat potential profile in the photoactive area, where the collected charge is being transferred to the FD only by diffusion mechanisms, on the other side – in the case of PPDs – it is caused by the high resistance of the fully depleted *n*-region.

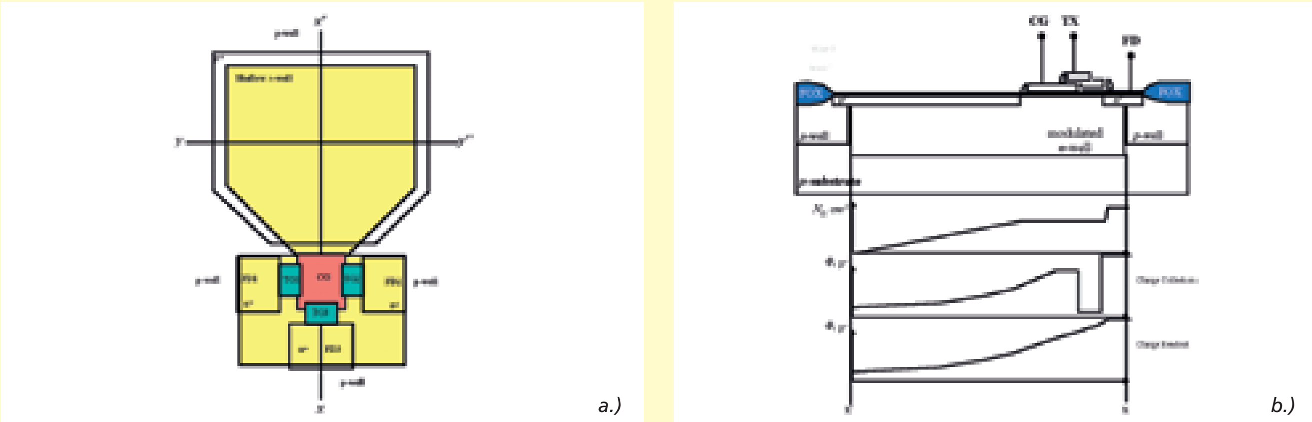

Figure 6: (a) Layout representation of the LDPD pixel configuration proposed; (b) schematic representation of the proposed CMOS compatible, low-noise, and high-response speed, lateral drift-field photodetector (LDPD).

Following the entire analysis just presented, a novel approach based on a lateral drift-field induced in the photoactive area by a concentration gradient is proposed. This gradient is created using a non-uniform lateral doping profile of an extra designed *n*-well to be fabricated in the 0.35 µm CMOS process described above. This is the essential idea behind the *lateral drift-field photodetector* (LDPD) introduced below.

IV Lateral Drift-Field Photodetector(LDPD) based ToF structure

The just mentioned extra *n*-well with a non-uniform lateral doping profile is located on the epitaxial substrate, as shown in Fig. 6(a). It remains fully depleted during operation if sandwiched between the substrate and a grounded p^+ layer, forming the pinned part of the photodetector. A metal-oxide-semiconductor (MOS) capacitor-based *collection-gate* (CG) is fabricated on the one end of the sandwiched well, in what can be defined as the unpinned region of the photodetector, which remains biased at a certain voltage and induces in this way an additional electrostatic potential maximum in the system, where the photo- and thermally-generated carriers are finally collected. The fact that the CG is fabricated on top of the same well used fort the pinned part resembles a "buried" photogate (or buried CCD), where the electrostatic potential maximum, if a perpendicular cut is made across the CG, is located away from the silicon surface, thus reducing the amount of charge carriers that are caused by the rapid surface-states to be mixed with the already collected photocharge. This potential maximum, as well as the extension of the CG are optimized to accumulate the desired amount of collected charge, also offering a means of external controlling of the lateral drift field in the structure proportional to the CG bias. Finally, a transfer-gate (TX) has been added which – by applying an adequate gate voltage – serves to create a potential barrier in the well to prevent the collected charge to be transferred into the floating-diffusion (FD) during the charge collection cycle. When properly biased, it enhances the drift field mechanism when the collected charge is being transferred into the FD during the readout and the reset cycles. The FD is used as a photodetector readout and reset node, just as it is he case in the surface-channel PG pixel structure described above. All the advantages of separated photoactive and readout regions and charge-coupling approach are still present in this pixel proposal.

According to the simulations performed so far for the LDPD pixel structure, if used in the same way as proposed for the PG pixel structures described in at the beginning, the expected charge-transfer times of less than 5ns are to be expected for this structures, in opposition to several hundreds of ns typically achieved by the PPD and PG pixel configurations, for similar pixel pitches. [7]

NEW CMOS PIXEL STRUCTURES FOR TIME-OF-FLIGHT IMAGING

V Conclusions

A fully standard CMOS technology compatible, surface-channel photogate based time-of-flight image sensor with optimized ambient light suppression, low noise, and improved response speed, has been proposed and described. Based on this principle, a demonstrator has been fabricated in a standard 0.35 µm CMOS process and proves fully the viability of the approach proposed. Moreover, the issues regarding limited charge transfer velocity and response speed of such a sensor have been analyzed, which are also typically present in pinned photodiode based pixel configurations. In order to solve this limitation present in the majority of pixel configurations used for ToF applications nowadays, a novel *lateral drift-field photodetector* (LDPD) pixel to be fabricated in the 0.35 µm CMOS process available at the Fraunhofer IMS has been presented. The proposed photodetector features a specially designed *n*-well with a non-uniform lateral doping profile that follows a square-root spatial dependence. The pixel based on this principle contains a "buried" MOS capacitor-based collection gate, a transfer gate, and a floating diffusion. The concentration gradient formed in the *n*-well requires a single extra implantation step and generates a lateral drift-field in the photoactive area of the pixel which enables a high transfer speed of photogenerated charge carriers at low noise.

References

[1] R. Lange, P. Seitz, "Solid-State Time-of-Flight Range Camera", IEEE Journal of Quantum Electronics, Vol. 37, No. 3, pp. 390-397, March 2001

[2] O. Elkhalili, O.M. Schrey, W. Ulfig, W. Brockherde, B.J. Hosticka, P. Mengel, L. Listl, "A 64x8 Pixel 3-D CMOS Time Of Flight Image Sensor for Car Safety Applications", Proc. ESSCIRC 2006, pp. 568-571, September 2006

[3] S. Kawahito, I.A. Izhal, T. Ushinaga, T. Sawada, M. Homma, Y. Maeda, "A CMOS Time-of-Flight Range Image Sensor With Gates-on-Field-Oxide Structure", IEEE Sensors Journal, Vol. 7, No. 12, pp. 1578-1586, December 2007

[4] A. Spickermann, Daniel Durini, Stefan Bröcker, Werner Brockherde, Bedrich J. Hosticka, Anton Grabmaier, "Pulsed Time-of-Flight 3D-CMOS Imaging Using Photogate-Based Active Pixel Sensors", Proc. ESSCIRC 2009, pp. 200-203, September 2009

[5] Lee et al. U.S. patent No. 5,903,021, 1995

[6] S. Ramaswami, S. Agwani, L. Loh, N. Bossemeyer, "Characterization of Pixel Response Time and Image Lag in CMOS Sensors", Image Capture Operation, Motorola Inc., Chandler, AZ, 2001

[7] Daniel Durini, Rana Mahdi, Andreas Spickermann, Werner Brockherde, Anton Grabmaier, Bedrich J. Hosticka, "Lateral Drift-Field Photodetector Based on a Non-Uniform Lateral Doping Profile Photodiode for Time-Of-Flight Imaging", ESSDERC 2009, Fringe Poster Session, September 2009

COMPASS PROJECT FOR MEASUREMENT OF PRESSURE AND TEMPERATURE IN THE PULMONARY ARTERY

N. Kordas, M. Görtz

The aim of the COMPASS project is the development of an implantable device for the permanent measurement of pressure and temperature in the human pulmonary artery (Fig. 1). Information about the pressure allows the calculation of the cardiac output. For patients with heart disease, the system offers remote diagnosis by an automated transfer of the measured data to the physician and thus an improvement of the therapy management. This allows a cost efficient monitoring of the patient in his own home without hospitalisation. A rapid change of the vital paramaters can be detected in a very early status.

The implantable device consists of a sensor tip and an RF-capsule for wireless communication with an external mobile reader, which forwards the data to the physician. The indicators to be measured are medically well established in the field of stationary monitoring. The partners collaborating in this project are BIOTRONIK SE & Co. KG, Helmholtz-Institute RWTH Aachen, Institut für Werkstoffe der Elektrotechnik RWTH Aachen and LITRONIK Batterietechnologie GmbH & Co. KG. Besides the design of the implantable electronics, the project comprises the development of suitable assembly techniques, reliable energy supply as well as methods and means for the implantation process.

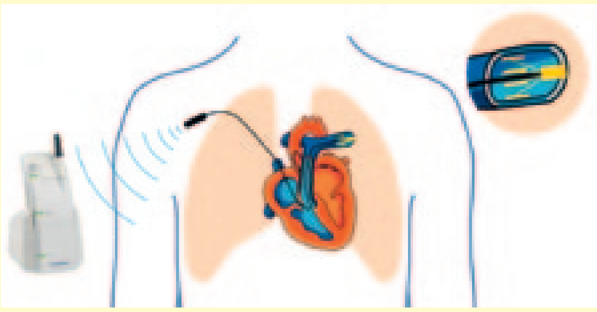

Figure 1: COMPASS System for the Measurement of Pressure and Temperature in the Pulmonary Artery (drawing by Biotronik)

Within the COMPASS project, Fraunhofer IMS develops and fabricates application specific integrated circuits for sensing, signal conditioning and interfacing between sensor tip and RF-capsule. The COMPASS system uses an integrated silicon pressure sensor with analog and digital signal conditioning.

Due to space requirements, the electronics of the sensor tip is distributed over two integrated circuits. The pressure sensor plus some basic signal conditioning is realised in a special technology suitable for micromachined structures like the pressure sensor. The more complex signal conditioning functions as well as digital control, EEPROM-memory for the permanent storage of calibration data and interfaces are located on a second ASIC, which is fabricated in a different technology using smaller structures. By this way, a maximum of functions can be realised within a relatively small area. Fig. 2 shows the main blocks of the implantable system. Fraunhofer IMS is responsible for the three application specific integrated circuits marked as DS, SPP and IEC.

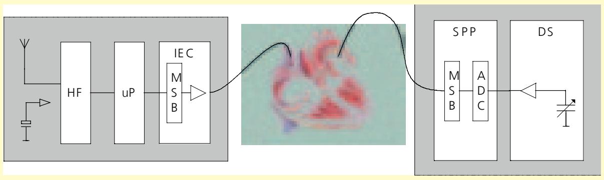

Figure 2: Main Blocks of the COMPASS Implant

The sensor is a capacitive micromachined silicon sensor made up of a polysilicicon membrane located above a conducting substrate. By applying pressure, the membrane bends and the capacitance between polysilicon and substrate changes. This principle has been proven in several industrial and medical applications, however, the COMPASS pressure sensor ASIC is the institute's smallest realisation so far.

In order to get a sufficient amount of capacitance, a large number of equally sized pressure sensors are combined as an array. Furthermore, a second array of reference sensors are

COMPASS PROJECT FOR MEASUREMENT OF PRESSURE AND TEMPERATURE IN THE PULMONARY ARTERY

used for the compensation of temperature effects. The modulation of the capacitance by changing pressure is transformed into a voltage via an analog amplifier circuit. The integrated pressure sensor with electronics is shown in Fig. 3. The size of the chip is 1.8 x 1.8 mm^2.

For assembly reasons, the sensor itself is located in the center of the ASIC. All electronic components are placed around the sensor. Connections to the post processor ASIC are established via 6 bond connections at one side of the pressure sensor.

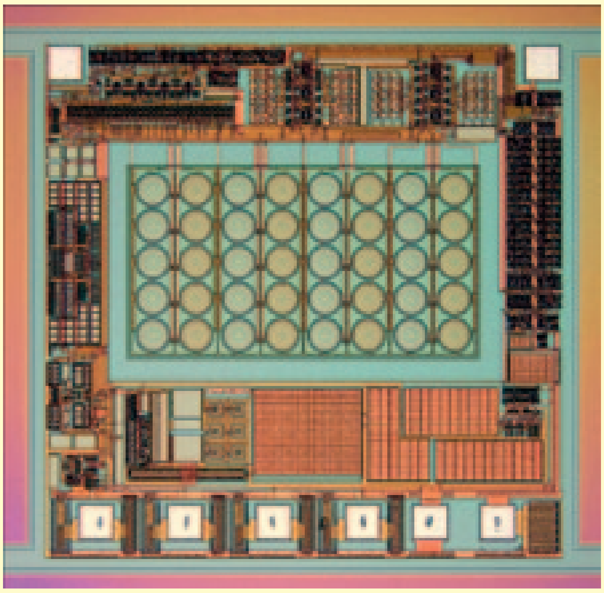

Figure 3: Chip Photo of the Integrated Pressure Sensor with Basic Signal Conditioning

After the pressure data have been forwarded to the sensor postprocessor, the analog voltage is converted into the digital format by a 13 Bit cyclic Analog-to-Digital-Converter. This ASIC also comprises voltage regulation, a local oscillator and an EEPROM memory for the permanent storage of calibration data. The digitised sensor values are then sent to the RF-capsule by a wired connection. The connection allows bidirectional data communication and also supplies the sensor tip with energy.

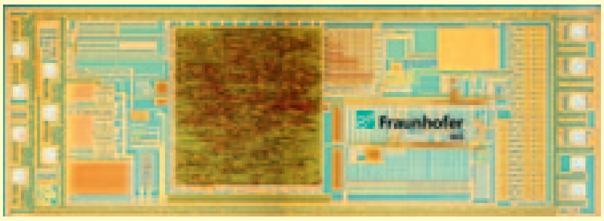

Figure 4: Chipphoto of the Sensor Postprocessor

The third ASIC of the chipset is a special interface circuit in the RF-capsule, called IEC. It serves as the counterpart for data communication with the sensor tip. This circuit also represents the interface to a microcontroller inside the implant. The RF-capsule is based on an existing device previously developed by the partner Biotronic and modified for the special requirements in this project.

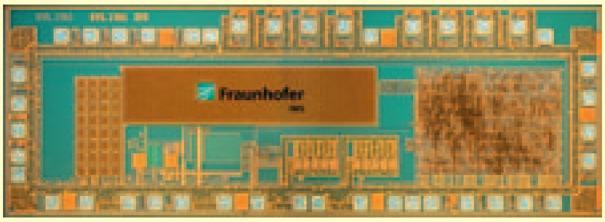

Figure 5: Chipphoto of the Interface-ASIC

In the current status of the project the first design phase is finished ; the ASICs have been fabricated and are currently being testet. The next steps are the assembly of the sensor tip and the Rf-capsule. The functional test of the complete system is envisaged subsequently. Experimental studies are also part of the project and will be performend by Biotronik and AME.

The project is funded by the German Ministerium für Bildung und Forschung.

RFID AND SENSOR TRANSPONDER SYSTEMS FOR MACHINE MAINTENANCE AND REPAIR

Frederic Meyer, Gerd vom Bögel, Martin van Ackeren, Martin Lörcks, Kosta Vasilev

Abstract
RFID and sensor transponder in the area of machine maintenance. RFID systems can support the maintenance and repair processes and provide important information. The susceptibility to metals, which shields the irradiation of the RFID, is a disadvantage of the system. For supporting effectively the process, the transponders have to be applied on and partially in metals.
Keywords: RFID, metal, transponder, sensor transponder, data logger

1 Introduction

RFID systems can support the processes for machine repair and maintenance. Important for a functional system are the boundary conditions for the working process e.g. metal, temperature, humidity, vibration…, these boundary conditions are furthermore interesting for the identifying of maintenance intervals as needed.
For some systems the identification for maintenance support suffices, for others the boundary conditions are important. The machining production depends on highest accuracy, often every hundredth millimeter counts. Worn out cutter and drills could not offer the demanded accuracy. The employees have to measure regularly the tools by hand in a complicated process before they can be assembled on a CNC machine. For detecting smallest irregularities of the misalignment, the fixtures of the cutter are rotary mounted and rotate while measuring. So far, the cutter and drills have been attached with a suited adapter to a mounting, the shaft. A serial number which is added to the adapter and the tool and other data like dimensions have to be copied by hand what leads to mistakes.
Another area is the maintenance of construction plants. Thereby the identification can help but decisive are the recording and storage of boundary conditions to determine the workload and the operation mode. That way, the ambient parameter can count the operating time and determine the operation mode, the normal operation or the intentional caused malfunction. Malfunction means, that the machines wear out earlier which results for example in gaskets which lose their effectiveness, leaking lubricants or hydraulic fluids, oil corrosion or the loss of lubricity etc… . The following chapter illustrates two RFID system solutions for supporting the repair and maintenance processes in detail.

2 Focusing the boundary conditions

Regarding the boundary conditions for support in the area of repair and maintenance a great range of rough ambient conditions can be detected. On one hand the ambience is full of metal, on the other hand humidity, great temperature fluctuations and vibrations limit the fields of application.

2.1 Boundary conditions by the identification of drills and cutters in the measurement transducer

Figure 1 depicts a fully automated measuring system for measuring drills and cutters.

Figure 1: Measuring system for measuring drills and cutters [1]

RFID AND SENSOR TRANSPONDER SYSTEMS FOR MACHINE MAINTENANCE AND REPAIR

Figure 2 depicts a simplified, schematic cross-section of the tool fixture with precision shaft and the stationary fixture in the pre-setting tool.
Tool fixture, stationary pre-setting tool, precision shaft

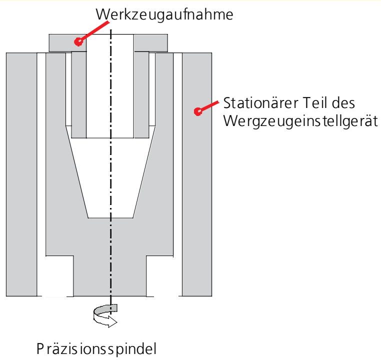

Figure 2: simplified, schematic cross-section

The pre-setting tool which has to be identified is rotary mounted and metallic capsuled.
The aerial of the reading device can only be integrated into the stationary part of the machine tool but it is not possible to identify the tool fixture which is placed in the shaft.

2.2 Boundary conditions of sensor transponder on construction plants

Construction plants have to face atmospheric influences 24 hours a day, 7 days a week.
The atmospheric influences range from frost in the Siberian Taiga or extreme highly temperatures in the desert up to humidity as well as impacts and shocks.
To limit the wide area of construction plants, the focus in the following chapter is on a machine to pitch and to sheet piles.

The machine to pitch and to sheet piles rams sheet piles into the ground. The main field of application is the protection of excavations, where the limited space does not allow slopes.

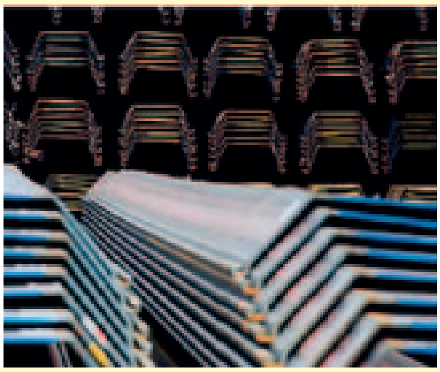

Figure 3: sheet piles [2]

Mostly, the machine is a temporary protection which is removed when the construction activity is finished. As a permanent component the machine is used in the area of water engineering for quay walls, moles, docks and channels.

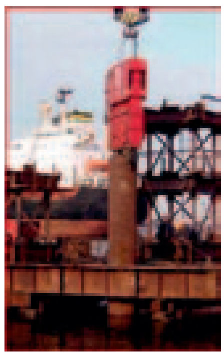

Figure 4: Machine to pitch and to sheet piles at a mole. [3]

Depending on the size of the machine to pitch and to sheet piles, the sheet pile is rammed into the ground by an amplitude swing which is about several centimeters and with frequencies between 30 and 60 Hz.

3 Approach

The problems are solved like shown in the following chapter.

3.1 Approach tool identification

The solution for the in chapter 2.1 described problem is a, like in figure 5 schematic depicted, inductive transformer, which is integrated into the precision shaft and transmits the field trough the shaft to the transponder.

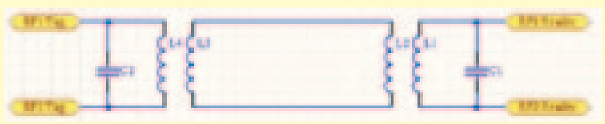

Figure 5: inductive transmission line

3.2 Approach machine to pitch and to sheet piles

The solution for measuring the ambient conditions is a semi active, discrete data logger with a LF- transceiver, a low-power-microcontroller, a temperature sensor, a vibration sensor, an EEPROM and a battery, as the block diagram in figure 7 clarifies.

Transmitter, receiver, battery, vibration sensor, temperature sensor, EEPROM, real time clock, low power micro controller

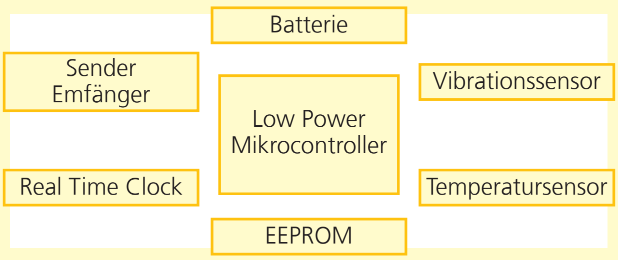

Figure 6: block diagram

4 Implementation

4.1 Implementation of the tool identification

The implemented system is composed of a reading device, the reader inductance {1}, the transducer {2} and the transponder {3}.

The mounting is schematically depicted in the following figure.

Figure 7: schematic mounting system

The system integration is depicted in figure 8 and 9.

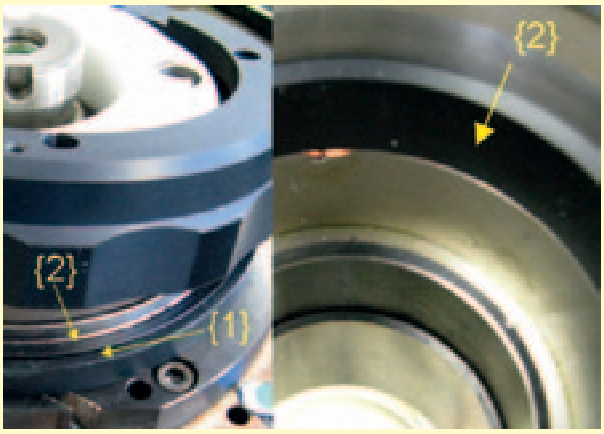

Figure 8: tool fixture and shaft with RFID aerial and transducer

In figure 8 the aerial of the reading device {1} which is integrated into the fully automated measuring system and the exterior transformer inductivity at the shaft {2} are depicted. On the right side, the interior transformer inductivity, which induces the energy into the transponder, is shown. Figure 9 depicts the transponder which is mounted on the tool fixture.

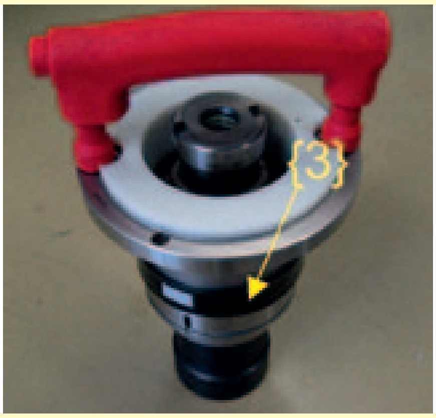

Figure 9: tool fixture with transponder

4.2 Implementation of the sensor transponder on construction plants

The production data acquisition is carried out by analyzing the sensor information of the 2D acceleration sensor and the temperature sensor.

4.2.1 Data processing

The measurement cycles of the sensor transponder are adjustable. The minimal measurement cycle is 60 seconds and is activated by the interrupt of a real time clock. At every measurement cycle a temperature data and 128 vibration data are recorded and analyzed. The data are Fourier transformed and evaluated in the frequency range. Figure 6 displays 128 scanned values which are produced by the vibration sensor. The following figures display sampled oscillations of 28 Hz and 48 Hz.

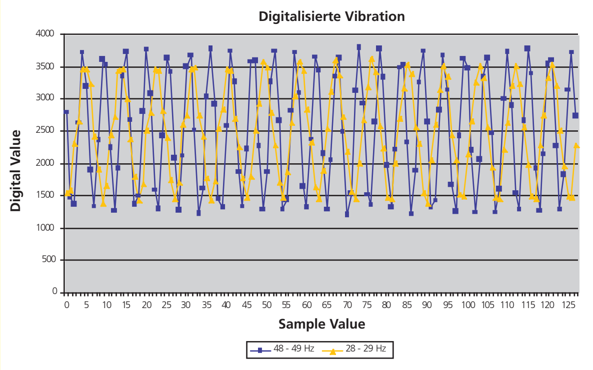

Figure 10: sampled acceleration sensor signal

The calculation of the Fourier transformation, according to the algorithm of Cooley and Turkey, is carried out by several steps. At first, a Hamming window is laid over the sampled values, displayed in figure 11.

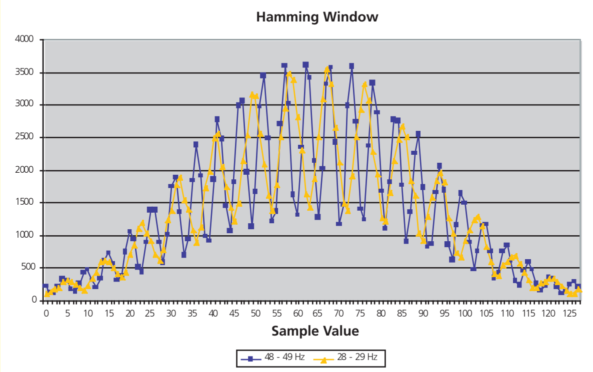

Figure 11: Hamming window

Secondly, the Butterfly calculation is carried out, which is displayed in the following figure.

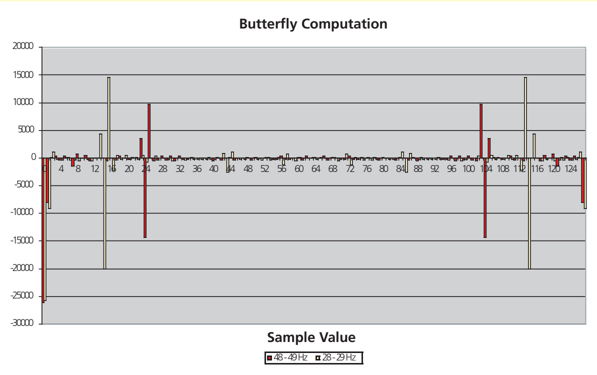

Figure 12: Butterfly calculation

Due to oversampling by a factor 2, the maxima of the butterfly calculation is on the half adjacent vibration frequency.
At last, the amplitude calculation is carried out. (Figure 13)

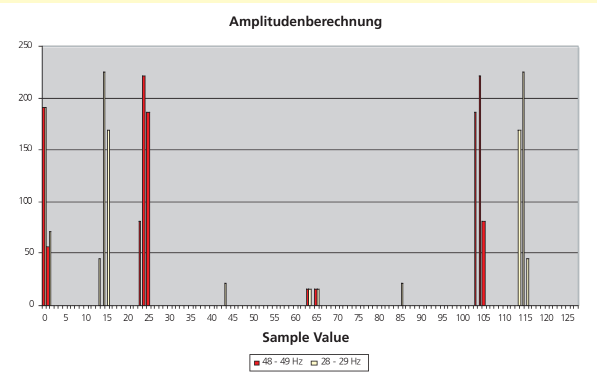

Figure 13: Butterfly calculation

At the identification of the maximum value the multiples of the vibration frequency are filtered out. The working frequency is determined by the calculated frequency and the temperature value gives information if normal operation, malfunction or no operation is existent.
The data of the measurement cycles are added up and stored as current values in an EEPROM.

4.2.2 Mounting

The transponder board is casted in 2 components epoxy resin to withstand the mechanic strains of a construction site.
A mounting with a mounting carrier that is not casted, is displayed in figure 14.

Temperature sensor, transceiver, RTC, EEPROM, vibration sensor, microcontroller

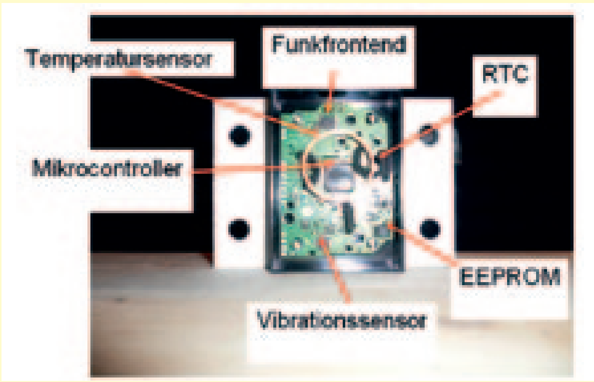

Figure 14: transponder that is not casted with epoxy resin

RFID AND SENSOR TRANSPONDER SYSTEMS FOR MACHINE MAINTENANCE AND REPAIR

4.2.3 Current consumption

The current consumption depends on the defined measurement cycle. The maximum current consumption is 2.9 mA during the measurement and the standby current consumption is 7.5 µA. Figure 15 displays the current consumption during active operation, which can be divided into 3 phases:

1) microcontroller active, ADC active, temperature sensor active, vibration sensor active (2.9 mA)
2) microcontroller active, ADC active, vibration sensor active (2.2 mA)
3) microcontroller active for data processing (1.2 mA)

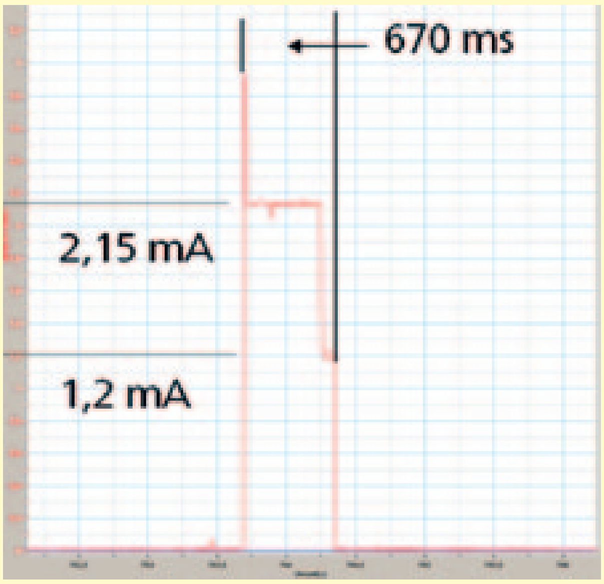

Figure 15: current consumption during active operation

Measuring cycle	battery capacity	durability
60 s	1000 mAh	2 Jahre
120 s	1000 mAh	4,5 Jahre
300 s	1000 mAh	> 7 Jahre
600 s	1000 mAh	> 10 Jahre

5 Résumé

This article explains how RFID systems can contribute to and provide information for maintenance processes. The example of the machine tool shows the successful application of RFID into a metallic environment. By this, the identification and the exchange of data between tools and the measurement transducer can be automated.

Using the example of the semi active data logger for construction machines, the article illustrates the system for measuring relevant operation data like duration normal operation, duration malfunction and temperature. Hereby, a data basis is given, which enables to decide promptly on a regular or irregular maintenance and its extent. This permits a more cost-effective operation of construction plants.

Bibliography:

[1] Kelch
http://www.kelch.de/?cat_id=76

[2] Hoesch Spundwand und Profile
http://www.spundwand.de/d/index.html

[3] Thyssen Krupp
http://www.thyssenkrupp-gft-tiefbautechnik.com/mueller/de/index.html

ANTENNA ANALYSIS AND OPTIMISATION FOR DEEPLY IMPLANTABLE MEDICAL SENSOR TRANSPONDERS

A. Hennig, G. vom Bögel

ABSTRACT

Deeply implanted sensor transponders are of interest in treatment of cardiovascular diseases. In such systems only small antennas in shape of a stick are supposed. To make a sensor transponder operatable, an optimisation of such an antenna is necessary. Therefor a mathematical expression is derived, that makes optimisation possible. A mathematical modell is derived, to describe physicall effects. Moreover, the influence of encapsulation and human tissue in direct contact to the antenna is analysed. Finally, an optimisation is done for typical requirements of such a system. Measuremts validate the theoretical examinations.

Index Terms – Sensor Transponder Medicine Implanted Antenna Energytransmission Human Tissue Optimisation

1. INTRODUCTION

The use of sensor transponder technologies in medicine opens valuable possibilities in the therapy of human cardiovascular system diseases. Medical studies [1] have shown, that the treatment of cardiovascular disease can be significantly improved by continuous monitoring of parameters such as blood pressure, temperature, and so on. A deeply implanted sensor transponder in human body can measure cardiovascular parameters and send it to a reader outside of the body. Implants normally stay inside the body for a longer period. Thus, a supply by a local battery is not possible, only so-called passive transponder systems are of interest. There are several requirements that have to be kept in mind. For example, a large transmission distance (up to half a meter for corpulent patients), low antenna dimensions (catheter implantation) and the influence of human tissue. Today, no system exist, that meet all these requirements. This work is focused on the analysis and optimisation of transponder antennas for such a system. Antenna characteristics will be investigated influenced by the encapsulation and human tissue. With the help of antenna models and mathematical expressions, that are derived in this work, an optimisation of antenna parameters is possible.

2. INDUCTIVE ENERGY TRANSMISSION

A sensor transponder system consists of a reader located outside the body and the implanted sensor transponder. The reader has a transmitter to produce an alternating magnetic field and a receiver for the transponder data. The sensor transponder consist of an antenna coil, a chip including analogue frontend, logic and integrated pressure and temperature sensor. Previous studies [2] have shown, than a frequency of 6.78 MHz is a good choice to transmit power to the transponder. At this frequency the maximum power transmission is possible. The transmission takes place in the so called nearfield. Only the magnetic component is used. Because of that, coils are used as antennas.

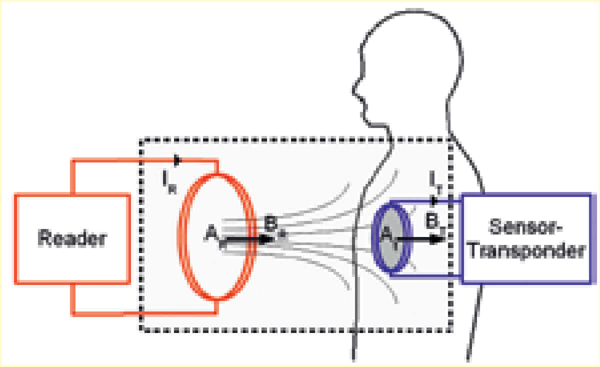

Figure 1: Sensor Transponder System

Figure 1 illustrates a sensor transponder system. The transmission channel consists of an antenna coil in the reader that produces an alternating magnetic field, the human body and the antenna coil of the transponder. The current in the antenna coil of the reader produces an magnetic flux. A small part of the magnetic flux couples with the transponder coil. In consequence, a voltage is induced in this coil. By this voltage, the electronic of the transponder is supplied with power. This voltage is proportional to the time derivation of the flux $\frac{D\Phi_T}{dt}$. Figure 2 shows an equivalent circuit of the inductive transmission channel. The resistors R_R and R_T model losses

ANTENNA ANALYSIS AND OPTIMISATION FOR DEEPLY IMPLANTABLE MEDICAL SENSOR TRANSPONDERS

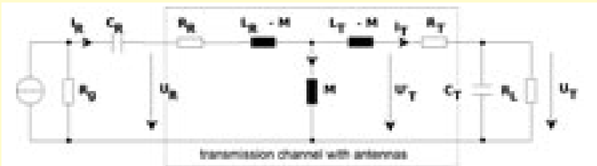

Figure 2: Equivalent Circuit

in antennas and human tissue. The current consumption of the transponder load is modelled by R_L. The function of the antenna coil in the reader is to generate a magnetic field at the transponders place, that provides it with enough energy for working. The purpose of the transponder antenna is, to produce the maximum possible voltage with the available magnetic field to provide power to the transponder's electronics. So, the transmission range can be maximised. The channel is modelled by a transformer equivalent circuit. Moreover it includes tuning capacitors at the primary and secondary side. The following mathematical expression is derived from this equivalent circuit that enables an optimisation of the antenna coil. This formula describes the achievable voltage over the load for an available field strength. It includes all parameters that describe the antenna characteristic.

$$\frac{|U_T|}{|B_T|} = \frac{\omega \cdot N_T A_T}{\sqrt{\left(\frac{R_T}{\omega L_T} + \frac{\omega L_T}{R_L}\right)^2 + \left(\frac{R_T}{R_L}\right)^2}} \quad (1)$$

The better the antenna is optimised, the larger is the value of this expression. The expression depends on some geometrical parameters, like the diameter and number of windings and electrical parameters, inductance, loss resistance and load resistance. To enable an optimisation of the antenna, it is necessary to have a mathematical model, that describes the dependences between the parameters. Moreover the influence of the human tissue has to be analysed. This is done in the following section.

3. THEORETICAL ANALYSIS OF IMPLANTED ANTENNA COILS

Following, the electrical characteristics of implanted antenna coils are analysed. Particularly, the influence of encapsulation and of human tissue in direct contact to the windings of the transponder coil are considered. For energy transmission, the parameters inductance, stray capacity and loss resistance are of interest. A part of available power is converted to heat. Stray capacity exists, because of the electric field between the windings. The electric field lines penetrate the encapsulation and the human tissue. These materials have higher permittivities. This causes a rise of the stray capacitance and can make the antenna unusable. In the end, these effects reduce the transmission range, which is is not acceptable in this application.

3.1. INDUCTANCE

The human tissue has no direct influence to the inductance, because it has no magnetic behaviour. However the measurable inductance of an antenna coil is influenced by the stray capacity. The following formula shows the interrelation between measurable inductance L_S, the parasitic capacity C and the real inductance L_L.

$$L_S = \frac{L_L}{1 - \omega^2 L_L C} \quad (2)$$

If the parasitic capacitance is known, the measuremable inductance can be predicted. By inserting the so called self resonant frequency $\omega_r = \frac{1}{\sqrt{L_L C}}$ we get:

$$L_S = \frac{L_L}{1 - \left(\frac{\omega}{\omega_r}\right)^2} \quad (3)$$

If the self resonant drops to the operation frequency ω, the effect of inductance and capacitance will cancel each other. If the operating frequency is higher than the self resonance ω_r, the coil will act as an capacitor.

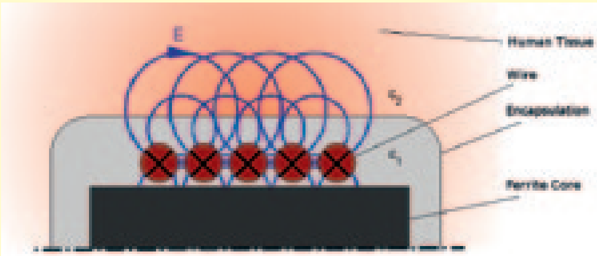

Figure 3: Electrical stray field of implanted antenna coil

3.2. STRAY CAPACITY

The windings of the transponder antenna are placed on a ferrite rod. They are surrounded by the encapsulation material and human tissue. Figure 3 shows a schematically structure of an implanted transponder antenna coil. Because of the voltage drop across each winding, an electric field appears. the electric field lines are indicated in the figure. There exist electric field lines between each winding, between the different windings, and to the core. Some of the field lines penetrate the encapsulation and the human tissue. Other field lines are just inside the encapsulation.

Figure 4 shows the simplified HF equivalent circuit of an antenna coil. It consists of inductivities L_n for each winding, resistors R_n for modelling losses, and capacities. The overall stray capacity is composed of several stray capacities between each winding C_t and between the core C_s. The field lines

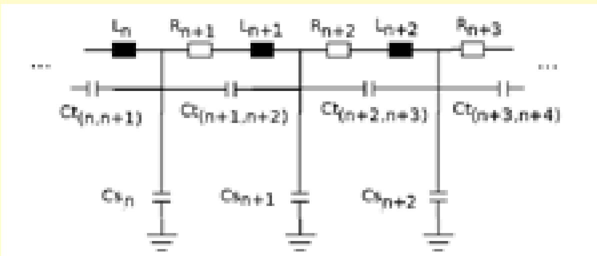

Figure 4: Equivalent circuit of implanted antenna coil

belonging to C_s penetrate just the encapsulation, whereas the field lines of C_t penetrates the human tissue. With the help of a mathematical description of this modell, the influence of encapsulation and the human tissue can be estimated. Various materials of encapsulation and human tissue can be considered. The influence of geometrical design parameters, like number of windings can be considered, as well. With the following formulas de-rived from this model [3], the stray capacity can be obtained.

$$C_t = \frac{\pi^2 D\varepsilon}{ln(p/2r + \sqrt{(p/2r)^2 - 1})} \quad (4)$$

$$C_S = \frac{2\pi^2 D\varepsilon}{ln(h/r + \sqrt{(h/r)^2 - 1})} \quad (5)$$

The overall capacity is composed of all single stray capacities together and can be found out by the following inductive formula:

$$C_{(n)} = \frac{C(n-2)C_t/2}{C(n-2) + C_t/2} + C_s/2 \quad (6)$$

Now, the influence of encapsulation and human tissue can be discussed. Geometrical parameters, like the dimension of the core, are given by the implantation technique. A searched parameter is the optimal number of windings. Additionally, one of the most importand question is, if the number of windings is limited by the parasitic capacity.

First of all, the influence of the human tissue is discussed. With the help of the formulas, the over all stray capacitance is calculated for several number of windings. Figure 5 shows the result. The over all stray capacitance of the transponder antenna is shown for differend kinds of surrounding materials. In all cases, silicone was chosen as encapsulation material. For each material, the corresponding permittivity at the operating frequency was used [4]. First of all, it can be said, that the stray capacitance is affected by the surrounding material. In an antenna coil with two windings, blood causes a value of 18pF, that is 25 times higher than 0.7pF for air. Heart tissue

ANTENNA ANALYSIS AND OPTIMISATION FOR DEEPLY IMPLANTABLE MEDICAL SENSOR TRANSPONDERS

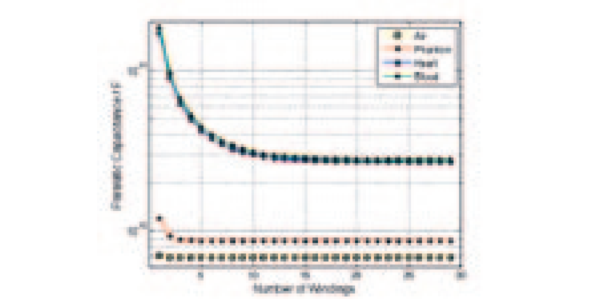

Figure 5: Stray capacitance over the number of windings for several kind of human tissues

has approximatelly the same effect. The over all capacitance is decreasing with rising number of windings. The reason is, that the over all capacitance of series connected capacities is smaller than the value of one single capacity. Moreover it can by seen, that the capacitance will not change significantly anymore, for more than about 20 windings. In this case, the capacities between the windings and the core C_s are decisively. To verify this, the over all capacitance is calculated for different kind of encapsulation materials. Figure 6 shows the result. It can be said, that the capacitance is not influenced by the capacity C_s for up to three windings. The question is now, how the usability is influenced.

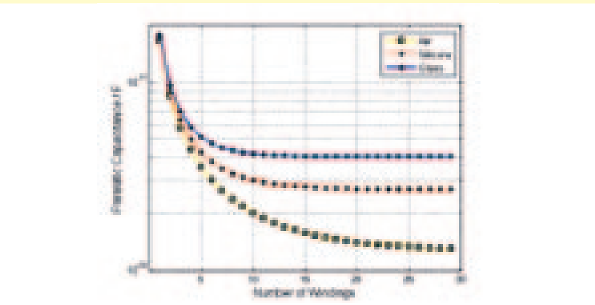

Figure 6: Dependency of over all capacitance on the number of windings for different encapsulation materials

As described in section 3.1, the measurable inductance of the antenna coil is influenced by the parasitic capacity. In the literature [5] can be found, that an antenna coil is usable, if the measurable inductance is maximal 10% raised by this effect. This means, that the self resonance caused by the inductivity and parasitic capacity should be $\sqrt{11}$ times higher than the operating frequency. Figure 7 shows the maximum recommend operating frequency in dependency to the number of windings.

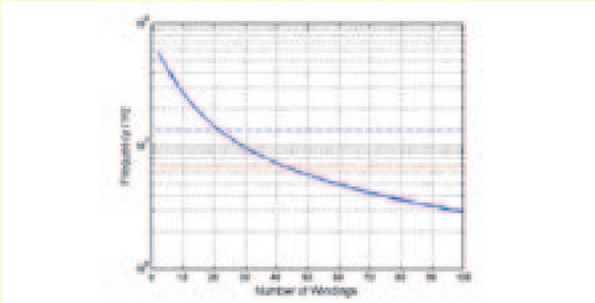

Figure 7: Maximum Recommend frequency over number of windings

The values are calculated for a silicone encapsulation and surrounded heart tissue. As can be seen, that the maximum recommend frequency is falling with rising number of windings. The reason for this is, that the inductivity rises faster than the parasitic capacitance falls with the number of windings. In this application, an operating frequency of 6.78 MHz or 13.56 MHz is of interest. These frequencies are shown by the dashed lines. It can be said, that antenna coils with no more than 20 windings can be used for 13.56 MHz and not more than 43 windings for 6.78 MHz.

3.3. LOSSES

Losses in antenna coils exist in the ferrite core, the wire, and the human tissue around the coil. A part of the energy is converted to heat. Losses in the wire are caused by the ohmic resistance, skin and proximity effects. Ferrite losses are caused by magnetisation of the material and eddy currents in the core. These effects are frequency depended.

DC resistance

The DC or ohmic resistance is caused by the limited conductivity of the wire, that means without frequency depending effects. It depends on the length of the wire, the thickness and the conductivity of the used material. The ohmic resistance should be expressed as a function of the number of windings respectively the inductance. With the following mathematical expression the DC resistance can be calculated:

$$R_{DC} = \frac{N_R D}{\sigma \pi d^2/4} \quad (7)$$

with d diameter of the wire and σ the conductivity of the material. E. g. for cupper $\sigma_{CU} = 57\frac{Sm}{mm^2}$. For a cylindric antenna coil D = 1.5 mm, d = 0.15 mm and N = 10 the DC resistance becomes $46.6 \cdot 10^{-6}\Omega$.

Skin Effect

Every electrical current is surrounded by a magnetic field. In case of ac current, eddy current will be induced in every conductive material next to the field. Insight the conductor, such eddy currents are as well. These eddy currents itself cause magnetic fields. These fields in turn interact with the current. In consequence, the current flow is driven to the surface of the wire. The bulk is currentless, and the cross section of the wire is not completely used. The resistance of the wire seems to rise. This effect is called skin effect. The ac resistance caused by this effect could be calculated with the following expression [6]:

$$A_{skin} = R_{DC} \cdot (x + \frac{1}{4} + \frac{3}{64x}) \quad ,$$

$$mitx = \frac{d}{4}\sqrt{\pi \int \sigma \mu}$$

Thus, the losses caused by the skin effect can be calculated. For example, the dc resistance caused by skin effect for a cylindric antenna coil with D = 1.5 mm, d = 0.15 mm and N = 10 at 6,78 MHz amounts to 9 $m\Omega$.

Proximity Effect

If a wire is arranged to a coil, an additionaly rise of the resistance will be observed. The reason is, that the magnetic field of induced eddy currents interacts with adjacent windings. This effect can be described mathematically. Kelvin-Besselfunctions are necessary. An expression to determine the ac resistance is given in [7]:

$$R_{AC} = R_{DC}\frac{\gamma}{2}\left[\frac{ber\gamma bei'\gamma - bei\gamma ber'\gamma}{ber'^2\gamma + bei'^2\gamma} - 2\pi\frac{ber_2\gamma ber'\gamma + bei_2\gamma bei'\gamma}{ber^2\gamma + bei^2\gamma}\right] \quad (8)$$

with $\gamma = \frac{d}{\delta\sqrt{2}}$ and δ the so called skin depth. "bei", "ber" are the Kelvin-Besselfuntions. The geometry of the conductor is considered.
Therefore, the losses caused by proximity effect can be described analytically.

Losses in human tissue

The losses inside human tissue for different frequencies were analysed in [2]. It can be said, that about 2 % up to 7 % of the energy is lost at 6.78 MHz. At 13.56 MHz about 5 % to 24 % is lost.

Losses in Ferrite Material

Additionally losses occur in the ferrite core. These are losses caused by eddy currents so called hysteresis losses. These effects are analytically difficult to be described. Because of that, it is more practicable to use an approximation with real measurement results. A polynomial function is fitted to these

ANTENNA ANALYSIS AND OPTIMISATION FOR DEEPLY IMPLANTABLE MEDICAL SENSOR TRANSPONDERS

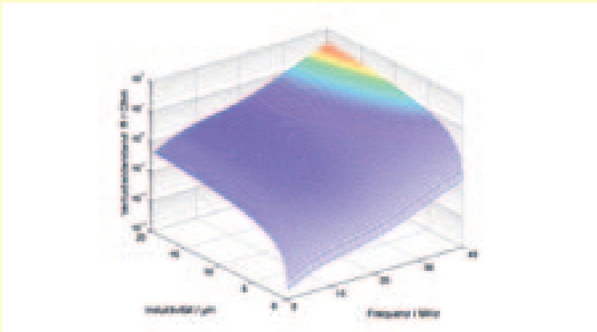

Figure 8: Modell of the used transponder antenna

measurement values. The measurements where done with a 2.5 mm x 10 mm ferrite rod that matches the requirements of the application.

Modelling of antenna coil

Now all loss effects are listed and the behaviour of the used antenna coil can be investigated. It is possible to build a modell that describes the dependences between the physical parameters inductance, frequency and loss resistance. All mathematical expressions and the fitting function where included into a Matlab [8] function. Figure 8 shows the result. The z-axis represents the loss resistor. The x-axis is the inductance and y-axis the frequency. For all frequencies and inductivities, the loss resistance is known yet. With this modell and the formula 1, it is possible to do an optimisation. This is done in the following section.

4. OPTIMISATION, CONSTRUCTION AND PRACTICAL VERIFICATION

With the help of the formula derived from the equivalent circuit in section 2 and the models derived in section 3, an optimisation of an implantable antenna coil is possible. With measurements on realized antenna coils inserted into a phantom fluid, the theoretical results are verified.

Geometrical parameters like core length and diameter are limited by the implantation technique. Hence, the number of windings respectively the inductance is optimised. By taking a look at formula 1, it can be seen, that the voltage at the load has a non linear dependence of the inductance. The inductance respectively the number of windings, is searched, for which the voltage is maximal. All voltage values were calculated with an field strength typical for the application. Figure 9 show the results. The reachable voltages at a load of $50\ k\Omega$ at 6.78 MHz are displayed, for inductances from 100 nH to 20 μH. The crossed curve shows the measurement results. The optimal inductance is 4 μH. This value is reached with 20 windings. Figure 10 shows a realized antenna. It was build with a 0.15 mm cupper wire on a 1.5 mm x 8 mm ferrite rod.

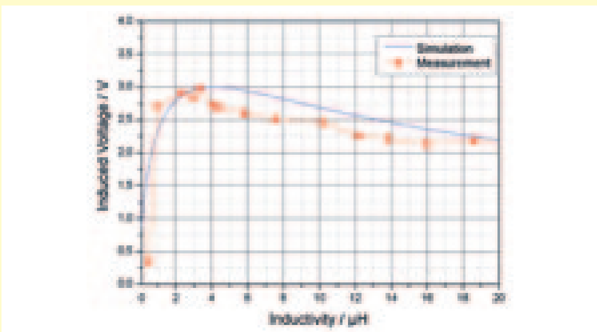

Figure 9: Equivalent circuit of implanted antenna coil

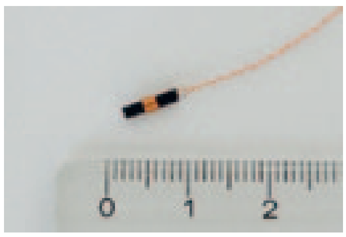

Figure 10: Realized transponder antenna

Now feasibility of an antenna coil with these parameters should be validated by taking care of stray capacity. By taking a look at figure 7 it can be stated, that this antenna coil is usable for frequencies up to 15 MHz.

The resonant frequency and the effective inductance were measured with a networkanalyser and an LCRmeter. For this, an antenna coil was build with 20 windings on a 1.5 mm x 10 mm ferrite core. To simulate the influence of the human tissue, the antenna coil was placed inside a phantom fluid. This fluid was prepared following a recipe described in [9]. The dc inductance of the builded antenna coil is about 4 μH. The measurements where done at 6.78 MHz.

	Air	Encaps	Phantom
Permittivity	1	2.69	12.54
Measured Ind.	5,7 μH	5,9 μH	6,3 μH
Self Resontantf.	58 MHz	46 MHz	13 MHz

Table 1: Determination of self resonant frequency by measurements

Table 1 shows the results. The measurements show a rise of the measurable inductance for materials with higher permittivities. As discussed in the theoretical part, the measurable inductance increases. The self resonant frequency drops down to 13 MHz if the antenna is placed inside the phantom fluid. The stray capacity is proportional to the permittivity. The capacitance should rise in the same manner. The self resonant frequency drops from 58 MHz to 46 MHz. This corresponse to an increase of the capacitance of the factor 1.6. The permittivity of silicone is specified with 2,69. Inside the phantom fluid, the self resonant drops additionally around a factor of 12.52. The permittiviy of the fluid is about 12.54.

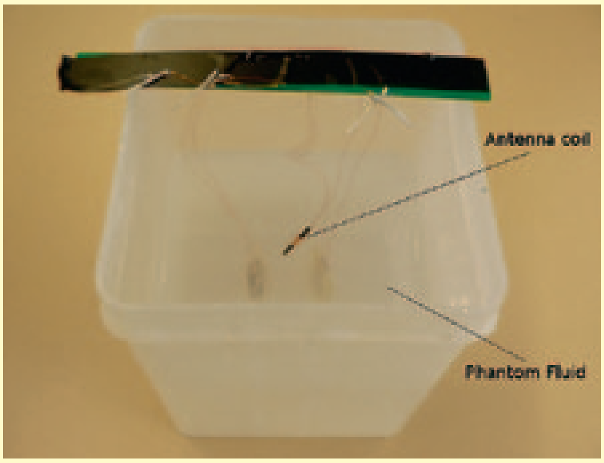

Figure 11: Measurement of antenna coil with phantom fluid

5. CONCLUSION

With the help of a mathematical expression, derived from an equivalent circuit of the transmission channel, an optimisation of an antenna coil was performed. Loss effects were considered by a developed model. The influence of the encapsulation and the human tissue to the stray capacity was analysed. For the presented application, a ferrite coil with 20 windings is an optimal choice. Usability was validated by determining the self resonant frequency. Practical measurements verified the influence of encapsulation and human tissue.

6. REFERENCES

[1] Priv.Doz. Dr. Andreas J. Morguet, Paul Kuehnelt, Antje Kallel, Dirk Russ, Marcus Waehner and Prof. Dr. Heinz-Peter Schulteiss. In Telemedizinische Betreuung und Ueberwachung von Patienten mit gering bis mittelgradiger chronischer Herzinsuffizienz in der haeuslichen Umgebung. VDE, 2004.

[2] A. Hennig. In RF Energy Transmission for Sensor Transponders Deeply Implanted in Human Bodies. IEEE, 2008.

ANTENNA ANALYSIS AND OPTIMISATION FOR DEEPLY IMPLANTABLE MEDICAL SENSOR TRANSPONDERS

[3] G.Grandi M.K., Kazimierczuk, A.Massarini and U.Reggiani. In Stray Capacitances of Single-Layer Air-Core Induktors for High-Frequency Applications.IEEE, 1996.

[4] S Gabriel, R W Lau, and C Gabriel. The dielectric properties of biological tissue: Iii. parametric models for the dielectric spectrum of tissues. Phys. Med. Biol. 41, 1996.

[5] Prof. Dr.-Ing K. Solbach. Microwave and rf technologie. Technical report, University of Duisburg, 2008.

[6] K. Kuepfmueller. Einfuehrung in die theoretische Elektrotechnik. Springer-Verlag, 1990.

[7] Jan A. Ferreira. In Improved Analytical Modeling of Conductive Losses in Magnetic Components. IEEE, 1993.

[8] http://www.mathworks.com.

[9] Standard test method for measurement of radio frequency induced heating near passive implants during magnetic resonance imaging.

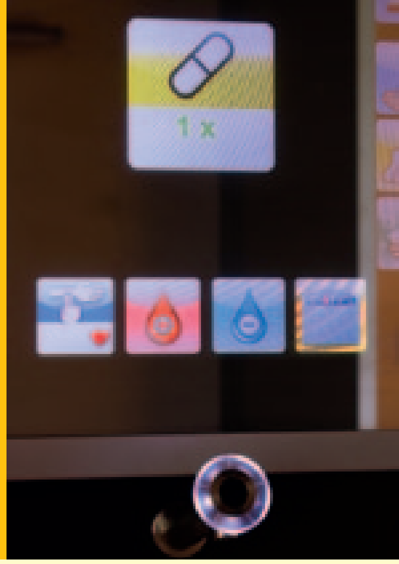

"INBATH" – ASSISTIVE ROOMSYSTEM FOR CARE APPLICATIONS

G. Stockmanns

The "inBath" project is especially oriented towards the support and development of hygiene-relevant care in a multigenerational household. With the help of new technologies, technical devices of aided recall are provided for the daily personal hygiene for elderly or disabled people. This does not only guarantee their personal autonomy but also enables them to live (longer) in their homes. The development of these systems, their testing and application are the core activities of the inHaus business field Health&Care.

The observationand support of residents withour disturbing them is the aim fo the inBath progject. The electronically eqqipped bathroom is liked by the whole family as it is barrier free and has a toilet that recognizes the residents automatically and adjusts its height accordingly.
The light is automatically switched on and off in order to save energy; so is the water tap. The only device that children do not approve of is the toothbrush alarm which reports whether the teeth have been brushed long enough.

The bathroom is especially helpful e.g. for grandpa who is slightly disoriented after a stroke. He forgets to shave and take his medication regularly. A mirror over the sink assists him. Illuminated pictograms show what is to do next: wash yourself, brush your teeth, shave and comb your hair. The days for showering are also stored. If the resident has to take pills, a voice from a loudspeaker reminds him of it. Alternatively, the medicine cabinet can also "talk" to him. It will also be decently illuminated when the medication is supposed to be taken.

"This custom-made assistance system is combined with the docu-mentation of processes that happen in the bathroom", says Dr. Gudrun Stockmanns, section leader of Health&Care Solutions at IMS. Sensors at the door, toilet, tap, light switches and carpet record every activity electronically. This is important if one day the grandfather needs professional care. Doctors or nursing staff read on a computer screen which electronic nursing functions have been used, how often the elderly person has used the bath-room or the toilet whether he fell down.

In emergency case the computer automatically phones the nursing station or one of the persons whose details are stored on the hard disk.

SMART METERING IN COMMERCIAL BUILDINGS AND PRIVATE HOMES

H.-J. Schliepkorte

Originally, the guideline 2006/32/EG by the European Parliament motivated "Smart Metering" in residential properties. The guideline states among other things:
"Member States shall ensure that, in so far as it is technically possible, financially reasonable and proportionate in relation to the potential energy savings, final customers for electricity, natural gas, district heating and/or cooling and domestic hot water are provided with competitively priced individual meters that accurately reflect the final customer's actual energy consumption and that provide information on actual time of use."
And furthermore: „Billing on the basis of actual consumption shall be performed frequently enough to enable customers to regulate their own energy consumption."[1]
Those provisions aim at reaching a guiding value of energy savings of 9 per cent within nine years.
The guideline demands new meters as well as storage and visualization of consumption data. This is why today, private households are furnished with electronic domestic supply meters, which include a technologically qualified interface, in order to read out and store consumption data in other facilities. These provisions originate in the current technological installation in private households: Basic collection and therefore analysis of energy consumption data is not possible at all or only exceedingly difficult. Taking a closer look, this problem also applies to commercial properties. But here, automatic collection of consumption data has been an issue for a long time and accordingly flexible rates are available. This motivates commercial customers to avoid consumption extremes in order to limit overall consumption as far as possible. Using current devices to analyse the overall consumption in commercial contexts often gives out insufficient information about the consumers, so that the evaluation of chances to cut down is very difficult. This shows that the often diverging demands of those very different areas correspond in the context of smart metering whenever it concerns the appropriate interpretation of automatically recorded consumption data.

In order to enable users to save energy, it is first of all important to inform him or her in detail and comprehensibly about his or her energy consumption. Here, it is important to distinguish who the end user is. If it is a technically accomplished facility manger, the application can be designed accordingly, e.g. including features to give out interesting details. Private users, on the other hand, are assumed to be less technically accomplished so that the application should be designed to be less technical. Regardless of the end user, the measured data should be edited before it is given out, in order to present them in a compressed format.

1: DIRECTIVE 2006/32/EC OF THE EUROPEAN PARLIAMENT AND OF THE COUNCIL of 5 April 2006

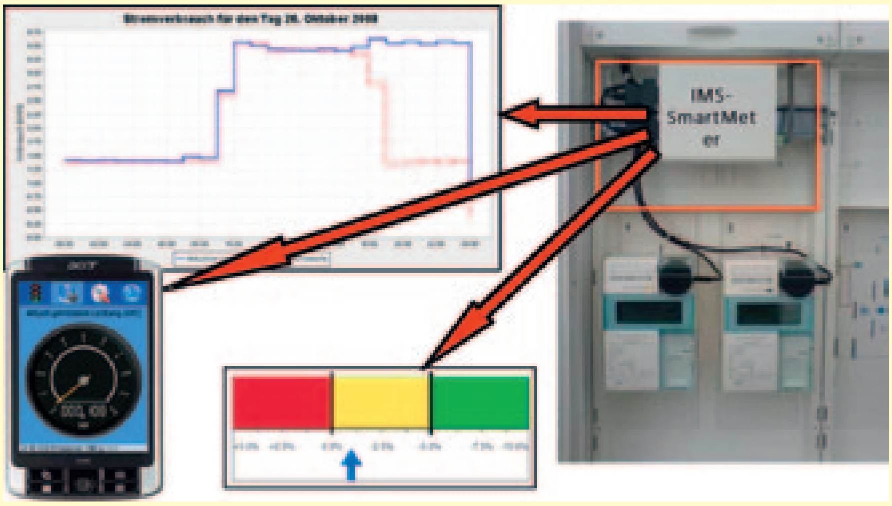

The IMS-SmartMeter is a new device, which takes advantage of the opportunities originating in the new electronic domestic supply meters. It supports up to four connected meters and is able to store all consumption data over a period of two years, before overwriting old data in the storage. Developing this new device, the focus was not on the technical feasibility but rather on the applications, which enable end users to save energy. For private households for instance, a special energy tachometer, which gives out information concerning the current energy consumption, was developed in cooperation with the electricity company RWE. Given out on a mobile, wireless device, the user is given the chance to operate different consumers in order to assess the influence on the overall energy consumption.

Another basic application gives out current energy consumption using the design of a traffic light: Current data is compared to last year's. The displayed arrow indicates divergences according to a self-determined goal of savings.

For technically accomplished end users, a load curve display was implemented. It reveals the consumption data of selectable periods of time. Using the integrated display of reference periods, changes in consumption can be analysed in detail.

A field experiment over a period of two years including fifty households was used to test the development. For this purpose, IMS-SmartMeter was specially supplied with technical alternatives to record and evaluate usage and user acceptance. IMS-SmartMeter is used in the facilities of inHaus1 and inHaus2 of the Fraunhofer-Gesellschaft to record energy consumption. This ensures long term testing and an extension of the range of features. Here, applications in commercial properties, which can be used to transmit user dependant consumption data, are of particular interest. In this context, SmartMeter serves to record the effectivity of implemented energy saving measures.

Further concepts of SmartMetering clearly exceed the basic recording of energy consumption. Due to an increasing percentage of regenerative energies in the area of power generation, the requirements for distribution networks are changing drastically. The new trend of several smaller generators instead of few bigger power plants, which brings about new requirements for distribution networks, serves as one possible explanation. Furthermore, generation can no longer be completely adapted to consumption, since e.g. wind- and solar-energy are not constantly available. Hereby, the importance of controlling consumption increases constantly. Also in this area, SmartMetering aims to help by offering flexible rates or directly piloting consumers.

SMART BUILDING: OPTIMIZATION OF OPERATION AND APPLICATION PROCESSES BY INTEGRATION OF IT AND DOMOTICS

K. Scherer

Convergence of technologies, devices and functions is one of the most important trends in the field of electronics, IT and communication. This means that due to digital signalling and extensive software application, more and more multifunctional devices and systems are dominating the market and mono functional devices like TV and phones are forced to the background in a mid-range time scale. The best known examples of multi-functionality are PCs, mobile phones and the internet. Besides the trend of convergence, *integration* of separately existing devices and functions in the form of complex, *integrated system environments* is another important concept.
In the future segments *SmartHome* and *SmartBuilding* the focus is on the integration of information-technology *(IT)* and *domotics* by data networking and multifunctional middleware-platforms.

Keywords
Domotics, Home- and Building-Technology, Information- and Communication-Technology, Middleware, Systems Integration, Systems-Solutions, Optimization of Operation- and Application-Processes: [1], [2], [3], [4]

1 Domotics, IT and open Systems Integration

Domotics is the common expression for technical equipment in homes and commercial buildings like heating and alarm systems, and in smart homes also appliances of the white goods segment, like washing machines and refrigerators. [13]
For data networking and systems integration of all these devices, there is a spectrum of interfacing and protocol standards. Examples are KNX/EIB (Konnex, European Installation Bus), LON (Local Operating Network), M-Bus (Metering Bus), Ethernet/TCP-IP, WLAN, DALI (Light-Systems-Bus) and BACnet (building automation control network). In combination with this we have to consider networking medias like coax, twisted pair, POF (polymer optical fibre), power line (data transmission over electric power cables) and the "data over air" technologies. [7], [8], [9]

More and more we also see innovative communication and information technology and products in homes and commercial buildings, e.g. office-buildings with LAN-, WLAN-Networks in combination with computation servers for intranets of companies. [14], [17], [18], [21], [23], [24], [25]
For an open integration of this technology, we need concepts like those of Fraunhofer IMS, which are based on middleware.

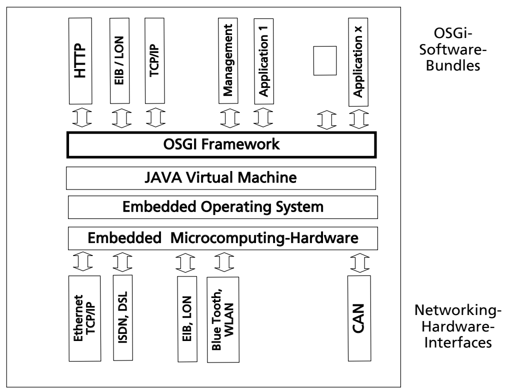

Figure 1: OSGi-Kernel-System with OSGi-Bundles and div. Data-Interfaces

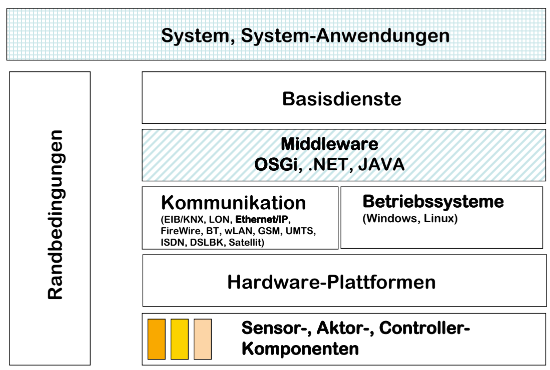

Figure 2: Basic structure of an open middleware systems integration platform

Mostly used middleware technologies are OSGi (open service gateway intitiative) and .NET. [6], [16, [26], but also UPnP (universal plug and play).
Figure 1 shows an OSGI-Kernel-Middleware-Platform and Figure 2 a basic structure of a middleware integration platform for open systems integration.

2 Two Examples of Application

Intelligent Care-Bath for Nursery Homes

The intelligent care bath (inBath) of IMS has been developed in cooperation with care experts. It aims to assist people suffering from dementia in their daily life environment, like the bathroom (AAL, ambient assisted living). The system assists in actions like personal hygiene, tooth brushing and medication. Diverse safety features like a sensor carpet for fall detection and a messaging system complete the range of benefits. [5]

Smart Metering for more Energy Transparency

More transparency in energy consumption is the first step in energy saving. In cooperation with RWE, Fraunhofer IMS developed in the inHaus-Center a smart metering prototype solution to be implemented in fifty dwellings in Wesel, a mid-sized town near Duisburg. The system is able to transmit consumption data from networked electronic electricity meters [12] via power-line to a home-PC with TV-functions, but also by a WLAN-Hotspot to smart phones and PDAs. Several screens show the yearly power consumption including costs as well as the CO_2-equivalent to the respective power consumption. In order to enhance usability, a traffic light signalling was integrated to show the amount of energy saving in the current year. Furthermore, power-consumption can be given out in car speed-meters. [8]

Figure 3: Intelligent Care-Bath in Fraunhofer-inHaus-Center

Figure 4: Smart-Metering User Interface on PC-TV and Mobile Phones like iPhone

SMART BUILDING: OPTIMIZATION OF OPERATION AND APPLICATION PROCESSES BY INTEGRATION OF IT AND DOMOTICS

3 Conclusion

In order to optimize operation and application processes in rooms and buildings, integrating domotics and ITC-functions in a whole system by means of middleware technology has become a very efficient concept, which offers diverse benefits. Examples are computer aided facility management (CAFM) with smart metering for energy transparency and an optimized management of processes in nursery homes, e.g. the intelligent bath room as well as care-documentation.

Further Reading

[1] www.inhaus.de
[2] www.ims.fraunhofer.de
[3] www.office21.de
[4] www.futurehotel.de
[5] www.aal-europe.eu
[6] www.osgi.org
[7] www.konnex.org
[8] www.lonmark.de
[9] www.develo.de
{10] www.iea.org
[11] www.theapplicationhome.com
[12] www.hager.de/menu/e-katalog/elektronische-haushaltszaehler-zubehoer/113644.htm
[13] www.vdi.de/41977.0.html
[14] www.ipv6-taskforce.org
[15] www.connectedhome.net
[16] www.internethomealliance.org
[17] www.ipv6forum.com
[18] www.plcforum.org
[19] www.homeplug.org
[20] www.teaha.org,
[21] www.wifitechnology.org
[22] www.upnp.org,
[23] www.zigbee.org
[24] www.intellon.com,
[25] www.wirelessethernet.org
[26] www.cenelec.org
[28] www.dlna.org

LIST OF PUBLICATIONS AND SCIENTIFIC THESES 2009

List of Publications and Scientific Theses 2009

LIST OF PUBLICATIONS AND SCIENTIFIC THESES 2009

1. Monographs

Grabmaier, A.:
Drahtlose Energieübertragung für Batterie betriebene mobile Geräte.
2009, Fulltext urn:nbn:de:0011-n-923923 (PDF)

2. Journals and Conference Papers

Betz, W.; Trieu, H.-K.; Vogt, H.:
In-vitro tests for biostability of materials for micro implants.
(MME <20, 2009, Toulouse>).
In: 20th Micromechanics Europe Workshop.
Toulouse: LAAS-CNRS, 2009, pp. D 27.1-3

Dierk, S.; Ünlübayir, S.; Boom, T. van den; Trieu, H.-K.:
BioProm: CMOS-biosensor based on an insulated gate with integrated membrane.
(Deutsches BioSensor Symposium <6, 2009, Freiburg).
In: 6. Deutsches BioSensor Symposium. Freiburg, 2009, p.136

Dimopoulos, T.; Schwarz, D.; Uhrmann, T.; Kirk, D.; Kohn, A.; Weyers, S.; Paschen, U., Brückl, H.:
Magnetic properties of embedded ferromagnetic contacts to silicon for spin injection.
In: Journal of physics / D 42 (2009) 8, 085004 [6pp]
http://www.iop.org/EJ/article/0022-3727/42/8/085004/d9_8_085004.pdf?request-id=9eb10d51-5ea0-4901-b10c-244913a93689

Dogangün, A.; Haverkamp, S.; Munstermann, M.; Stockmanns, G.; Naroska, E.:
"inBath" – assistive Badumgebung.
(Konferenz Mensch und Computer <9, 2009, Berlin>).
In: Mensch & Computer 2009. München [u.a.]: Oldenbourg, 2009, pp. 423-426

Dünnebacke, D.; Schönherr, F.; Heidemann, B.; Amini, A.:
MeDiNa: Telemedizinische Rehabilitationsunterstützung in den eigenen vier Wänden.
In: Unternehmen der Zukunft (2009) 3, p. 22-25

Durini, D.; Brockherde, W.; Hosticka, B. J.:
Charge-injection photogate pixel fabricated in CMOS silicon-on-insulator technology.
In: International journal of circuit theory and applications 37 (2009) 2, pp. 179-192

Durini, D.; Brockherde, W.; Grabmaier, A.; Hosticka, B. J.:
Development of a CMOS-optoprocess for particle and radiation detection.
(European Symposium on Semiconductor Detectors <11, 2009, Wildbad Kreuth>).
In: 11th European Symposium on Semiconductor Detectors: Conference Program & Abstract Book. Wildbad Kreuth, 2009, without pagination

Durini, D.; Aurola, A.; Brockherde, W.; Hosticka, B. J.; Grabmaier, A.:
Double modified internal gate (MIG) pixel for fluorescence imaging applications.
(ECCTD <19, 2009, Antalya>).
In: ECCTD 2009. Piscataway, NJ: IEEE, 2009, pp. 9-12

Durini, D.; Dreiner, S.; Vogt, H.:
Indium-Tin-Oxide (ITO) layer integration in single-poly-silicon standard CMOS processes to improve the CTE in photogate pixels.
(Conference on Frontiers in Electronic Imaging <2009, München>).
In: Proceedings of the EOS Conferences at the World of Photonics Congress 2009.
Hannover: EOS, 2009, without pagination

Durini, D.; Mahdi, R.; Spickermann, A.; Brockherde, W.; Grabmaier, A.; Hosticka, B. J.:
Lateral drift-field photodetector based on a non-uniform lateral doping profile photodiode for time-of-flight imaging.
(ESSDERC <39, 2009, Athen>).
In: ESSDERC ESSCIRC 2009: Fringe Poster Session. Piscataway, NJ: IEEE [u.a.], 2009, without pagination

Feldengut, T.; Kokozinski, R.; Kolnsberg, S.:
A UHF voltage multiplier circuit using a threshold-voltage cancellation technique.
(PRIME <5, 2009, Cork>).
In: PRIME 2009. Piscataway, NJ: IEEE, 2009, pp. 288-291

Feldengut, T.; Kolnsberg, S.; Kokozinski, R.:
A long range passive UHF transponder ASIC with temperature sensor.
(Internationales Wissenschaftliches Kolloquium <57, 2009, Ilmenau>).
In: 54. Internationales Wissenschaftliches Kolloquium. Ilmenau: Technische Univ., 2009, without pagination

Feldengut, T.; Kolnsberg, S.; Kokozinski, R.:
Voltage rectification: The energy-bottleneck for passive RFID systems.
(European Workshop on RFID Systems and Technologies <5, 2009, Bremen>).
In: RFID SysTech 2009. Berlin [u.a.]: VDE-Verl., 2009, without pagination

Gräfe, M.; Göttsche, T.; Osypka, P.; Görtz, M.; Trieu, H.-K.; Fassbender, H.; Mokwa, W.; Urban, U.; Schmitz-Rode, T.; Bender, B.; Glocker, R.; Fähnle, M.:
HYPER-IMS: a fully implantable blood pressure sensor for hypertensive patients.
(Sensor <14, 2009, Nürnberg>).
In: SENSOR 2009. Wunstorf: AMA Service GmbH, 2009, B 1.2

Hennig, A.; Vom Bögel, G.:
Antenna analysis and optimisation for deeply implantable medical sensor transponders.
(Internationales Wissenschaftliches Kolloquium <57, 2009, Ilmenau>).
In: 54. Internationales Wissenschaftliches Kolloquium. Ilmenau: Technische Univ., 2009, without pagination

Hennig, A.; Vom Bögel, G.:
Antenna design for deeply implantable sensor transponder systems in medicine.
(European Workshop on RFID Systems and Technologies <5, 2009, Bremen>).
In: RFID SysTech 2009. Berlin [u.a.]: VDE-Verl., 2009, without pagination

Hosticka, B. J.:
Scannerless 3D-ToF-Sensors.
(Conference on Frontiers in Electronic Imaging <2009, München>).
In: Proceedings of the EOS Conferences at the World of Photonics Congress 2009
Hannover: EOS, 2009, without pagination

Klauke, S.; Görtz, M.; Rein, S.; Hoehl, D.; Thomas, U.; Eckhorn, R.; Bremmer, F.; Wachtler, T.:
Electrical stimulation of the human retina with a wireless intraocular retinal prosthesis.
(Göttingen Meeting of the German Neuroscience Society <8, 2009, Göttingen>).
In: Eight Göttingen Meeting of the German Neuroscience Society. Göttingen, 2009, T15-6B
PDF Volltext: Konferenz http://www.nwg-goettingen.de/2009/

Klieber, R.; Goehlich, A.; Trieu, H.-K.; Kappert, H.; Grabmaier, A.:
Assembly of pressure sensor chips as an example for integrated MEMS for high temperature applications.
Mikrosystemtechnik-Kongress <3, 2009, Berlin>)
In: MikroSystemTechnik. Berlin [u.a.]: VDE-Verl., 2009, Paper P1.21

LIST OF PUBLICATIONS AND SCIENTIFIC THESES 2009

Marx, M.; Kokozinski, R.; Müller, H.-C.:
High resolution delay locked loop for time synchronization with multi path mitigation.
(PRIME <5, 2009, Cork>).
In: PRIME 2009. Piscataway, NJ: IEEE, 2009, pp. 204-207

Marx, M.; Kokozinski, R.; Müller, H.-C.:
Time synchronization for real time localization systems with multi path mitigation.
(IEEE MTT-S International Microwave Workshop <1, 2009, Cavtat>).
In: IEEE MTT-S International Microwave Workshop Series on Wireless Sensing, Local Positioning, and RFID. Piscataway, NJ: IEEE, 2009, pp. 57-60

Menges, M.; Schmidt, A.; Bonath, W.:
Open Source-/Freeware IC Design Flow am Beispiel einer DPLL.
(Workshop Multiprojekt-Chip-Gruppe Baden-Württemberg <2009, Karlsruhe>).
In: Tagungsband zum Workshop der Multiprojekt-Chip-Gruppe Baden-Württemberg 42 (2009) Juli, pp. 17-23

Meyer, F.; Vom Bögel, G.; Van Ackeren, M.; Lörcks, M.; Vasilev, K.:
RFID- und Sensortranspondersysteme in Wartung und Instandhaltung.
(European Workshop on RFID Systems and Technologies <5, 2009, Bremen>).
In: RFID SysTech 2009. Berlin [u.a.]: VDE-Verl., 2009, without pagination

Naroska, E.; Stockmanns, G.; Dimitrov, T.; Haverkamp, S.; Kurzschenkel, M., Meyer, W.; Perszewiski, H.:
Fallstudie: Verhaltensanalyse einer an Demenz erkrankten Seniorin.
(Kongress Ambient Assisted Living <2, 2009, Berlin>).
In: Ambient Assisted Living. Berlin [u.a.]: VDE, 2009, without pagination

Naroska, E.; Stockmanns, G.; Dimitrov, T.; Hensel, T.; Meyer, W.; Perszewiski, H.:
Eine Low-cost Infrastruktur zur Erfassung und Analyse von Bewohnerverhaltensdaten in betreuten Wohngemeinschaften.
(Kongress Ambient Assisted Living <2, 2009, Berlin>).
In: Ambient Assisted Living. Berlin [u.a.]: VDE, 2009, without pagination

Roessler, G.; Laube, T.; Brockmann, C.; Kirschkamp, T.; Mazinani, B.; Görtz, M.; Koch, C.; Krisch, I.; Sellhaus, B.; Trieu, H.-K.; Weis, J.; Bornfeld, N.; Röthgen, H.; Messner, A.; Mokwa, W.; Walter, P.:
Implantation and explantation of a wireless epiretinal retina implant device.
In: Investigative ophthalmology and visual science 50 (2009) 6, pp. 3003-3008

Scherer, K.:
Smart Building: Optimierung von Betriebs- und Anwendungsprozessen durch Integration von IT und Domotik.
In: Information Management und Consulting 24 (2009) 3, pp. 28-32

Schliepkorte, H.-J.:
Fraunhofer inHaus-Zentrum – Innovationswerkstatt für optimierten Objektbau.
(Gebäudeeffizienz <2009, Frankfurt, Main>).
In: GebäudeEffizenz 2009. Aachen: TEMA Technologie Marketing AG, 2009, pp. 157-171

Schliepkorte, H.-J.:
Smart Home: Zukünftige Kundenerwartungen/ -anforderungen.
(E-World Kongress <2009, Essen>).
In: E-World. Essen: Messe, 2009, without pagination

Schmidt, A.; Feldengut, T.; Kolnsberg, S.; Kokozinski, R.:
A low quiescent current LDO voltage regulator for passive RFID transponder-tags using SMCNR-compensation.
(Germany Student Conference <1, 2009, Hamburg>).
In: Proceedings of the First IEEE Germany Student Conference 2009. Hamburg: IEEE, 2009, P. 12 [4 pp.]

Sommer, S. P.; Paschen, U.; Figge, M.; Vogt, H.:
Light switched plasma charging damage protection device allowing high field characterization.
(ESSDERC <39, 2009, Athen>).
In: ESSDERC ESSCIRC 2009: Conference Proceedings. Piscataway, NJ: IEEE [u.a.], 2009, without pagination

Spickermann, A.; Hosticka, B. J.; Grabmaier, A.:
Performance considerations for photogate based active pixel sensors.
(PRIME <5, 2009, Cork>).
In: PRIME 2009. Piscataway, NJ: IEEE, 2009, pp. 216-219

Spickermann, A.; Durini, D.; Bröcker, S.; Brockherde, W.; Grabmaier, A.:
Pulsed time-of-flight 3D-CMOS imaging using photogate-based active pixel sensors.
(ESSDERC <39, 2009, Athen>).
In: ESSDERC ESSCIRC 2009: Conference Proceedings. Piscataway, NJ: IEEE [u.a.], 2009, without pagination

Stockmanns, G.:
Entwicklung assistiver Umgebungen für ein selbstbestimmtes Leben im Alter bei kognitiven Einschränkungen.
(Deutsche Gesellschaft für Physikalische Medizin und Rehabilitation / Jahreskongress <114, 2009, Leipzig>).
In: Physikalische Medizin und Rehabilitation. Leipzig, 2009, without pagination

Trieu, H.-K.; Görtz, M.; Koch, C.; Mokwa, W.; Walter, P.:
Implants for epiretinal stimulation of retinitis pigmentosa patients.
(World Congress on Medical Physics and Biomedical Engineering <2009, München>).
In: World Congress on Medical Physics and Biomedical Engineering. Heidelberg: Springer, 2009, pp. 80-83

Ünlübayir, S.; Weiler, D.; Boom, T. van den; Trieu, H.-K.:
Immunosensor based on specifity enhanced field effect transistor (seFET).
(Deutsches BioSensor Symposium <6, 2009, Freiburg).
In: 6. Deutsches BioSensor Symposium. Freiburg, 2009, p. 96

Uhlemann, A.; Aal, A.; Vogt, H.:
A fast WLR test for the evaluation of EEPROM endurance.
(Integrated Reliability Workshop <2009, Lake Tahoe, Calif.>).
In: International Integrated Reliability Workshop <2009, Lake Tahoe, Calif.>: Final Report. Piscataway, NJ: IEEE [u.a.], 2009, pp. 20-24

Uhrmann, T.; Dimopoulos, T.; Kovacs, A.; Kohn, A.; Weyers, S.; Paschen, U., Smoliner, J.; Brückl, H.:
Evaluation of Schottky and MgO-based tunnelling diodes with different ferromagnets for spin injection in n-Si.
In: Journal of physics / D 42 (2009) 14, 145114 [9pp]
http://www.iop.org/EJ/article/-search=68566905.1/0022-3727/42/14/145114/d9_14_145114.pdf?request-id=3260fc4c-470f-448d-bd70-0c3548d24e19

Urban, U.; Fassbender, H.; Fürst, P.; Göttsche, T.; Bender, B.; Becker, R.; Mokwa, W.; Trieu, H.-K.; Osypka, P.; Glocker, R.; Steinseifer, U.; Schmitz-Rode, T.:
Fully implantable blood pressure system: Implantation experiences.
(World Congress on Medical Physics and Biomedical Engineering <2009, München>).
In: World Congress on Medical Physics and Biomedical Engineering. Heidelberg: Springer, 2009, pp. 214–217

Vogt, H.:
CMOS Post-Processing für kompakte, intelligente Mikrosysteme.
(Mikrosystemtechnik-Kongress <3, 2009, Berlin>)
In: MikroSystemTechnik. Berlin [u.a.]: VDE-Verl., 2009, Paper 19

Vogt, H.; Vogt, H.:
Simulation des Laserabgleichs von Dünnfilmwiderständen mit Widerstandsnetzwerk im Schaltungssimulator.
(Mikrosystemtechnik-Kongress <3, 2009, Berlin>).
In: MikroSystemTechnik. Berlin [u.a.]: VDE-Verl., 2009, Paper P8.18

3. Oral Presentations

Scherer, K.:
Fraunhofer inHaus-Zentrum – Innovationswerkstatt für die Prozessoptimierung durch integrierte Raum- und Gebäudesysteme.
VDI-Gesellschaft für Bauen und Gebäudetechnik, Erfurt, October 10, 2009

4. Patents

4.1 Granted Patents

Köster, O.; Slotkowski, J.:
Verfahren und Vorrichtung zum Testen oder Kalibrieren eines Drucksensors an einem Wafer.
May 6, 2009
EP 1 397 656 B1

Krisch, I.; Brockherde, W.:
Videoendoskopievorrichtung.
March 11, 2009
EP 1 773 178 B1

Trieu, H.-K.; Bollerott, M.; Kemmerling, M.; Hildebrand, R.; van Hest, J.; Rutjes, F.; Koch, K.; van Beek, T.A.; Sudhölter, E. J. R.; Boom, R. M.; Janssen, A. E.M.:
Chip-holder for a micro-fluid chip.
December 23, 2009
EP 1 919 623 B1

4.2 Laid Open Patent Documents

Görtz, M.; Trieu, H.-K.; Mokwa, W.:
Flexible Sehprothese und ein Verfahren zur Herstellung einer flexiblen Sehprothese.
March 11, 2009
EP 2 033 682 A1

Huppertz, J.:
Konzept zum Bestimmen eines Messwerts an einem Bauelement.
June 18, 2009
DE 10 2007 056 731 A1

Huppertz, J.:
Concept for determining a mearsurement value at a component
May 28, 2009
US 2009/0134330 A1

Huppertz, J.:
Vorrichtung und Verfahren zur effizienten Analog-Zu-Digital-Wandlung.
May 28, 2009
DE 10 2007 056 732 A1

Klieber, R.; Schelle, B.:
Schaltungsanordnung und ein Verfahren zum Verkapseln derselben.
March 05, 2009
DE 10 2007 041 229 A1

Naroska, E.; Jalali, L.; Dimitrov, T.:
Vorrichtung und Verfahren zur Bestimmung eines Leistungsverbrauchs einer leistungsverbrauchenden Einrichtung aus einer Mehrzahl von leistungsverbrauchenden Einrichtungen.
July 16, 2009
DE 10 2007 051 347 A1

Schelle, B.; Klieber, R.:
Circuit arrangement and method for the encapsulation thereof.
March 12, 2009
PCT/EP2008/006526

Schrey, O. M.; Brockherde, W.; Hosticka, B. J.; Ulfig, W.:
Optical distance meter and method for the optical distance measurement.
October 22, 2009
PCT/EP2009/002570

Schrey, O. M.; Brockherde, W.; Hosticka, B. J.; Ulfig, W.:
Optischer Abstandsmesser und Verfahren zur optischen Abstandsmessung.
October 15, 2009
DE 10 2008 018 718 A1

Trieu, H.-K.; Slotkowski, J.; Klieber, R.; Cornelis, J.; Van Hest, M.; Koch, K.; Rutjes, F. P. J. T.; Nieuwland, P.; Wiebe, P.:
Chip holder, fluidic system and a chip holder system.
December 10, 2009
US 2009/0302190 A1

Ünlübayir, S.; Trieu, H.-K.:
Biosensor und ein Verfahren zum Messen einer Konzentration eines Analyten in einem Medium.
April 2, 2009
DE 10 2007 043 132 A1

Vogt, H.; Ruß, M.:
Bolometer und Verfahren zum Herstellen eines Bolometers.
August 19, 2009
CN 101512308 A

5. Theses

5.1 Dissertations

Durini Romero, D.:
Solid-State imaging in standard CMOS processes.
Duisburg-Essen, Campus Duisburg, Univ., Diss., 2009

Jeremias, Ralf F.:
CMOS-Bildsensoren mit Kurzzeitverschluß zur Tiefenerfassung nach dem Lichtlaufzeit-Messprinzip.
Duisburg-Essen, Campus Duisburg, Univ., Diss., 2009

Thoß, S.:
Neuartiges Ausleseverfahren für induktive Näherungssensoren auf Basis von Sigma-Delta Modulation.
Duisburg-Essen, Campus Duisburg, Univ., Diss., 2009

5.2 Diploma Theses

Böttcher, M.:
Entwurf und Optimierung eines Taktgenerators für passive RFID Transponder.
Zittau-Görlitz, Campus Zittau, Hochsch., Dipl.-Arb., 2009

Breßer, P.;
Konzeptionierung, Aufbau und Verifikation eines RFID Transponder Testplatzes für das europäische UHF ISM Band bei 865 - 868 MHz.
Dortmund, Fachhochsch., Dipl.-Arb., 2009

Fladung, J.-E.:
Schaltungsentwurf und Realisierung eines PROMs für 250 °C in einer SOI-Hochtemperatur-Technologie.
Lübeck, Fachhochsch., Dipl.-Arb., 2009

Hillebrand, C.:
Optimierung und Erweiterung eines Vier-Sensor-Systems zur Gewichtsmessung von Gegenständen mit piezoelektrischen Drucksensoren.
Duisburg-Essen, Campus Duisburg, Univ., Dipl.-Arb., 2009

Mat Jizat, J. A.:
Silicone as encapsulation material for micro implants: Silicone's adhesion properties.
Karlsruhe, Hochsch., Dipl.-Arb., 2009

Nawrocki, M.:
Untersuchung von Bildverarbeitungsalgorithmen zur Optimierung von streuungsdominierten Bildern in der kardiovaskulären Angiographie.
Krefeld-Mönchengladbach, Campus Krefeld, Hochsch., Dipl.-Arb., 2009

Ragunathan, D.:
Aufbau einer Testumgebung zur Messung von Signalstärken in Funknetzen innerhalb von Gebäuden mit den „Fraunhofer µNodes".
Dortmund, Fachhochsch., Dipl.-Arb., 2009

Schmidt, A.:
Entwurf eines integrierten Spannungsreglers für passive UHF-Transponder.
Gießen-Friedberg, Campus Gießen, Fachhochsch., Dipl.-Arb., 2009

Weber, D.:
Intellectual Capital Report – Gestaltungsmöglichkeiten am Beispiel des Fraunhofer-Instituts, Duisburg.
Duisburg-Essen, Campus Duisburg, Univ., Dipl.-Arb., 2009

5.3 Master Theses

Baccar, D.:
Anpassung und Evaluierung einer FPGA basierten Rapid-Prototyping Umgebung und Funktionsdemonstration durch Umsetzung von Signalverarbeitungsfunktionen.
Gelsenkirchen, Fachhochsch., Master Thesis, 2009

Grey Oropeza, S.:
Analysis of commerically available USB-modules and design of a comparable framework for microcontrollers.
Duisburg-Essen, Campus Duisburg, Univ., Master Thesis, 2009

5.4 Bachelor Theses

Giacalone, G.:
Entwicklung eines über LabView gesteuerten Messplatzes zur parallelen Ansteuerung und Charakterisierung von integrierten, mikromechanischen Druck- und Temperatursensoren für medizinische Implantate.
Gelsenkirchen, Fachhochsch., Bachelor-Thesis, 2009

Gräfe, K.:
Aufbau und Inbetriebnahme eines elektrochemischen Messplatzes.
Duisburg-Essen, Campus Duisburg, Univ., Bachelor-Thesis, 2009

Günter, S.:
Simulation und Charakterisierung von Photogate basierten Photodetektoren in einem 0,35 µm Standard-CMOS-Prozess.
Duisburg-Essen, Campus Duisburg, Univ., Bachelor-Thesis, 2009

Law, K. H.:
Verification for testability of digital circuits forming part of a mixed signal ASIC fabricated in a 0.35 µm CMOS process, and generation of wafer level digital design test pattern.
Duisburg-Essen, Campus Duisburg, Univ., Bachelor Thesis, 2009

Pfeiffer, D.:
Analyse von Stromlastgängen aus Privathaushalten und Untersuchung der Möglichkeiten für neue Anwendungen im Bereich Energieeffizienz.
Duisburg-Essen, Campus Duisburg, Univ., Bachelor Thesis, 2009

Saxler, M.:
Realisierung und Test von Verfahren zur Signalunterdrückung in RFID Transceiver Modulen.
Düsseldorf, Fachhochsch., Bachelor Thesis, 2009

Tarhuni, H.:
Optimising bidirectional data transmission process of the requirements of a sensor transponder system.
Duisburg-Essen, Campus Duisburg, Univ., Bachelor-Thesis, 2009

Volgmann, S.:
Charakterisierung von Hochspannungstransistoren einer SOI CMOS Technologie.
Düsseldorf, Fachhochsch., Bachelor Thesis, 2009

5.5 Project Theses

Breßer, P.:
Aufbau und Evaluierung eines I/Q Demodulators für einen UHF RFID Reader.
Dortmund, Fachhochsch., Project Thesis, 2009

Weitz, K.:
Entwurf und Layout von skalierbaren Schaltungsmodulen für ein RAM-Generatorsystem.
Dortmund, Techn. Univ., Project Thesis, 2009

CHRONICLE 2009

Chronicle

ENERGY EFFICIENCY BY SMART FACILITY MANAGEMENT

The Fraunhofer-Gesellschaft together with the Chambers of commerce and industry of North Rhine-Westphalia invited industrial companies to a conference on "Energy Efficiency by Smart Facility Management".

More than 250 representatives of various companies took part in this event which took place on February 5th 2009 in the Fraunhofer-inHaus-Center in Duisburg. They all learned more about techniques to save and to gain energy in order to stay competitive and to act environmentally friendly.

In close cooperation with manufacturers the Fraunhofer-inHaus-Center conducts research activities on new integrated energy concepts for buildings as well as materials to supply and save energy in an intelligent way.

New techniques and examples were presented in speeches and demonstrations.

Examples for saving energy

- A smart meter shows the energy consumption in detail and monitors it so that the user gets more information on his behaviour.

- Intelligent heating and lighting management with networked components save energy.

- New Building materials including energy-efficient windows, well-sealed doors, and additional thermal insulation of walls can reduce heat loss.

Renewable Power Supply

- Geothermal energy is power extracted from heat stored in the earth and is supplied to private households and business bildings.

- Photovoltaic solar energy as a prinicipal or additional source of energy

KICKOFF FOR A NEW GENERATION OF EVEN MORE INTELLIGENT SYSTEMS

The Fraunhofer Institute for Microelectronic Circuits and Systems wins the scientific competition "NanoMikro + Werkstoffe.NRW" and invests 16 Million Euro in a new Microsystems technologlogy lab (MST-Lab).

North Rhine-Westphalia and the Federal Ministry of Research contribute 25 % of the subsidy amount each. The European Commission contributes another 50 % of the amount.

Fraunhofer IMS advances in MEMS-Technology **(M**icro-**E**lectro-**M**echanical **S**ystems) which combines the traditional CMOS-Technology **(C**omplemantary **M**etal **O**xide **S**emiconductor) with new procedures and new materials on a chip. Researchers integrate different micro- and nanofunctions directly on top of signal processing CMOS circuits. They combine mechanical elements such as sensors and actors with electronic components on a common silicon substrate.

The new equipment will expand the existing capabilities for microbolometer arrays (incl. galvanic and flip chip bonding for encapsulation) with a stepper capable of alignment to the wafer backside, thinning and through Silicon via processes, deposition and etching of special dielectrics and metals, as well as a broad range of process control tools.

This will increase the stability of the processes and expand the options for further sophistication in existing core competencies:

- Bio-compatible metallizations will allow higher flexibility for advanced implanted pressure monitors.
- In the automotive sector, miniaturized infrared sensors warn drivers against pedestrians and animals in their way and colour enabled CMOS cameras with high dynamic range enable a detailed rear view for drivers even with blocked rear vision.
- Surveillance in low light conditions will be improved by single photon detection systems, enabled by the sophisticated processes to be developed in the new facilities.
- Rugged and simply constructed pressure sensors for industrial applications will be possible with newly available processes like Through Silicon Via etch, wafer bonding and thinning.

Business companies as well as public research centers collaborate with Fraunhofer IMS in order to develop new MEMS which are asked for in different commercial sectors e.g. automotive industry, consumer electronics and medical technology.

FRAUNHOFER TRUCK STOPPED IN DUISBURG ON NOVEMBER 18TH 2009

People need healthcare, mobility, environment, security, communications and energy. Fraunhofer scientists are always looking for innovative solutions in all these thematic areas. People, their needs and their desires, lie at the heart of this endeavor: Which products, technologies and processes will make people healthier, safer and happier in their daily lives? The Fraunhofer Truck enabled us to show the visitors in a readily understandable way the results of scientific research from the following six areas: healthcare, security, communications, mobility, energy and environment.

FRAUNHOFER IMS PRESENTED ITS IMPLANTABLE BLOOD PRESSURE SENSOR

Patients with high blood pressure often need to be monitored over long periods until drugs can be used to control their blood pressure. In the past, patients had to wear a sleeve on their arm that was inflated at regular intervals. All of which would be very inconvenient for the patient, especially at night. In future, a small pressure sensor, which is introduced into the femoral artery in the groin, will be used to measure blood pressure. The sensor is connected using a small transponder under the skin. This transponder then digitizes and sends the data to a reader on the patient’s belt.

VISIONS ON THE FAIRS: LASER AND VISION

For the first time Fraunhofer IMS was present on the fair "LASER – World of Photonics" which took place in Munich from June 15th to 18th. On the booth of the German network for optical technologies OpTech-Net we presented the latest results of CMOS optical sensor technology at IMS. Moreover, an invited talk and a contributed paper were given at the accompanying "World of Photonics Congress". These presentations received highest interest from the international expert forum.

As in the years before Fraunhofer IMS presented its news in the field of CMOS image sensors on the "VISION" fair in Stuttgart, this time from 9th to 11th November, 2009. The financial crisis couldn't disturbe the interest of visitors and also exhibitors who were present in the same number than in the last year. After a decade of continuous IMS presence at this important forum it is already good tradition now meeting our customers there! They know finding us and get informed about important novelties. On a 25 m² stand we informed about our main themes which is at the moment the 3D CMOS image sensor technology working on the time-of-flight principle. Our recent spin-off TriDiCam who is using this technology was also present at the fair with an own booth. A second main focus was layed on our new CMOS opto process for imaging sensors which is running at the Fraunhofer IMS wafer fab. We informed about the features of this 0.35 µm CMOS process and the high performance in optical device design and fabrication. Novel photodiodes, color filters, UV enhanced devices, stitching and more special devices are possible in this standard 0.35 µm CMOS process. Further on we announced our 5th Fraunhofer IMS Workshop on CMOS Imaging on 4th and 5th May, 2010 which is going to take place at our institute in Duisburg. According to the high number of contacts and their quality all of these themes were highly interesting for our customers who are already planning to meeting us again at the VISION 2010.


INHAUS-CENTER EVENTS 2009

In 2009, Fraunhofer inHaus-Center hosted many events for professional audiences. Highlights include the following:

February 5, 2009: Energy-Efficiency by Means of Intelligent Facility Management

About 250 participants accepted the invitation of Fraunhofer-Gesellschaft and the chamber of commerce and industry to the event 'Energy-Efficiency by means of Intelligent Facility Management'. Considering that companies can only guarantee cost advantages and advantages in competition if they succeed in consequently making use of all possible savings, ways to optimize energy costs were pointed out.
Both examples of particular companies and innovative methods were presented. Guided tours and demonstrators completed the event.

May 27, 2009: Innovative Living – Additional Benefits of Modernization

This year's inHaus-Forum-spezial presented approaches and innovations to enhance the quality of living conditions and to use new technologies efficiently. The event outlined solutions in the areas of comfortable living, cost savings and protection of the environment by means of energy-efficiency and assistive environments, which allow independent living despite handicaps. About a hundred participants took advantage of this event and its complementary exhibition to be informed about new application solutions and to network.

September 2/3, 2009: Design and Operation of Intelligent and Energy-Efficient Buildings – Composing European Networks for Innovations

This international event attracted participants from all over Europe and was initiated by Smart Building Cluster Cork (Ireland), Zenit and Fraunhofer-inHaus-Center. It aimed at showing the potential of innovations in the area of intelligent buildings. Furthermore, participants were given the opportunity to discuss European Research & Development projects within the limits of the seventh EU general program and to establish a network 'European Innovation for Intelligent and Energy-Efficient Buildings'. Following up presentations covering all relevant issues during the first day, participants from industry, research facilities and science worked in workshops during the second day to develop research proposals.

November 19, 2009: inHaus-Forum 2009

InHaus-Forum 2009 presented the new potential of integrated system solutions for rooms and buildings for investors, manufacturers, service providers, operators and users. The event focused on findings, conclusions and current and future innovation-activities of the inHaus-Center and its partners. It was again an event of intense networking.
In the morning, each business area of Fraunhofer-inHaus-Center presented previous conclusions and strategies for 2010. During the afternoon, keynotes dealing with 'New Market Opportunities by means of System Solutions' were followed by a panel discussion of leading experts.

Panel Discussion
Participants – right to left: Prof. Dr. Georg Wilking, Hochschule Niederrhein,
Dr. Gerd vom Bögel, Fraunhofer IMS, Dirk Unsenos, ISIS IC, Otto Domke, Landwirtschaftskammer NRW

FORUM ON RFID IN AGRICULTURE

September 3rd 2009: More than 70 scientists, logistician, horticulturists and farmer met at the Fraunhofer Institute for Microelectronic Circuits and Systems in order to discuss new applications of RFID (Radio Frequency Identification) technologies in agriculture. The workshop was organized by Fraunhofer IMS in cooperation with the initiative agrobusiness and the Duisburg Chamber of Industry and Commerce.

Topics as quality control and cost-efficiency by optimized production processes are of utmost importance in every company as well on farms and in a greenhouses. Therefore innovative technologies such as RFID may strengthen agricultural productivity.

Fraunhofer IMS has designed numerous applications for practical use in farming and environmental management. Examples are: measuring the temperature in greenhouses, observing the ecological situation in forests with ground sensors, the monitoring of bovine health via the stomach and aiding the plant protection in potato crops

A few words about RFID: It is a wireless identification method, relying on storing and remotely retrieving data using devices called RFID tags or transponders. An RFID tag is a small label that can be attached to or incorporated into a product, animal or person. RFID tags contain silicon chips and antennas to enable them to receive and respond to radio-frequency queries from an RFID transceiver. Passive tags require no internal power source, whereas active tags require a power source. This technology allows the documentation of processes and offers many applications in agriculture.

PRESS REVIEW

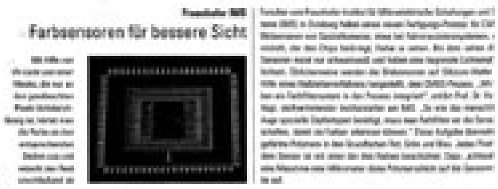

ATZelektronik Juni 2009

tw Juni 2009

SciTechs 2009

Physik Journal 8 2009

WAZ Juni 2009


Sensor in Arterie misst Blutdruck

Ergo Med Januar 2009


Schaf testet Duisburger Medizin-Sensation

Super-Chip misst den Blutdruck unter der Haut

Früher mussten die Patienten tagelang eine Manschette tragen. Bald funkt ein Mini-Sensor die Werte zum Arzt

Bild Februar 2009


Mehr als 28 Nanosekunden

Weinheimer Nachrichten März 2009


Dem Stick bleibt nichts verborgen

Wissenschaftler der Energie forschen nach einem Gerät, das alle Inhaltsstoffe von Lebensmitteln erkennt. Auch geringe Spuren.

Neue Ruhr Zeitung März 2009

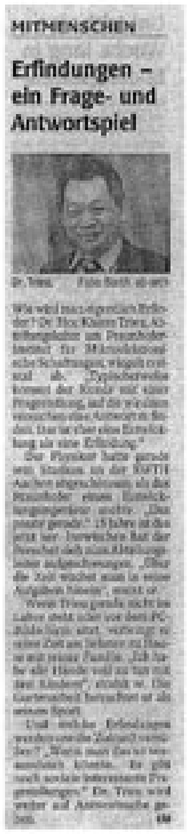
MITMENSCHEN

Erfindungen – ein Frage- und Antwortspiel

Dr. Trieu

WAZ Juni 2009

Measuring blood pressure

A new sensor will make it easier to carry out long-term blood pressure measurements. The device determines the blood pressure directly in the artery and transmits the data wirelessly to a reader attached to the patient's belt. The system was developed by researchers at the Fraunhofer Institute for Microelectronic Circuits and Systems IMS in Duisburg together with the company Dr. Osypka and other partners. The first clinical trials are already underway. In order to find a suitable drug and the correct dosage for patients with high blood pressure, doctors often have to monitor the patients' blood pressure over a longer period of time – a tedious process. The patient has to wear a blood pressure meter on their body, and a pressure sleeve on their arm regularly inflates itself to record the latest values – even at night.

The new sensor measures the blood pressure 30 times per second, but without the patient even noticing. It is no more than about a millimeter in diameter, including its casing. The doctor inserts the tiny helper into the patient's femoral artery in the groin. The data are forwarded via the connected transponder and the external reader to a monitoring station, where the medic analyzes them.

The tiny pressure sensor measures the blood pressure directly inside the femoral artery. © Fraunhofer IMS

Fraunhofer Magazin 02/2009

ATZ Januar 2008

Autonomes Fahren

Objektverfolgung und Wegplanung für das Team-Lux-Roboterfahrzeug

ATZ Januar 2008

ATZ Januar 2008

Fraunhofer

Die Hoffnung im Auge

Fraunhofer Journal 2009

Durchblick im Herzen

TECHNOLOGY REVIEW Juni 2008

Blinde sehen wieder Licht

Rheinische Post 2009

2009

Senioren Ratgeber April 2009

Deutsches Ärzteblatt Oktober 2009

tw November 2009

Rheinische Post Mai 2009

RFID-Signale durch Metall verlustfrei übertragen

elektronikpraxis.de Februar 2009

RFID-Chips funken durch Gegenstände aus Metall

ElektronikPraxis März 2009

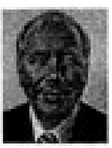

Moderne Baustellenlogistik durch Einsatz neuer Informations- und Kommunikations-Technologien

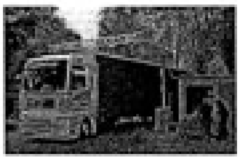

Management Praxis 2009

RFID und Sensorcheck – neue Technologien

TASPO MAGAZIN Juni 2009

RFID lieben Metall

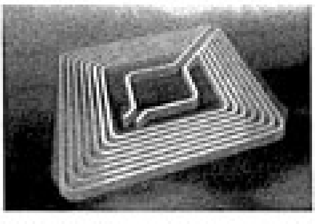

Imprint

Hansastraße 27 c
80686 München

ISSN 1435-0874
Annual Report
Fraunhofer-Institut für Mikroelektronische
Schaltungen und Systeme

Director: Prof. Dr. rer. nat. A. Grabmaier

Adresses:
IMS Duisburg
Finkenstraße 61
47057 Duisburg
Phone +49(0)2 03/37 83-0
Fax +49(0)2 03/37 83-2 66
E-mail martin.van.ackeren@ims.fraunhofer.de
Internet www.ims.fraunhofer.de

Editorial Staff: Martin van Ackeren